

# **Proton Exchange Membranes and Membrane Electrode Assemblies for Enhanced Direct Methanol Fuel Cell Performance**

A Major Qualifying Project Report:

Submitted to the Faculty

of the

WORCESTER POLYTECHNIC INSTITUTE

in partial fulfillment of the requirements for the

Degree of Bachelor of Science

By

---

**Denise A. Gleason**

---

**Kristoffer G. Jensen**

---

**Garima Painuly**

Date: April 22<sup>nd</sup>, 2008

Approved:

---

**Professor Ravindra Datta, Advisor**

---

# TABLE OF CONTENTS

<b>Abstract.....</b>	<b>7</b>
<b>Chapter 1: Introduction .....</b>	<b>8</b>
Advantages and Applications of Direct Methanol Fuel Cells .....	8
How a Direct Methanol Fuel Cell Works .....	9
Problems with Direct Methanol Fuel Cells.....	11
Nafion® Membrane .....	12
Literature Review .....	14
Membrane Modification .....	14
Membrane Electrode Assembly Fabrication.....	21
Passive Direct Methanol Fuel Cell .....	24
<b>Chapter 2: Goals, Hypothesis, &amp; Plan of Work.....</b>	<b>30</b>
Goals .....	30
DMFC Performance.....	30
Design of Experiments.....	35
<b>Chapter 3: Experimental Methods.....</b>	<b>43</b>
Nafion 115 Membrane .....	44
Membrane Pretreatment.....	44
Catalyst Deposition.....	45
Post-treatment .....	47
Hotpressing .....	48
Fuel Cell Assembly.....	49
Fuel Cell Test Station Description.....	51
Fuel Cell Activation.....	53
Fuel Cell Test Conditions .....	54
Bilayer Membrane .....	54
Carboxylic Acid Membrane.....	54
Silica Membrane .....	55
Aldrich Silica .....	58
<b>Chapter 4: Results &amp; Discussion .....</b>	<b>59</b>
Establishing Base Operating Conditions using E-TEK MEAs.....	59
Effect of Methanol Feed Concentration.....	59
Effect of Cell Temperature .....	60
Vapor Methanol Feed .....	61
Effect of Cathode Humidifier Conditions.....	62
Base Operating Conditions .....	63
Optimizing Nafion 115 MEA Fabrication .....	64
Catalyst Ink Deposition: GDL-Application and Membrane-Application.....	64
Nafion Loading .....	66
Effects of Hot-Pressing.....	68
Effects of Pre-Treatment of Post-Treatment of Catalyzed Membranes.....	70

Comparison of Homemade Nafion 115 MEA with E-TEK MEA.....	71
Membrane Comparisons .....	74
Membranes Tested with Electrochem® Gas Diffusion Electrodes .....	74
Fabrication of Homemade Bilayer and Silica Membranes .....	78
Home-made Membrane Comparison – Best Membranes .....	79
<b>Chapter 5: Conclusions &amp; Future Work .....</b>	<b>85</b>
Conclusion .....	85
Recommendations for Future Work .....	87
<b>References .....</b>	<b>89</b>
<b>Acknowledgements .....</b>	<b>93</b>
<b>Appendices.....</b>	<b>94</b>
Appendix 1: Membrane Treatment Procedures .....	94
Appendix 2: Calibration of Cathode Flow Meter for Oxygen and Air.....	96
Appendix 3: Synthesis Procedure for Nafion-SiO <sub>2</sub> Sol-Gel Membrane.....	97
Appendix 4: Temperature Calibration for Vacuum Oven .....	99
Appendix 5: Raw Data.....	100

## List of Figures

Figure 1: Schematic of Direct Methanol Fuel Cell (Hackquard, 2005).....	9
Figure 2: Molecular structure of Nafion (Dyck, et al., 2002).....	12
Figure 3: Diffusion Mechanisms in Nafion (Choi, et al., 2005).....	15
Figure 4: Preparation of Carboxylic/Sulfonic Acid Membranes & Performance (Hensley, et al., 2007).....	18
Figure 5: Silca Particle in Nafion: Non-acidic vs. Acidic.....	19
Figure 6: Polarization Curve for S-ZrO <sub>2</sub> /Nafion membranes (Ren, et al., 2006).....	21
Figure 7: Three-Phase Interface in the Catalyst (Hackquard, 2005) and Sites of Interfacial Contact.....	23
Figure 8: Scanning electron micrograph of a catalyst layer with cracks.....	23
Figure 9: Schematic of Direct Methanol Fuel Cell Hardware (Liu, et al., 2005).....	25
Figure 10: Schemcatic of water transportation mechanism in DMFC (Jewett, et al., 2007).....	28
Figure 11: General Polarization Curve for DMFC.....	31
Figure 12: DMFC potential energy loss diagram (Datta, 2008).....	33
Figure 13: General Performance Density and Polarization Curves for DMFC.....	34
Figure 14: Expected Polarization Curves for Membranes with Different Conductivities.....	35
Figure 15: Design of Experiments.....	36
Figure 16: Photo of an E-TEK MEA.....	37
Figure 17: Schematic of Nafion 115 Membrane.....	38
Figure 18: Photo of Bilayer Membrane from Aldrich.....	38
Figure 19: Schematic of Bilayer Membrane - Orientation Recommended by Aldrich.....	39
Figure 20: Schematic of Bilayer Membrane Switched.....	40
Figure 21: Structure of Carboxylic Acid Membrane.....	41
Figure 22: Spraying homde-made catalyst directly onto membrane using a spray gun.....	46
Figure 23: A catalyzed- membrane upon completion of the spray step.....	46
Figure 24: Full Pretreatment Method vs. Post-treatment Method.....	47
Figure 25: Hotpress Machine.....	48
Figure 26: Fuel Cell Assembly.....	49
Figure 27: Schematic of DMFC Test Station.....	51
Figure 28: DMFC Test Station.....	52
Figure 29: Fuel Cell in Test Station.....	52
Figure 30: Photo of a warped carboxylic acid membrane (N982).....	55
Figure 31: Silica-Nafion Membrane Preparation.....	58
Figure 32: Effect of Methanol Feed Concentration on E-TEK MEA, Cathode humidifier at 85°C.....	60
Figure 33: Polarization and Performance Density Curves on Effect of Cell Temperature on E-TEK MEA.....	61
Figure 34: Effect of Cathode Humidifier Conditions.....	62
Figure 35: E-TEK MEA Performance at Base Operating Conditions.....	63
Figure 36: Effect of Methods of Catalyst Application.....	64
Figure 37: Effect of Nafion Loading in Catalyst Area.....	66
Figure 38: Effect of Nafion Loading in Catalyst Slurry for Homemade MEAs.....	68
Figure 39: Effect of Hotpressing Conditions.....	69
Figure 40: Effect of Full Pretreatment vs. Post-treatment on Nafion 115.....	70

Figure 41: E-TEK MEA Performance vs. Optimal Home-made Nafion 115 MEA Performance .....	71
Figure 42: EDX spectrum for a catalyst layer from an E-TEK MEA. ....	72
Figure 43:EDX spectrum for the catalyst layer from an Electrochem electrode.....	72
Figure 44: SEM image of a catalyst layer from an E-TEK MEA: 50x and 500x.....	73
Figure 45: SEM image of a catalyst layer of an MEA hot-pressed with Electrochem GDLs.: 50x and 500x.....	73
Figure 46: Electrochem GDE Membrane Comparison – Polarization Curves .....	75
Figure 47: Electrochem GDE Comparison – Power Density .....	75
Figure 48: Photo of a Carboxylic Acid MEA (Nafion 982) .....	76
Figure 49: Aldrich Silica MEA.....	77
Figure 50: Homemade Bilayer MEA - Fully Pretreated vs. Post-treated .....	78
Figure 51: Membrane Comparison at 3M.....	80
Figure 52: Different Membrane Comparison at 5M MeOH.....	81
Figure 53: Different Membrane Comparison at 7M MeOH.....	82
Figure 54: Performance Drop between 3M and 7M across Various Voltages for Different Membranes.....	83

## List of Tables

Table 1: Catalyst Ink Ingredients ..... 45

# Abstract

Direct methanol fuel cell (DMFC) performance is limited by methanol permeation through Nafion® membranes and interfacial resistances between membrane electrode assembly (MEA) layers. An analysis of several membrane systems showed that Nafion impregnated with Silica nanoparticles and bilayer membranes incorporating two equivalent weights of Nafion exhibited the most favorable balance between protonic conductivity and methanol crossover at high methanol concentrations. In terms of MEA fabrication, spraying catalyst directly on the membrane achieved closest contact between the membrane and catalyst.

# Chapter 1: Introduction

## Advantages and Applications of Direct Methanol Fuel Cells

Fuel cells have received widespread recognition as an alternative energy generation technology that is highly efficient and that operates in a renewable fuel economy. This electrochemically-based energy technology operates with high efficiency as it converts chemical energy directly to electricity (O'Hayre, et al., 2006). Unlike internal combustion engines, fuel cells bypass any thermal step during energy conversion, and therefore, they are not limited by the Carnot efficiency, which only permits approximately 40 percent of the converted chemical energy to be used for work, depending on the temperatures employed.

Mechanically, fuel cells have no moving parts providing high durability, long lifetimes, and silent performance. In addition to being mechanically rigid systems, fuel cells are not consumed during operation like batteries. Instead, they continue to generate electricity as long as fuel is fed to them. Durability in fuel cells is beneficial since long-lasting energy systems are needed for the global push for a sustainable future.

The direct methanol fuel cell (DMFC) is a highly contending energy technology for application in portable micropower systems (Iojoiu, et al., 2005; Farhat, et al., 2006). Methanol is an energy dense fuel with a gravimetric power density that is at least double that of hydrogen (O'Hayre, Cha et al. 2006). Additionally, methanol is much easier and safer to store than compressed hydrogen (Schultz, et al., 2001). This lends to portability since methanol does not require bulky storage capsules. DMFCs can also operate at low temperatures which are needed for devices that are transported by humans. A light-weight and compact DMFC that operates at low temperatures, produces power as long as fuel is supplied, and that is easy to refuel promises

to be a next-generation energy conversion technology with benefits far exceeding conventional batteries. Unlike lithium ion batteries, where improvement is merely incremental, DMFCs are an example of radical innovation in the sense that as long as fuel is provided, it will churn out electricity. In other words, DMFCs offer “unlimited battery life”, which is unheard of in the portable micropower industry.

## How a Direct Methanol Fuel Cell Works

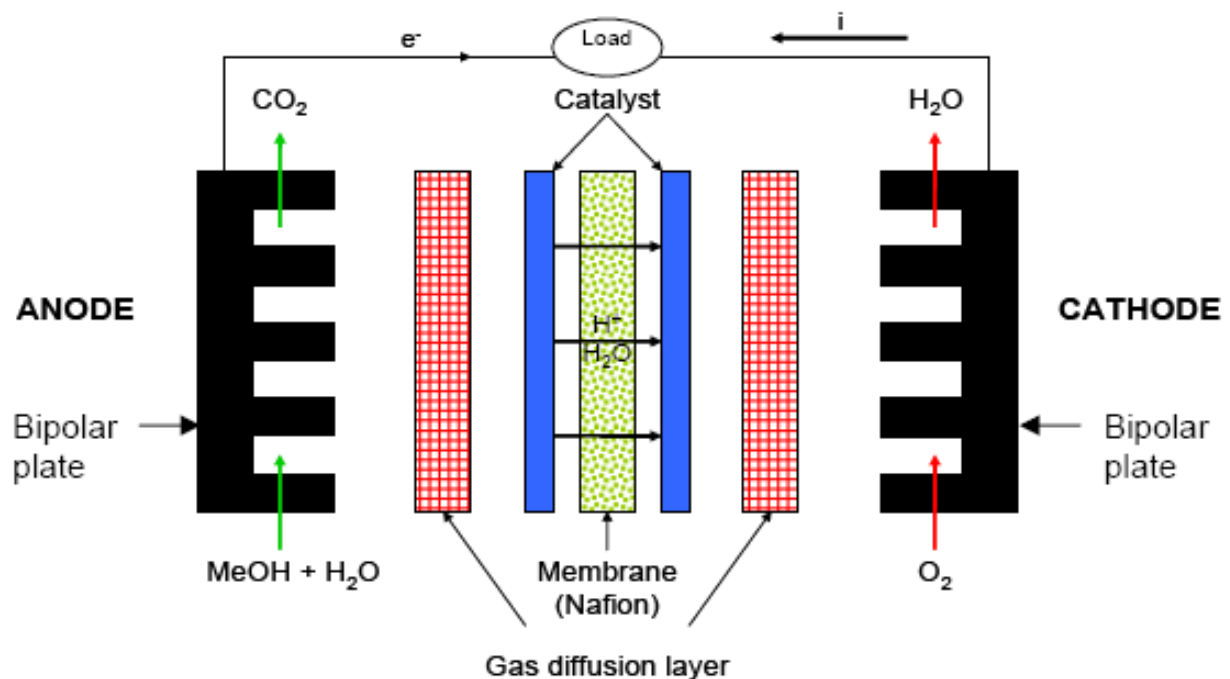
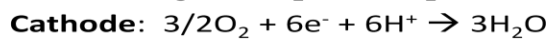
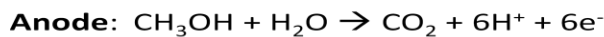


Figure 1: Schematic of Direct Methanol Fuel Cell (Hackquard, 2005)



As shown in Figure 1, DMFCs generate an electrical current by spatially separating a methanol oxidation reaction and an oxygen reduction reaction. Methanol is oxidized by water to form carbon dioxide, protons, and electrons at the anode. These protons and electrons

subsequently react with oxygen to reproduce water at the cathode. Upon separation of the two redox half reactions, the electrons participating in the reaction can be extracted and directed through an external circuit, thus producing an electrical current. A potential load can be applied on the electrical current to produce usable work to power an electrical device. Electrons flow from the anode (oxidation electrode) to the cathode (reduction electrode) so that oxygen will have electrons to react with at the cathodic reaction. However, in order to complete the overall oxidation-reduction reaction, a medium is also required for proton transport. The direct methanol fuel cell utilizes a polymer electrolyte membrane (PEM) as its proton transport medium. The standard material in industry for PEMs is Nafion<sup>®</sup> because it is a superior proton conductor.

The proton exchange membrane (PEM) lies at the core of the cell. Since protons conduct through Nafion at a rate that is at least three orders of magnitude less than the rate at which electrons conduct through carbon cloth for a given potential drop, then the distance over which protons conduct must be minimized. Therefore, the thickness of PEMs is typically between 50 to 250  $\mu\text{m}$ . Catalyst layers are directly adjacent to the PEM on each side. Catalysts are employed to speed up the kinetics of the anodic and cathodic reactions. Moving outwards, the catalyst is in contact with gas diffusion layers (GDLs). GDLs have two primary roles. First, they provide routes by which fuel – aqueous methanol at the anode, and oxygen or air at the cathode – can reach reactive catalytic sites, and by which byproducts of reaction -namely carbon dioxide at the anode and water at the cathode- can diffuse back towards the bipolar plates and the outlet. To serve this function, GDLs are highly porous layers to facilitate fluid flow. Second, GDLs extract electrons from reaction as they are typically made of carbon cloth or carbon fibers, which conduct electricity at around  $200 \text{ Scm}^{-1}$ . The PEM, the catalyst layers, and the GDLs make up

the heart of the fuel cell called the Membrane Electrode Assembly (MEA). The catalyst layers and GDLs taken together make up the electrodes.

Bipolar plates are current collectors that provide a conduit for electrons to flow through an external circuit. The anodic plate harnesses the electrons received from the anodic reaction, and directs these electrons to the cathodic plate through a circuit. The cathodic plate receives electrons from the circuit, and conducts electrons through the GDL to the loci of oxygen reduction.

## **Problems with Direct Methanol Fuel Cells**

DMFC performance is limited by three primary problems: slow anode oxidation due to carbon monoxide poisoning of the catalyst, high methanol permeation from the anode to the cathode, obstruction to fuel flow at the anode by carbon dioxide formation (Schultz, et al., 2001).

Carbon monoxide is an extremely stable intermediate species in the methanol oxidation reaction at the anode. Therefore, carbon monoxide poisons the anode catalyst by clinging to surface sites thus reducing the overall amount of active catalytic reaction sites available for methanol oxidation. For high reaction density at the anode, carbon monoxide must be removed from catalytic sites. Although, platinum is typically the catalyst used for methanol oxidation, ruthenium is often added to the anode catalyst since it forms powerful hydroxyl radicals with water that oxidize carbon monoxide to free up the catalytic sites. Additionally, high operating temperature reduces carbon monoxide poisoning (Lobato, et al., 2006).

Nafion is limited by its poor methanol permeation and water uptake characteristics (Schultz, et al., 2001). Water uptake compromises the mechanical strength of the membrane due to the stress of unmanageable swelling and contraction and also fosters a domain for methanol transport. Methanol permeates through Nafion membranes by means of vehicular diffusion

through hydrated ionic channels (Schultz, et al., 2001). The detriment of this fuel permeation culminates in the oxidation of methanol at the cathode causing reduction of electrode potential (Schultz, et al., 2001), and consequently, reduced fuel cell power density (Walker, et al., 1999). To minimize crossover, very dilute feed is used at the anode, specifically 1 M or 3 wt % methanol. This reduces the energy density of DMFCs therefore one of the goals of this research was to investigate designs in which higher methanol concentrations could be employed.

## Nafion<sup>®</sup> Membrane

The industry standard for PEMs is Nafion<sup>®</sup>, a supreme ion conductor developed and manufactured by Dupont<sup>®</sup>. Its perfluorinated backbone provides significant mechanical strength and hydrophobicity. Pendent to the tetrafluoroethylene (Teflon) backbone are perfluorovinyl ether chains that end with a sulfonic acid functional group (Heitner-Wirguin, 1996; Mauritz, et al., 2004). The sulfonic acid group is an exceptional ion-conducting moiety because its conjugate base is highly resonance stabilized. If R-SO<sub>3</sub>H loses a proton, H<sup>+</sup>, the negative charge is distributed over three oxygen atoms providing high stability. Figure 2 shows the molecular structure of Nafion.

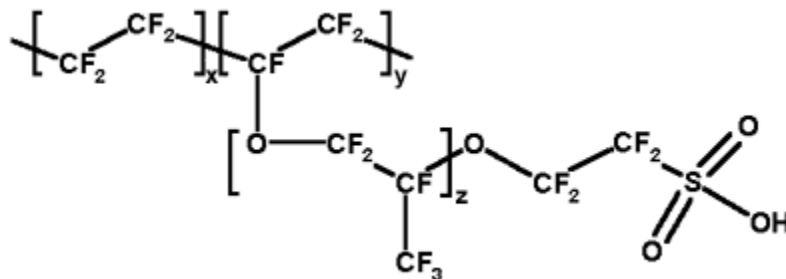


Figure 2: Molecular structure of Nafion (Dyck, et al., 2002)

Since sulfonic acid sites in Nafion are highly acidic they contribute hydrophilicity to an otherwise hydrophobic organic macromolecule, thus, promoting the formation of ion clusters in Nafion. When coupled with sufficient water uptake, the proton-conducting ion clusters expand to become the dominant domain. In fact, hydration initiates the formation of continuous ionic channels that give protons direct access through the Nafion system (Yang, et al., 2005). Unfortunately, in DMFCs, these ionic channels are the same channels through which methanol diffuses from the anode to the cathode causing unwanted methanol crossover and the concomitant loss of performance as well as fuel

An ideal equivalent weight for Nafion in fuel cells is required since too high a concentration of hydrophilic sulfonic acid groups in Nafion compromises the polymer's mechanical strength (Hickner, et al., 2004). A highly hydrophilic membrane can be overly sensitive to water. Long-term durability of membrane polymers is adversely affected by the large quantities of water adsorbed and exuded in start-up and shutdown sequences during fuel cell operation. Repetitious large-scale swelling and contraction can crack the catalyst layers, and in extreme cases, tear the membrane and render it inoperable. Furthermore, excessive water uptake shapes a polyelectrolyte morphology that is less conducive to proton transport than less hydrated morphologies because of dilution of proton moiety. For example, Rajendran R. G. (Rajendran, 2005) reports that an equivalent weight (EW) of 800-1100 for Nafion promotes highest ionic conductivity. Fuel cell reaction kinetics also suffer due to high water transport as water accumulates at the cathode and decreases the driving force of the overall reaction according to LeChatelier's Principle. Excessive water uptake also causes the membrane to become spongy and allow methanol to diffuse through by osmotic drag. Therefore, a desirable equivalent weight must demonstrate a favorable balance between protonic conductivity and water uptake (Hickner, et al., 2004).

## Literature Review

Recent academic literature was surveyed to find applicable work on membrane electrode assemblies, proton exchange membranes, and direct methanol fuel cells. Topics of interest included membrane modification to reduce methanol crossover, membrane electrode assembly fabrication techniques, and passive for DMFCs.

### *Membrane Modification*

Methanol crossover occurs in PEMs of DMFCs due to the concentration gradient of water and methanol across the membrane. Since methanol is fed at the anode, the resulting concentration gradient drives mass transfer from the anode side to the cathode side. This leads to an electrode overpotential since methanol that has permeated to the cathode side will oxidize to liberate electrons at the electrode where reduction and absorption of electrons should occur instead. A lower potential drop between the electrodes reduces the attainable power density of the fuel cell.

Reducing methanol crossover over the membrane involves reducing proton conductivity as well. This is because the mechanism of methanol crossover through the membrane is the same as the mechanism of proton transfer. It is very likely that due to the dipole-dipole attraction, the  $\text{OH}^-$  present in methanol is attracted to the  $\text{H}_3\text{O}^+$  and so methanol is transferred through the membrane to the cathode side along with protons ( $\text{H}^+$ ) and water molecules ( $\text{H}_2\text{O}$ ). So modifications to the membrane material to reduce methanol crossover would reduce conductivity as well. A balance has to be found between the two when evaluating techniques for methanol crossover reduction.

Proton transport in the membrane is thought to occur with a combination of three mechanisms (Choi, et al., 2005) – surface diffusion, Grotthuss diffusion and vehicular diffusion.

The three mechanisms are illustrated in Figure 3 below:

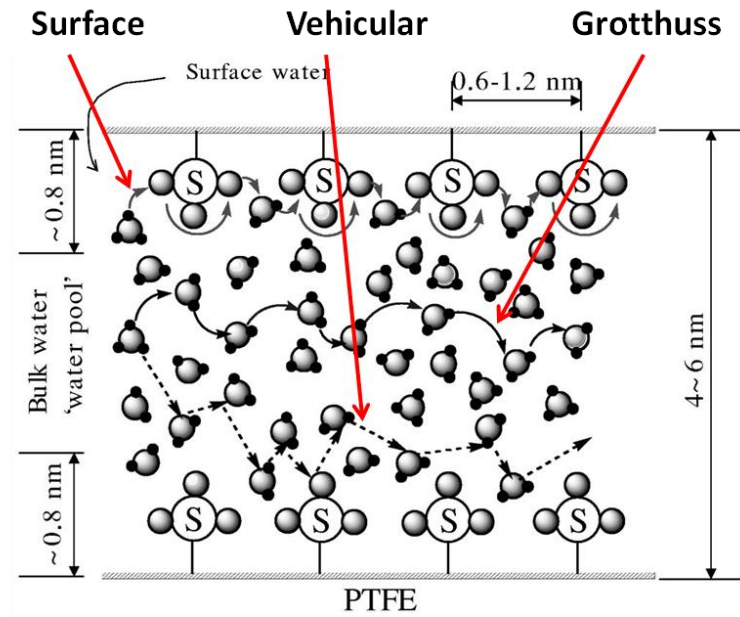


Figure 3: Diffusion Mechanisms in Nafion (Choi, et al., 2005)

Both protons and methanol travel through the same ionic channels in the membrane. The ionic channels in the membrane can be divided into two regions: the surface region and the bulk water region. The surface region is populated with sulfonic acid sites at the wall of the channels and water. The bulk water region is at the center of ionic channels and makes up the majority of the cross-sectional area of the channel.

Surface diffusion involves the hopping of protons between water molecules and sulfonate groups. It occurs near the sulfonic acid sites, at the surface, and is the slowest of the diffusion mechanisms due to the high Coulombic interaction at the surface (Jalani, 2006). Both vehicular diffusion and Grotthuss diffusion take place in the bulk water region and are relatively rapid. Vehicular diffusion is *en masse* migration of proton carriers,  $\text{H}_3\text{O}^+$  ions through the membrane.

Grotthuss diffusion accounts for about 80% of the proton transport in the bulk phase. Protons hop from one water molecule to another through the network of hydrogen bonds across the membrane.

Effective membranes must exhibit a favorable balance between protonic conductivity and methanol crossover. In order to tune the transport properties of membranes, the diffusion mechanisms for protons and methanol must be understood. Protons are transported through ionomer membranes such as Nafion by means of surface, vehicular, and Grotthuss diffusion. However, methanol only migrates through Nafion *en masse*. Therefore, this research hypothesized that altering the structure and properties of ionic channels in Nafion would change the protonic conductivity and methanol permeability of the membrane to different extents.

For example, it is desirable to decrease the level of vehicular diffusion to limit methanol crossover while maintaining the rates of Grotius and surface diffusion to prevent a sizeable decrease in proton conduction. One of the ways to accomplish this could be to decrease water uptake of the membrane. Reducing the water permeability of the membrane impedes vehicular diffusion as less proton carriers are able to migrate through the membrane. Grotthuss diffusion would be affected as well, but to a lesser extent because it relies less on the amount of water in the membrane. As long as there is some water in the membrane protons will be able to hop from one water molecule to another. So when looking at techniques to reduce methanol crossover through the membrane, it is important to focus on increasing the contribution of Grotthuss diffusion versus vehicular diffusion.

It is hypothesized that the following points are important to impede proton transport (and hence methanol crossover) across Nafion membranes:

- Increasing thickness of membrane

- Decreasing acidity of the membrane
- Incorporating fillers and dopants into the membrane

In simplified terms, the flux of methanol across the membrane can be described as:

$$J_{MeOH} = -D_{MeOH} \frac{\partial C}{\partial z}$$

Increasing the thickness of the membrane would reduce the concentration gradient of water and methanol and so less methanol would crossover to the cathode.

Acid groups are negatively charged and therefore attract protons and encourage proton transport. Decreasing the acidity of the membrane would reduce the concentration of protons available for transport. Further it would reduce hydrophilicity of the membrane and hence water uptake. So reducing the number and strength of acid groups would impede proton conductivity and methanol crossover. Decreasing the acidity of Nafion membranes can be done in the following ways:

- Using a membrane with higher equivalent weight
- Substituting some of the sulfonic acid groups for carboxylic acid groups as carboxylic acid is less acidic

In a report by Hensley et al. (Hensley, et al., 2007), using sulfonyl fluoride precursor films (1100 EW), carboxylic/sulfonic acid Nafion membranes were prepared. The schematic in Figure 4 below summarizes the preparation. Contact with hydrazine reduces sulfonyl fluoride to sulfonic acid. Oxidation desulfonates the polymer, leaving carboxylic acid at the end of the side chains. This is followed by annealing and cleaning.

Figure 4 also shows proton conductivities obtained for various carboxylate contents. There are a few trends visible from this graph. As the carboxylate content increases proton conductivity decreases proportionally, but water permeability decreases exponentially. This

would mean that overall methanol crossover may be reduced more than proton conductivity, which is desirable. Decreasing water permeability also implies that the contribution of Grotthuss diffusion increases as compared to vehicular diffusion in the bulk phase.

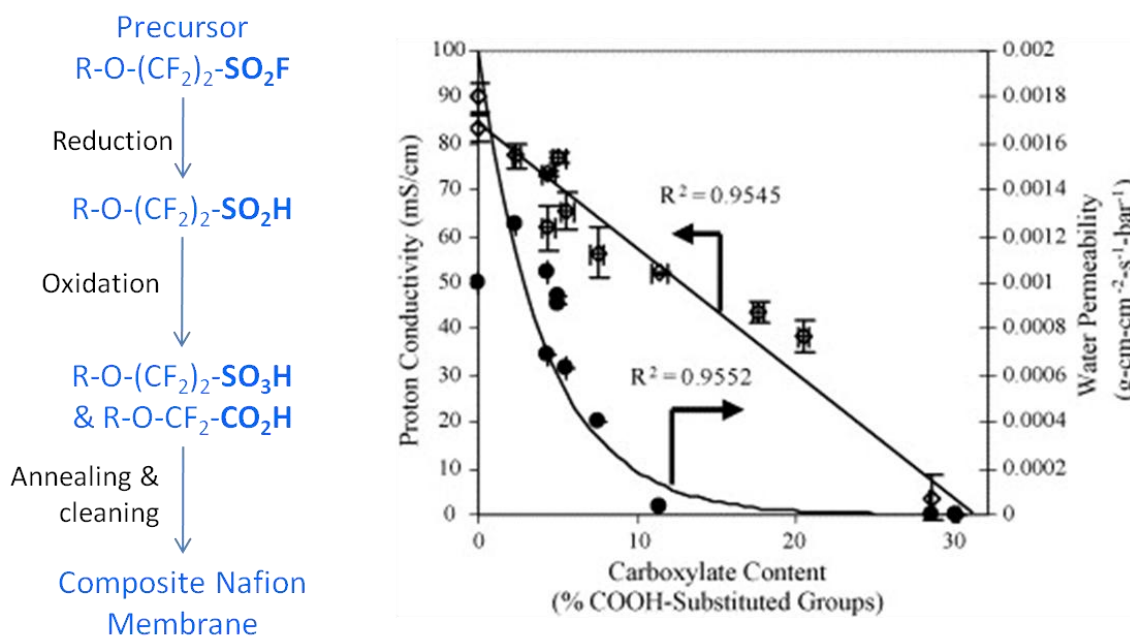


Figure 4: Preparation of Carboxylic/Sulfonic Acid Membranes & Performance (Hensley, et al., 2007)

The best balance between proton conductivity and low water permeability were achieved when the carboxylate content was 10 – 25%. The carboxylate content should not exceed 20% as SAXS data showed that the morphology of the membrane is significantly altered beyond it (Hensley, et al., 2007).

Generally with carboxylic acid membranes, there is no preferential permeation of water or methanol; both decrease with increasing carboxylate content. For unmodified Nafion membranes, and for Nafion membranes with low carboxylate contents the total flux of methanol and water increases with increasing temperature and feed methanol concentration. Therefore it

was determined that carboxylic acid membranes seem promising and are worth investigating for DMFC application.

Some examples of dopants incorporated in the membrane include zirconia, silica, titania, zeolites and montmorillonite. They are incorporated into membrane pores by a variety of methods. The effect of incorporating inorganic dopants in the membrane depends on the nature of the dopant in question. If the dopant is not acidic it simply acts as a barrier to both proton and methanol flow as shown schematically on the left side of Figure 5 below. The dopant in this case is non-conducting and acts as a barrier to both vehicular diffusion and Grotthuss diffusion. It obstructs the former by preventing the vehicular transport of hydronium ions. And it obstructs the latter by disturbing the hydrogen bond network. This should be especially effective in blocking methanol flow as methanol molecules are much larger than protons, but it will also affect proton conductivity adversely.

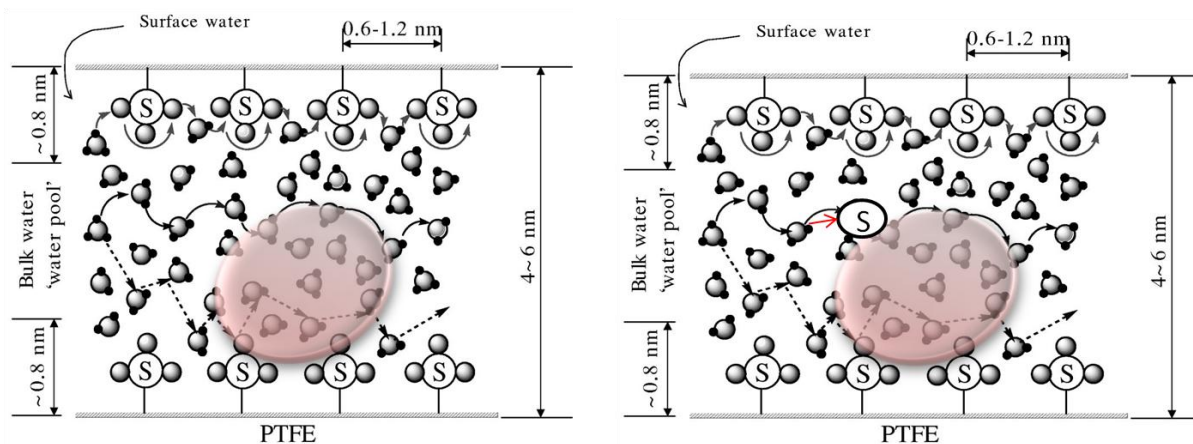


**Figure 5: Silica Particle in Nafion: Non-acidic vs. Acidic**

The image on the right side shows a dopant with a sulfated (acidic) surface. The particle has an  $\text{SO}_4^{2-}$  group attached that attracts protons and continues the hydrogen bond network (shown by red arrow). This particle will still block vehicular diffusion but it will only slightly reduce Grotthuss diffusion, if at all. Depending on the acidity of the particles, it might

even increase the proton exchange sites and so increase Grotthuss diffusion and overall conductivity.

Sulfated dopants, such as sulfated zirconia and sulfated silica are especially popular in current research (Jalani, 2006). Extensive research has been done with these inorganic particles in PEMFCs. Incorporation of sulfated zirconia particles ( $\text{ZrO}_2/\text{SO}_4^{2-}$ ) into Nafion via the sol-gel method has shown increased water uptake and proton conductivity in hydrogen/oxygen fuel cells due to the additional acid sites (Choi, et al., 2005). However, increased water uptake is undesirable in DMFCs due to methanol crossover. The acidity of the membrane should be such that overall methanol crossover is reduced while maintaining conductivity.

The inorganic content needed for the right balance varies. It is reported to be between 5 – 12% in literature (Jiang, et al., 2005) for DMFCs in general. Beyond 12% the morphology of the membrane is altered significantly and proton conductivity is severely compromised. Ladewig et al. tested  $\text{SiO}_2/\text{SO}_3\text{H}$  Nafion 117 membranes in hydrogen/oxygen fuel cells. Membranes with 16.7 wt % inorganic content showed an 89% reduction in methanol permeability at 50°C and 68% reduction in proton conductivity (Ladewig, et al., 2006). A 68% reduction in conductivity is too much, however, and is undesirable.

Ren et al. reported fairly good results with S- $\text{ZrO}_2$ /Nafion membranes in DMFCs. Figure 6 shows the polarization curve.

So sulfated forms of silica doped into Nafion membranes have potential advantages for DMFCs over plain Nafion membranes, as do membranes with up to 20% carboxylic acid content.

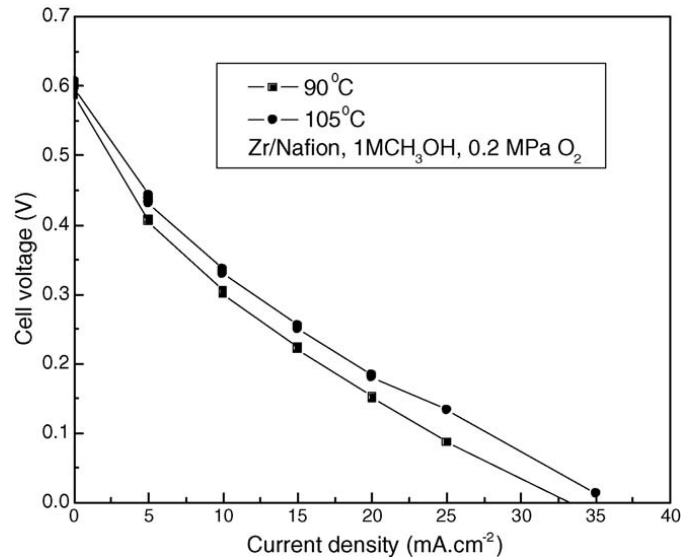


Figure 6: Polarization Curve for S-ZrO<sub>2</sub>/Nafion membranes (Ren, et al., 2006)

### ***Membrane Electrode Assembly Fabrication***

Several factors in the membrane electrode assembly strongly affect fuel cell performance. This research sought to increase the quality of MEAs by tweaking specific properties so that each specific subsection of the MEA would be conducive to improved fuel cell performance. Wilson and Gottesfeld have stressed the importance for close catalyst contact with the ionomer (Wilson, et al., 1992). Since the conductivity of protons through ionomers such as Nafion is typically several orders of magnitude less than the conductivity of electrons in the carbon cloth or carbon fiber material that makes up gas diffusion layers, then it is essential to provide good contact between the catalyst and the membrane to encourage proton transport between the spatially separated electrodes. In terms of charge transport, protonic transport limit reaction and fuel cell performance much more than electron transport does. Wilson and Gottesfeld used impedance analysis to show that “direct application [of catalyst on membranes] apparently improves the interfacial continuity between the ionomer in the membrane and the ionomer in the

catalyst layers” (Wilson, et al., 1992). Catalyzing membranes instead of GDLs facilitates proton transport and increases the overall level of reaction and reduces the resistance of the assembly.

Although, Wilson and Gottesfeld used the decal method to transfer catalyst onto the membrane (Wilson, et al., 1992), this research applied catalyst via the direct spray method since this method even further reduced the resistance of the electrodes (Sun, et al., 2008). This research hypothesized that the direct spray method would achieve highly uniform catalyst layers with high catalyst dispersion (Song, et al., 2005). Since interfacial contact and adhesion between the catalyst and the PEM are paramount for minimizing Ohmic losses (Han, et al., 2007), then steps such as varying catalyst deposition, changing Nafion loading in catalyst slurries, and altering hot-pressing protocol were taken to insure close interfacial contact and high levels of three-phase interface within the catalyst.

Another interesting method to facilitate adhesion between Nafion and catalyst is to modify the surface of Nafion through roughening and gold-sputtering (Han, et al., 2007). SEM imaging of catalyst-membrane interfaces have shown that roughening and gold-sputtering vastly increase the amount of intertwining of Nafion within the catalyst and the amount of interfacial contact area between the two layers (Han, et al., 2007).

The three-phase interface includes contact among catalyst, carbon particles or fibers, and Nafion or ionomers. Electrical current in fuel cells is generated by spatially separating two redox half-reactions, methanol oxidation and oxygen reduction. Therefore, the catalytic reaction sites must be in contact with the medium for electron transport (carbon cloth) so that electrical current can be extracted. Additionally, reaction sites must be in contact with Nafion, the medium for proton transport, so that the overall redox reaction can be completed. In the research of this project, the issue of the three-phase interface was investigated by varying Nafion loading in

catalyst inks. Figure 7 below shows a schematic of a 3-phase interface and sites where interfacial contact is important.

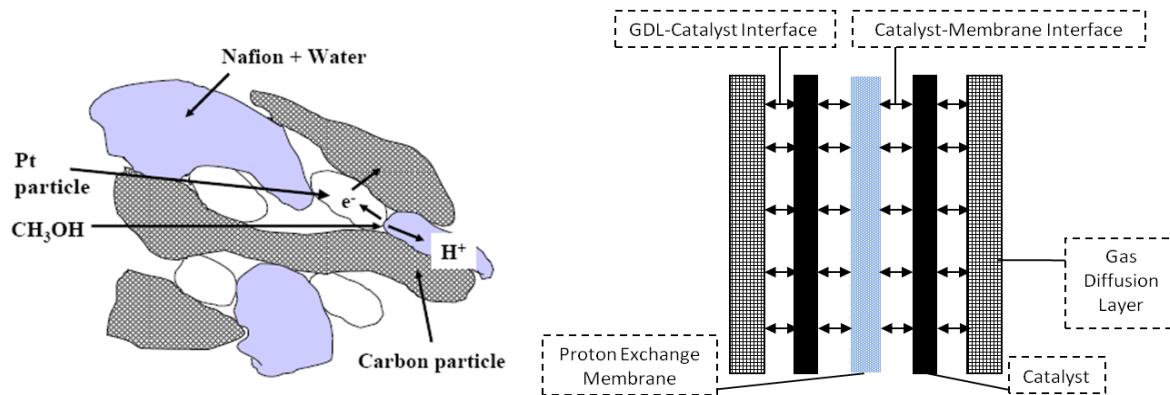


**Figure 7: Three-Phase Interface in the Catalyst (Hackquard, 2005) and Sites of Interfacial Contact**

In addition to maximizing interfacial contact and three-phase interface, it is important to inhibit cracking in the catalyst layer. Cracks are conduits for methanol to diffuse through the anodic layer without significant reaction to directly access the ionomer membrane, thus, increasing methanol crossover. This research sought to minimize cracking in the catalyst layer by utilizing the minimum applied pressure in the hot-pressing step that still provided sufficient interfacial contact between the GDL and the membrane to reduce losses due to resistance. Figure 8 below shows an SEM image of a cracked catalyst layer. The integrity of the catalyst layer is compromised by cracks which reduce the amount of reaction sites and give methanol direct access to the membrane at the anode causing increased methanol crossover.

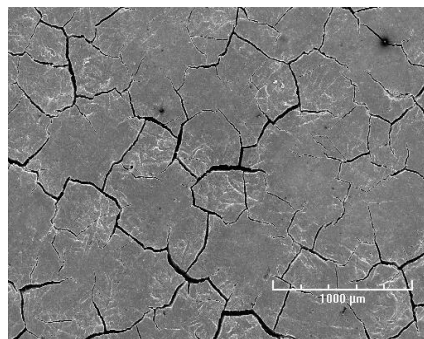


**Figure 8: Scanning electron micrograph of a catalyst layer with cracks.**

J. Zhang et al. studied hot-pressing protocol thoroughly by varying parameters such as temperature, pressure, and time (Zhang, et al., 2007). J. Zhang et al. found that overly high pressures and hot-pressing times compromised the porosity and internal structure of GDLs, and limiting the conduction of electrons. It is ideal to operate at a hot-pressing temperature of 135°C since this is slightly above the glass transition temperature of Nafion (Zhang, et al., 2007). This allows Nafion to become slightly gel-like during hot-pressing and intertwine with the catalyst.

### ***Passive Direct Methanol Fuel Cell***

One of the potential advantages of DMFCs is the high energy density of methanol, which is needed for portable applications. However, conventional DMFCs have external devices such as a humidifier, compressor, cooling system, heating system, and fuel pump that make them difficult to be used as portable devices. Furthermore, these auxiliary components decrease the achievable potential energy and power density due to parasitic power losses (Liu, et al., 2005). Therefore, passive, air-breathing DMFCs that operate without the use of energy sapping peripheral devices are desirable for powering portable appliances. A passive DMFC does all the functions of the above-mentioned external components such as the supply of methanol fuel and oxygen as well as the removal of products and heat, which minimizes the parasitic power losses. A schematic of passive DMFC hardware is shown in Figure 9.

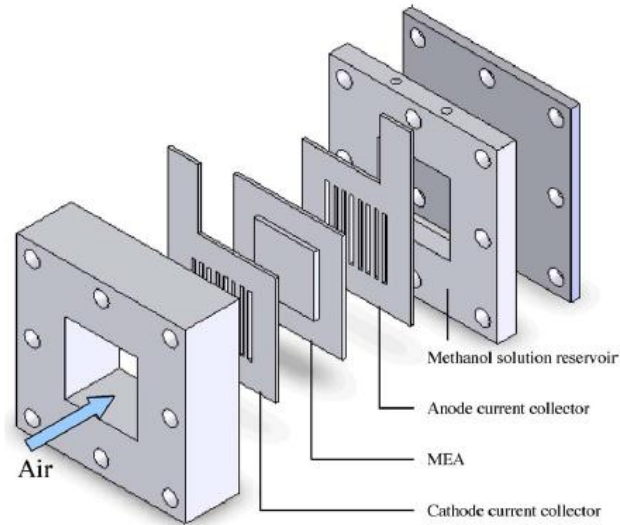


**Figure 9: Schematic of Direct Methanol Fuel Cell Hardware (Liu, et al., 2005)**

Moreover, vapor methanol feed is used for passive DMFC so that it can achieve the most potential energy and power density. A study by Kim et al. showed that vapor-feed passive DMFCs not only had a higher performance and fuel efficiency but also longer lifespan than liquid-feed passive DMFCs (Chen, et al., 2007).

### Passive DMFCs vs. Active DMFCs

Since the designs of active and passive DMFCs are quite different, the optimal design parameters used in active DMFCs are not appropriate for passive DMFCs. For example, a study by Liu et al. showed that the performance of passive DMFC increased with increase in methanol concentration; whereas for active DMFC, increase in concentration does not increase the performance (Liu, et al., 2005). This is due to the fact that both active and passive DMFCs are affected by methanol crossover. The relationship between methanol crossover and concentration for DMFCs is that as the methanol concentration increases, the methanol crossover increases, which decreases performance. However, the performance of the passive DMFC increased with increasing methanol concentration due to the increase in the cell temperature. The increase in the

cell temperature was a result of the energy released from the exothermic reaction between permeated methanol and oxygen on the cathode side. Since the methanol oxidation reaction on the anode side is a slow electrochemical kinetic reaction, the energy produced from methanol crossover at the cathode provided some energy for the activation of methanol oxidation. The energy produced by the methanol crossover affects the performance of the passive DMFC, which is operated at room temperature due to lack of an external heating device. It has no influence on the performance for active DMFCs since it is already heated to an optimal cell temperature using a heater. As a result, the optimal methanol concentration for active DMFC is 1M; while for passive DMFC it is 5M (Liu, et al., 2005) . Another reason for this concentration difference is that the liquid phase methanol concentration in the anode determines the performance. A vapor phase in equilibrium with a liquid methanol-water structure would have a higher concentration as methanol is the more volatile species.

### Issues in Passive DMFCs

An important factor in the performance of passive DMFCs is oxygen transportation. DMFCs are usually in an oxygen-starved condition because they have no external means of air movement at the cathode side since they rely on the diffusion of ambient air for oxygen supply. In passive DMFCs, there is an increase in the cathode loss due to mass transfer resistance which is caused by mass transport in GDL. The mass transport in the GDL is due to the oxygen transportation from the ambient air to the cathode catalyst and the water transportation from the cathode to ambient air. The water transportation to the ambient air from the cathode is due to water concentration gradient. As a result, the increase in the cathode resistance decreases the performance of the cell (Chen, et al., 2007). In order to decrease the cathode resistance, Chen et al., enhanced the oxygen transport on the cathode side by using a porous metal foam current

collector rather than the conventional or perforated -plate current collector. The porous current collector enhanced the oxygen transportation to the cathode due to an increase in the region of transport area of the oxygen by the pores. The enhancement of oxygen transportation reduced the cathode resistance, which increased the performance. However, Chen et al. found that larger pores did not create good contact between the GDL and the current collector; the larger the pore size, the higher was the internal resistance (Chen, et al., 2007).

Furthermore, the heat generated in the cell is mostly lost by the current collector. In order to reduce heat loss it is desirable that the material for current collectors have low effective thermal conductivity. Since the metal foam had a low effective thermal conductivity, less heat was lost to the environment; therefore the cell temperature was not decreased. This has a favorable effect on the kinetics of electrochemical reactions (Chen, et al., 2007).

Another important parameter to consider for passive DMFCs is water transportation. In general, the proton exchange membrane must have enough hydration to allow proton conductivity. Previous studies illustrated that a liquid-feed passive DMFC operates effectively at high methanol concentrations since the only mechanism of methanol transport from the reservoir to the anode catalyst is through diffusion. The lack of water in the methanol feed creates a water management issue for passive DMFCs due to the different water transportation mechanisms. Figure 10 is a schematic of the different water transportation mechanisms in the DMFC membrane.

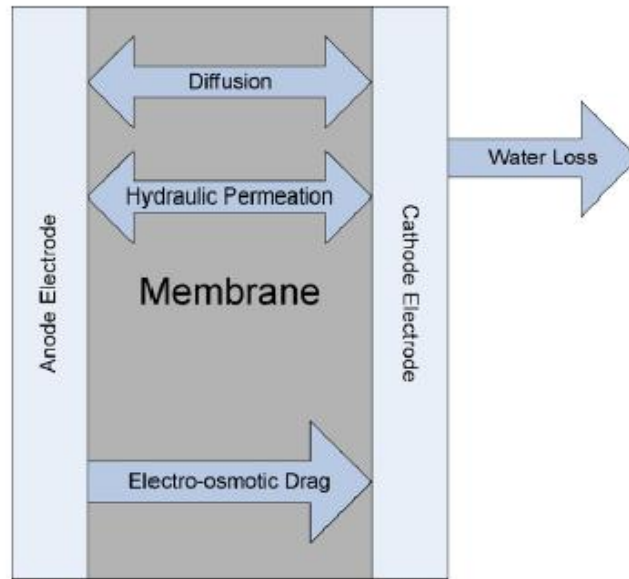


**Figure 10: Schematic of water transportation mechanism in DMFC (Jewett, et al., 2007)**

There are three main water transportation mechanisms in the PEM membrane: Diffusion, Electro-osmotic Drag, and Hydraulic Permeation. The diffusion mechanism is due to species concentration gradients, and this diffusion is the main reason for methanol crossover. The transport of water increased as methanol concentration increased due to evaporation on the cathode side. The electro-osmotic drag is due to proton conductivity across the membrane, which also increases with methanol concentration because more fuel is being oxidized at the anode. Finally, the hydraulic permeation mechanism is caused by pressure gradients in the cathode side. This is caused because the rate of water production from the oxygen reduction reaction is greater than the rate of water evaporation. Since passive DMFCs are exposed to ambient air there is evaporation of water from the cathode side to the ambient air. Therefore the pressure gradient will drive the water from cathode to anode (Jewett, et al., 2007).

In order to retain sufficient water in the membrane, the hydraulic permeation mechanism is crucial because it creates a negative concentration gradient across the membrane.

Studies conducted by Peled et al. used a hydrophilic liquid-water leak-proof layer before and after the cathode current collector to reduce water evaporation. Jewett et al. studied the effect of adding thicker hydrophobic gas diffusion layers before the current collector to increase the hydraulic permeation mechanism (Jewett, et al., 2007).

## **Chapter 2: Goals, Hypothesis, & Plan of Work**

This chapter discusses the objective goals of our research, and the theory behind our hypotheses on how to improve DMFC performance. In particular, energy losses are explained in terms of the effect of kinetics, conduction, and transport in the shape of the voltage-current curve. Also included is a detailed description of the membranes analyzed in this study.

### ***Goals***

The objectives of this Major Qualifying Project (MQP) were to optimize membrane electrode assembly performance by optimizing MEA fabrication techniques and by testing alternate proton exchange membranes with different properties. The focus was on decreasing methanol crossover without impacting proton conductivity too adversely. Both membrane properties and MEA fabrication play an important role in DMFC performance.

In order to evaluate fuel cell and membrane performance, some background is necessary on DMFC performance.

### ***DMFC Performance***

The polarization curve, also known as voltage-current density (V-I) curve, is commonly used to evaluate fuel cell performance. Figure 11 is a representation of a typical polarization curve for Direct Methanol Fuel Cells.

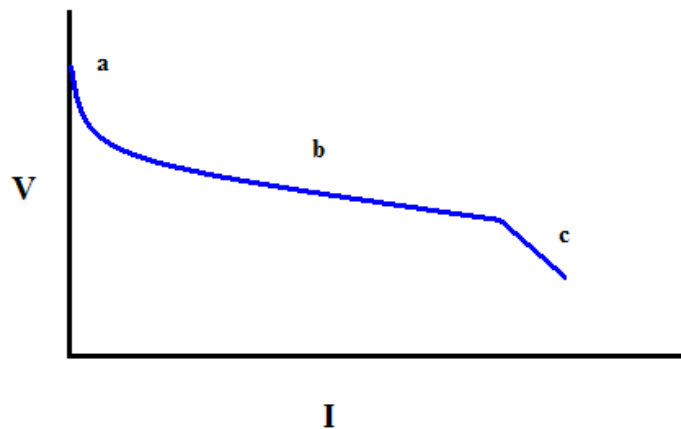


**Figure 11: General Polarization Curve for DMFC**

The x-axis plots the current density ( $\text{mA}/\text{cm}^2$ ) and the y-axis plots the voltage (V). The y-intercept on the graph is the so-called Open Circuit Potential (OCP), which is typically less than the ideal voltage obtainable from a specific fuel cell system as determined by thermodynamics. The thermodynamic voltage for DMFCs is 1.12 V. However, DMFCs operate below the ideal thermodynamically-determined voltage because of three primary forms of energy losses that dominate at different current densities. The three forms of energy losses correspond to distinct regions of the V-I curve.

At low current densities, slow anodic and cathodic reactions result in activation losses and further methanol crossover causes an electrode overpotential that results in a voltage drop. Activation losses dominate in region *a* of Figure 11, which is termed the *activation region*. Oxidation of methanol at the anode is slowed by the accumulation of carbon monoxide on the catalyst surface. Carbon monoxide is a stable reaction intermediate in the anodic reaction and occupies the active catalytic surface sites of platinum, and therefore reduces the overall amount of reaction. To combat carbon monoxide poisoning, ruthenium is often added to the anode catalyst, since it generates hydroxyl radicals that oxidize carbon monoxide to free up catalyst sites to speed up reaction.

The methanol crossover is another factor influencing the energy loss for the activation region. The fuel consumption is proportional to the current density. Since region *a* is in the low current density area, the fuel consumption by the electrode is low so that the methanol crossover is significant. Since proton flux is insignificant, Proton Exchange Membrane (PEM) losses may be negligible. Therefore, the only loss as affecting Region *a* are the losses at the anode and the kinetic losses at the cathode, which are strongly affected by the methanol flux. The combination of these two factors determines the energy losses in region *a*.

Region *b* in Figure 11 represents the *Ohmic region* where performance losses are primarily due to limitations on protonic and electronic conduction (O'Hayre, et al., 2006). The V-I curve in this region is characteristically linear with a slope that corresponds to the overall resistance of the MEA. The slope of the Ohmic region corresponds to the overall resistance of the MEA. This region can be modeled by Ohm's Law:  $V = IR$ , where  $V$  is the voltage (dependent variable, y-axis),  $I$  is the current density (independent variable, x-axis), and  $R$  is the resistance (slope).

At high current densities, energy losses due to mass transfer inefficiencies dominate. Region *c* in Figure 11 is called the *transport region* since losses are caused by insufficient transport of reactants to the catalytic reaction sites and insufficient removal of products, carbon dioxide and water.

These losses are expressed in the following equation:

$$V = V_0 - \eta_A + \eta_C - \eta_{EL} - \eta_I \quad (\text{Thampan, et al., 2006})$$

where  $V$  = ideal voltage of DMFC

$V_0$  = actual voltage of DMFC

$\eta_A$  = anode loss or anode overpotential

$\eta_C$  = cathode loss or cathode overpotential

$\eta_{EL}$  = Ohmic loss

$\eta_I$  = interface loss.

These losses are also shown schematically in Figure 12 for the hydrogen/oxygen fuel cell, in which cathode losses are dominant.

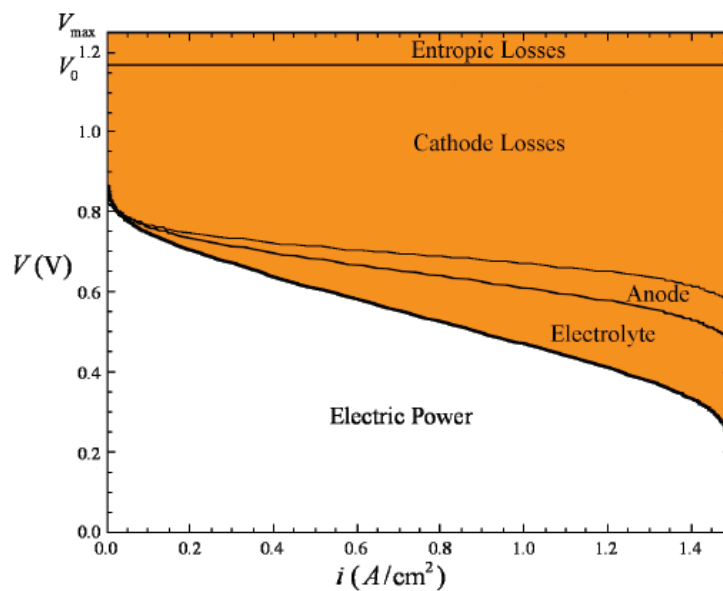
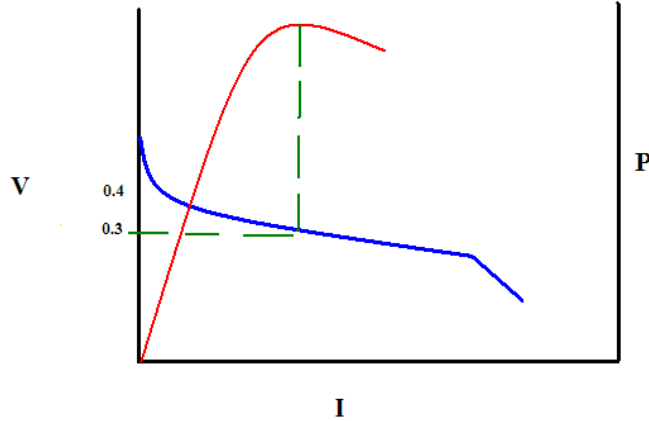


Figure 12: DMFC potential energy loss diagram (Datta, 2008)

To gauge fuel cell performance, polarization curves are used to compare competing systems. A specific region of interest lies between 0.3 V and 0.4 V since this region corresponds to more efficient use of fuel. These voltages correspond to power densities that are typically less than and to the left of the maximum (peak) on the power density curve. Figure 13 presents a graphical representation of this concept.



**Figure 13: General Performance Density and Polarization Curves for DMFC**

The efficiency of DMFC at any voltage is determined by following equation:

$$E = \frac{V}{V_o}$$

In the equation above E is the efficiency, V is the operating voltage, and  $V_o$  is the thermodynamic potential, i.e. 1.12 V. This understanding of the characteristic shape of the current density/voltage curve with the respective potential energy losses of the DMFCs provides the necessary background information to develop a hypothesis for this experiment. The overall goal for this experiment is to optimize the performance of the DMFC by reducing methanol crossover and by improved interfacial contact via improved fabrication. In order to reduce methanol crossover, the diffusion coefficient for methanol is to be reduced, hence the conductivity of protons will be decreased as well, since the diffusion coefficient for methanol is proportional to the proton conductivity. Figure 14 shows a graphical representation of our hypothesis with respect to altering properties of the membrane. If Membrane B is considered to be the base case (Nafion 115 membrane) Membrane A is a lower conducting membrane for which the OCP is higher and the slope in the Ohmic region is steeper. Membrane C on the other hand is a higher conducting membrane. Although the OCP is lower, it performs well in the high current density region and the slope is flatter.

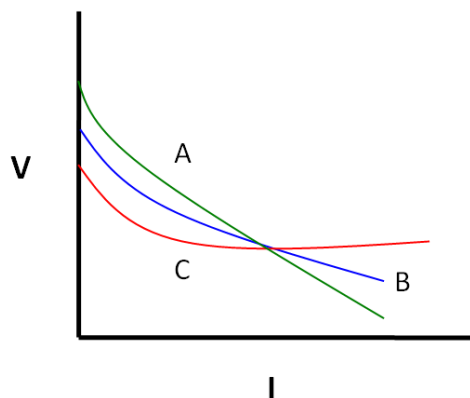


**Figure 14: Expected Polarization Curves for Membranes with Different Conductivities**

It is hypothesized that reduction in the diffusion coefficient of methanol will improve the performance in the low current density region since the energy losses associated with this region is due to methanol crossover and the resulting overpotential at the cathode. However, reduction in diffusion coefficient also decreases proton conductivity which will decrease the performance in the high current density region, since the energy losses associated with this region are largely due to PEM losses. Furthermore, if the proton conductivity is increased, the diffusion coefficient will increase and the performance in the low current density region will decrease due to increased cathode overpotential. But it will increase in the high current density region.

### ***Design of Experiments***

First a baseline for performance was established by testing commercial MEAs for DMFCs, purchased from E-TEK. Then MEAs based on Nafion 115 membranes were fabricated in the lab. Several parameters are involved in MEA fabrication; these were varied one at a time to determine optimal MEA fabrication conditions for Nafion membranes. These fabrication conditions were then utilized for the other membranes, with a few necessary modifications.

Besides the E-TEK MEA and Nafion 115 membranes, 5 other membranes were thus investigated: a bilayer membrane, home-made silica membranes, an Aldrich Silica membrane,

and a DuPont Carboxylic Acid membrane. A description of each of these membranes is provided below. The schematic in Figure 15 below shows the experimental plan followed.

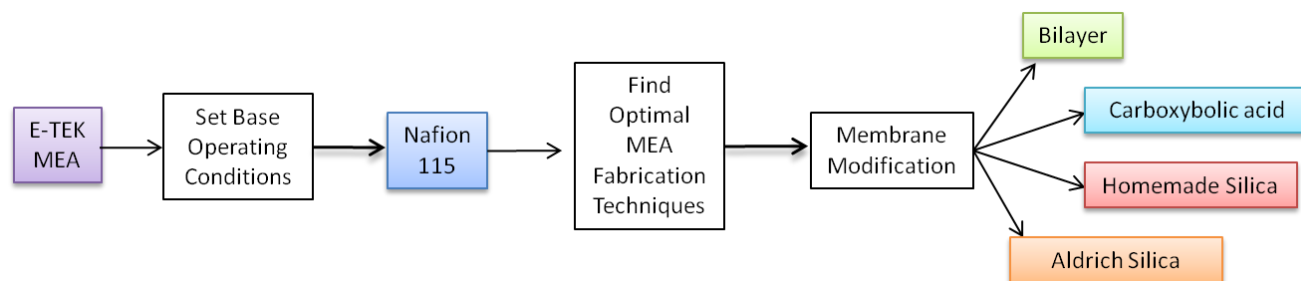


**Figure 15: Design of Experiments**

In order to accurately compare the performance of the various membranes, catalyzed commercial electrodes were purchased from ElectroChem and hotpressed to the membranes instead of using the Direct Spray Method for catalyst deposition. This eliminated the variables associated with spraying the catalyst.

### MEA Fabrication

Several factors are important in MEA fabrication, the most important among them being good interfacial contact between the membrane and the catalyst, and between the catalyst and the gas diffusion layer. Pressure is applied to press these layers together in close contact. However if the pressure is too high the catalyst layer may develop cracks, allowing methanol to leak through. Thus an intact catalyst layer is equally important as interfacial contact. Membrane, catalyst, and gas diffusion layer properties also play a role in fabrication.

### ElectroChem<sup>®</sup> Gas Diffusion Electrodes

The ElectroChem gas diffusion electrodes (GDEs) had a catalyst loading of the 4 mg/cm<sup>2</sup> with a carbon cloth backing. The cathode catalyst was Platinum supported on carbon and the

anode catalyst was Platinum-Ruthenium supported on carbon. The catalyst layers were coated with Nafion. It should be noted that the homemade MEAs were made with unsupported catalysts.

### E-TEK MEA

“Series 12D-W MEA” membrane electrode assemblies were purchased from E-TEK. They are designed for use in DMFCs. They came with the GDLs hotpressed to the catalyst layers and just had to be assembled in the cell. Figure 16 below is a photo of the E-TEK MEA. The catalyst area is almost a perfect square with little warping of the membrane, indicating sophisticated MEA fabrication techniques developed by the manufacturer.

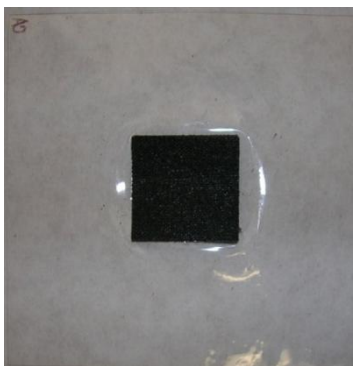


**Figure 16: Photo of an E-TEK MEA**

The membrane was Nafion 115 with unsupported Platinum on the cathode and unsupported Platinum-Ruthenium on the anode. The catalyst loading was  $5 \text{ mg/cm}^2$ .

### Membranes

#### **Nafion 115**

Nafion 115 membranes were purchased from Ion-Power. They are transparent membranes with a smooth surface. They have 1100 equivalent weight and are 5 mil, or 125 micrometers thick. Figure 17 shows a cross-section of the membrane.

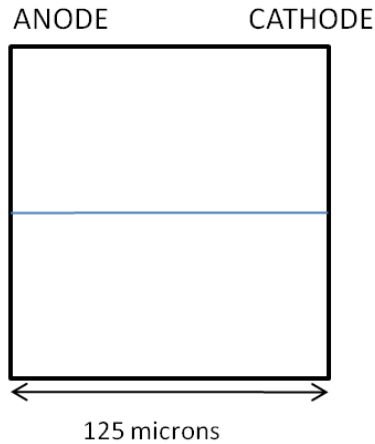


**Figure 17: Schematic of Nafion 115 Membrane**

Methanol and protons flow from the anode to the cathode. The blue line represents the concentration gradient of the protons across the membrane, which should be constant because of the constant acidity throughout the membrane.

### **Bilayer**

The bilayer membrane was purchased from Aldrich. It is a Nafion membrane, specifically “Nafion 324”. The membrane has an overall thickness of 152 micrometers and is reinforced with PTFE fiber. Figure 18 below shows a photo of the membrane face.



**Figure 18: Photo of Bilayer Membrane from Aldrich**

The PTFE support fiber is very visible in this photo and in the actual membrane as well. It protrudes out of the membrane. This is actually two layer composite membrane. One side of

the membrane has equivalent weight 1500 and a thickness of 25 micrometers while the other side has equivalent weight 1000 and a thickness of 127 micrometers. The higher equivalent weight side is smoother and shinier. Aldrich recommended using the higher equivalent weight side as the cathode side. Figure 19 below shows a schematic of the membrane, with the blue line showing the proton concentration levels in the two layers, the higher equivalent weight side possessing lower acidity.

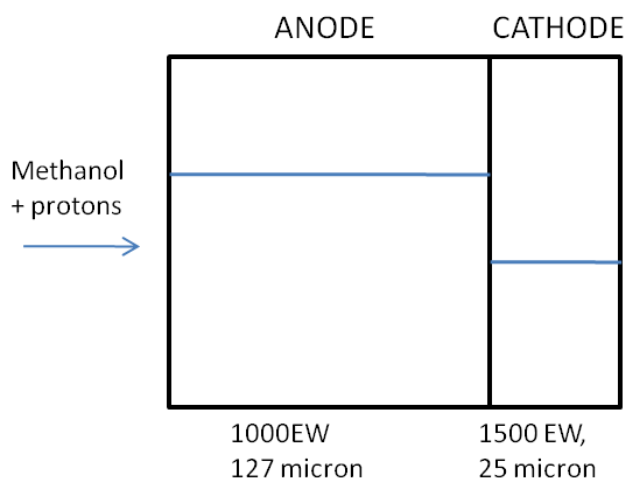


**Figure 19: Schematic of Bilayer Membrane - Orientation Recommended by Aldrich**

Since the cathode side is less acidic than the anode side, a concentration gradient is created to assist proton conduction from the anode to the cathode. The line between the anode and cathode represents an interface. The overall flux of methanol over the membrane should be lower than for Nafion 115 because of the increased thickness, presence of an interface, and reduced flux are due to the presence of the PTFE fiber. The favorable concentration gradient of protons however assists in methanol flux.

It was hypothesized that methanol crossover could be decreased even further if the membrane sides were switched. That is, the recommended cathode side could be used as the anode instead. Refer to the schematic in Figure 20 below.

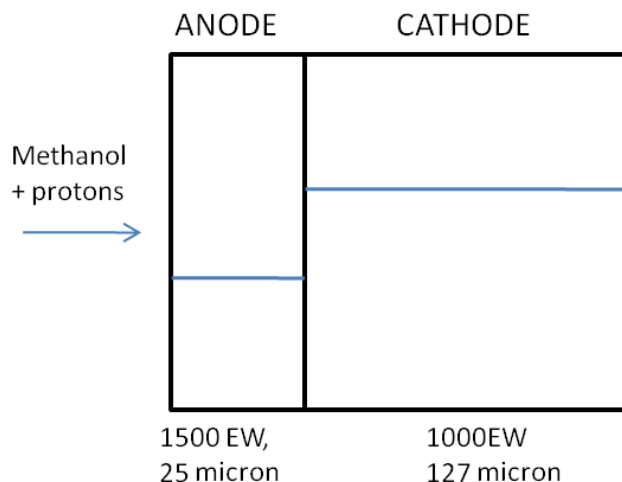


**Figure 20: Schematic of Bilayer Membrane Switched**

If the anode side is less acidic the concentration gradient for protons is reversed. Creating a negative concentration gradient would decrease proton as well as methanol flux and could result in improved performance at the low current density region.

### **Carboxylic Acid Membrane**

A sample of Nafion 982 was obtained from DuPont. This membrane is manufactured for the electrolysis of brine. The membrane has macroscopic roughness and is thicker than Nafion 115. A thicker membranes should have less methanol crossover. The membrane is in dry sodium form.

Figure 21 below shows the structure of the membrane from the DuPont product information document. In fact, one side of the membrane has sulfonic acid groups and the other side has carboxylic acid groups. The sulfonic acid side also has fabric which adds resistance. (The anode and cathode sides denoted in the figure are recommended by DuPont for the electrolysis of brine so they need not apply here). Using the carboxylic acid side on the anode would create a negative concentration gradient for methanol as carboxylic acid is less acidic. This would reduce flux and increase performance, at least in the lower current density region.

Also, the fabric on the cathode would prevent methanol crossover. Both sides were tested to test this hypothesis.

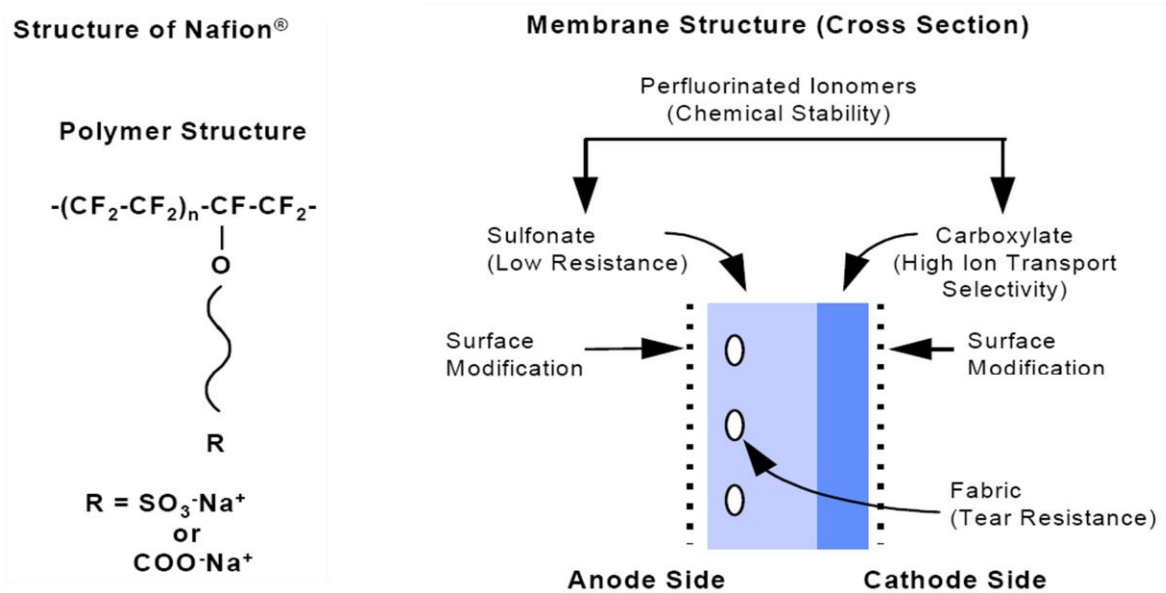


Figure 21: Structure of Carboxylic Acid Membrane

### Homemade Silica Nafion 115

Homemade Nafion-nano-silica membranes were made via the Sol Gel method. This method provides a relatively uniform and homogenous distribution of silica nanoparticles within the membrane. Nafion 115 membranes were used as the host membrane. The Nafion membrane was impregnated with a precursor solution of tetraethylorthosilicate (TEOS) and methanol. The membrane undergoes condensation reactions at an elevated temperature. The product is silica nanoparticles in the membrane pores, which should block methanol crossover. (Refer to Figure 5).

## **Aldrich Silica Membrane**

Silica-polymer composite membranes were purchased from Sigma-Aldrich. These membranes are manufactured by Aldrich; they are supposed to be a Nafion replacement in fuel cells. Sulfonic acid groups are grafted on silica and this lends the membrane good proton-exchange properties (SigmaAldrich, 2007), while still limiting methanol crossover due to the silica. The membrane is very thin, at 60 microns.

The experimental methodologies and the results obtained with the different membranes are described.

## Chapter 3: Experimental Methods

Since DMFCs deliver less power than hydrogen/oxygen fuel cells, fabrication conditions play an important role in DMFC performance. A slight variation in fabrication procedures would result in a significant difference in the power density delivered.

A number of factors are important in MEA fabrication. The smoothness and thickness of the membrane, and the membrane surface morphology affect the ease with which the catalyst may be deposited on the membrane. Membrane swelling is a concern in DMFC MEA synthesis; due to the high catalyst loading more solvent is needed, and the solvent causes membrane swelling and warping. Some other factors that affect MEA performance are whether the catalyst is applied to the gas diffusion layer or the membrane, the properties of the gas diffusion layer, solvent properties, and the evenness of the catalyst layer.

The fabrication procedure used was extrapolated from the 'Direct Spray' procedure used for hydrogen/oxygen fuel cells by Elias and Kurek (Elias, et al., 2007). However, the catalyst composition and hotpressing conditions were necessarily different for DMFCs.

First MEA fabrication methods based on Nafion 115 membranes were explored to optimize performance and compare with the commercial E-TEK MEA performance (Elias, et al., 2007). After optimal fabrication conditions were determined for Nafion 115, a similar procedure was applied for the other membranes: bilayer, carboxylic acid, silica, and Aldrich silica membranes. Due to differences in the membrane structures and properties, the treatment methods and the hotpressing conditions were slightly different for each membrane. The catalyst deposition protocol was kept fairly constant though.

# Nafion 115 Membrane

## *Membrane Pretreatment*

Membrane pretreatment involves cleaning the as received Nafion membrane. When the catalyst is being applied to the gas diffusion layer, the membrane must be converted to proton prior to catalyst application. This is also true when using the ElectroChem gas diffusion electrodes. When the catalyst is being applied to the membrane, the membrane may be converted to proton form either before catalyst application *or* after application.

### Full Pretreatment Method

This method was used when the membrane was converted to proton form *before* catalyst application. The as-received Nafion membrane was cut into a square with each side measuring 2.0 inches. It was boiled in DI water for one hour, followed by boiling in 150 mL of 3 wt % hydrogen peroxide for an hour and a half, and then DI water again for one hour. It was converted to proton form by boiling in 0.5M sulfuric acid for an hour and a half and then cleaned by boiling in water for one hour again. The membrane was then stored in water until catalyst application. It should be noted that ‘boiling’ denotes gentle boiling. Vigorous boiling could damage the membrane surface.

### Post-treatment Method

This method was used when the membrane was converted to proton form *after* catalyst application. The full pretreatment method was followed until the sulfuric acid step. The membrane was then stored in DI water until catalyst application. Please see Appendix 1 for step-by-step instructions for both methods.

## *Catalyst Deposition*

### Catalyst Ink Preparation

Anode Catalyst Ink Slurry	Cathode Catalyst Ink Slurry
24mg (4mgcm <sup>-2</sup> ) Platinum:Ruthenium black	24mg (4mgcm <sup>-2</sup> ) Platinum Black
2-3 Drops Deionized Water	2-3 Drops Deionized Water
35mg 10% 1100EW Nafion	35mg 10% 1100EW Nafion
5mL Methanol	5mL Methanol

**Table 1: Catalyst Ink Ingredients**

Separate catalyst ink slurries were prepared for the anode and the cathode. Each side had a catalyst loading of 4mgcm<sup>-2</sup> for a 5cm<sup>2</sup> area. The Nafion loading for the catalyst layers was 0.7mgcm<sup>-2</sup>. Catalyst powders were wetted with deionized water to prevent combustion upon the addition of methanol. To achieve the aforementioned catalyst and Nafion loadings, a mixture of catalyst, deionized water, Nafion slurry, and methanol was prepared with proportions according to Table 1. These mixtures were sonicated in a Fisher Scientific<sup>®</sup> Solid State/Ultrasonic FS-14 for three hours.

The inks were sprayed directly onto either a GDL or a membrane using a Badger<sup>®</sup> Professional 150.

### Spraying Catalyst on the GDL

The GDL was purchased from E-TEK; the product is called LT1400W, microporous carbon cloth GDL. The catalyst was sprayed onto the GDL. The flow rate of the ink spray was minimized to prevent penetration of the ink through the GDL. In order to form a uniform layer, catalyst was sprayed from side to side in a steady motion to insure that the same amount of catalyst was deposited on the entire 5cm<sup>2</sup> area of the GDL. After each spraying round, the wet catalyst was blow dried with a low flow rate of unheated air for 30 seconds to 1 minute. When spraying was completed, the catalyzed GDL was placed in an oven for 90 minutes at 80°C.

## Spraying Catalyst Directly onto the Membrane

A proton exchange membrane (stored in water) was dried and flattened by pressing it with Kim<sup>®</sup> wipes in flat metal plates for 10 minutes. This membrane was aligned and clamped between two metal plates with a 5cm<sup>2</sup> square opening for catalyst deposition. Catalyst was sprayed on one side at a time. Figure 22 shows a photo of a membrane being sprayed and Figure 23 shows a sprayed membrane.

After each spraying round, the wet catalyst on the GDL or the membrane was blow dried with a low flow rate of unheated air. To form a uniform layer, catalyst was sprayed from side to side in a steady manner. To prevent cracking of the catalyst layer, catalyst had to be sprayed at a low flow rate to minimize swelling of the membrane. Swelling occurred when methanol in the ink diffused into the membrane. Repetitious swelling from catalyst application and contraction from blow drying could cause microscopic cracks in the catalyst layer. When spraying was completed, the catalyzed membrane was placed in an oven for 90 minutes at 70°C.

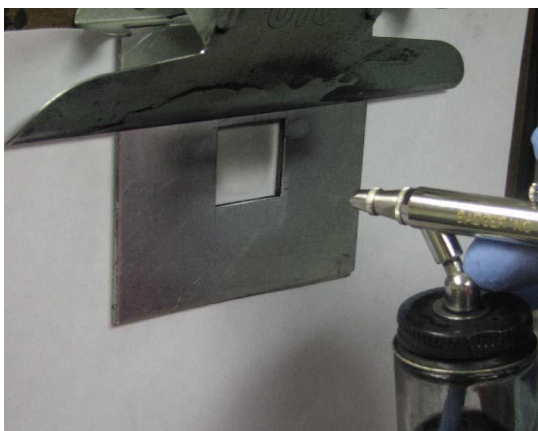


**Figure 22: Spraying homemade catalyst directly onto membrane using a spray gun**

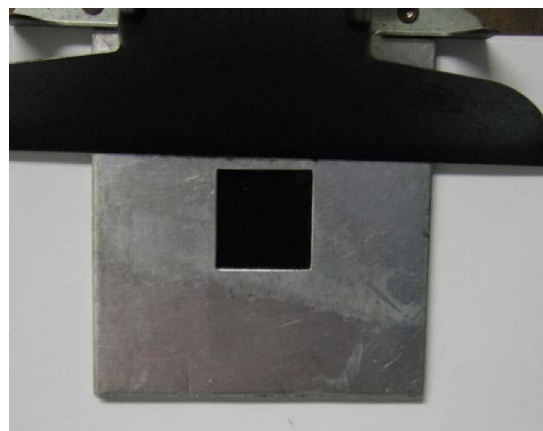
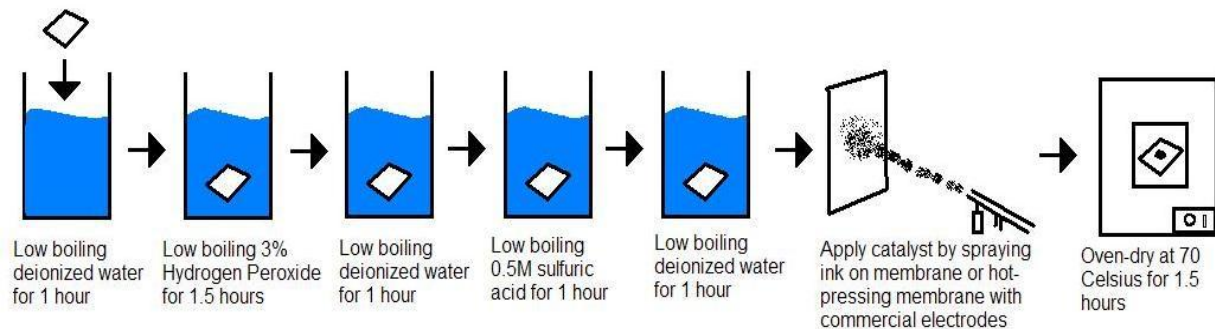


**Figure 23: A catalyzed membrane upon completion of the spray step**

## Post-treatment

This step was only followed for membranes pretreated via the ‘Post-treatment Method’ denoted in the ‘Membrane Pretreatment’ section. After the catalyzed membrane was removed from the oven, it was boiled for one hour in 0.5M sulfuric acid, followed by heating in DI water for one hour. It was then dried in the hotpress with Kim wipes without any heat or pressure. It was hotpressed immediately afterwards. Figure 24 below shows a schematic comparing the Full Pretreatment and the Post-treatment methods.

### Catalyst Application on Completely Pre-Treated Membranes



### Fabrication via Post-Treatment Procedure

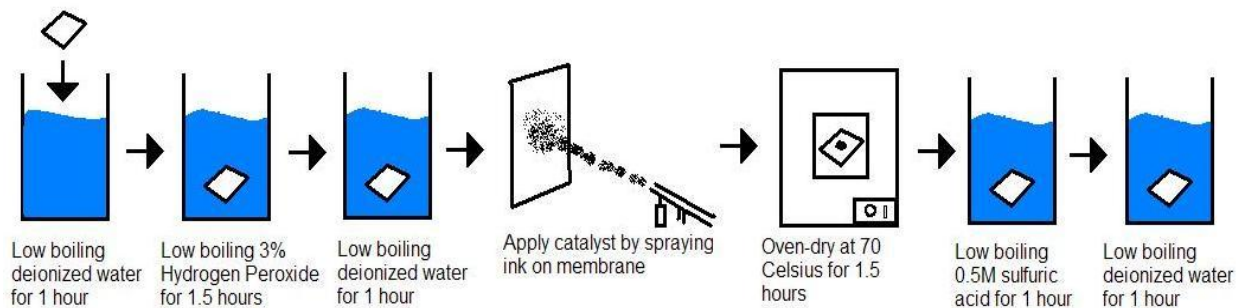


Figure 24: Full Pretreatment Method vs. Post-treatment Method

## *Hotpressing*



**Figure 25: Hotpress Machine**

Hot-pressing is used for adhesion and transfer of catalyst on the membrane to obtain good interfacial contact between the membrane and the catalyst. This is essential because it creates a good continuity of Nafion between the membrane and the catalyst that will allow quick transport of the protons from the anode to the cathode side. Therefore, the temperature, time span, and pressure are all key parameters when hot-pressing the membrane and the catalyst. The temperature of the hot-press was at the glass transition temperature of Nafion, which is approximately 135°C.

To hotpress the Nafion 115 membrane, first a Teflon sheet was placed on a metal plate. Then the GDL was carefully placed on the center of the Teflon sheet. The membrane was placed on top of the GDL and it was aligned so that the GDL was located at the center of the membrane. If the membrane was warped, then the edges of the membrane could be taped to flatten the membrane. Then another GDL was placed on top of the membrane with caution. It is vital that

the two GDLs are aligned completely together to ensure even distribution of the reactants to the catalyst and removal of the unwanted products, such as carbon dioxide, from the catalyst. Once the GDLs are aligned, a second metal plate was placed after the Teflon sheet. Meanwhile, the hotpress machine should have been set to 135°C, and as soon as the temperature was reached, it was hotpressed at a pressure of 2 metric tons for 2 minutes. Then the membrane was removed from the machine and cooled for 2 minutes before assembling in the cell. Unless stated otherwise, a hotpressing pressure of 2 metric tons was applied for 2 minutes.

### ***Fuel Cell Assembly***

A setup of the apparatus of Direct Methanol Fuel Cell assembly is shown in Figure 26.

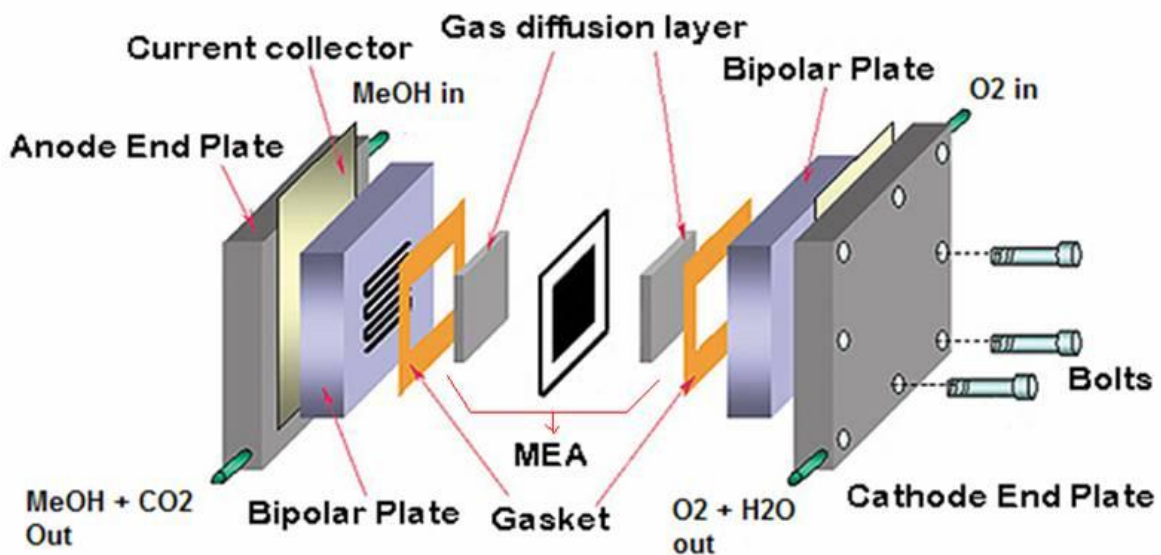


Figure 26: Fuel Cell Assembly

The center of the sketch is the MEA Membrane Electrode Assembly, which is the heart of DMFC. The MEA consists of gas diffusion layers, anode and cathode catalyst layers, and a proton exchange membrane (such as Nafion 115). The anode catalyst consists of Platinum,

Ruthenium, and Nafion particles where the methanol oxidation reaction takes place. The cathode catalyst consists of Platinum and Nafion particles. The two catalyst layers are separated by the proton exchange membrane that conducts protons from the anode to cathode.

Attached to the catalyst layers on either side of the membrane are the gas diffusion layers (GDLs). The primary purpose of GDLs is to collect and transport electrons, provide mechanical support, distribute gases to and from the catalyst, and manage water. The GDLs are made of carbon fiber paper or carbon fiber cloth. The GDLs can be treated with PTFE polymer, which gives them both hydrophilic and hydrophobic characteristics. This allows reactant gases and water vapor to pass through the pores to the catalyst while still preventing the GDLs from becoming saturated by liquid water. It is also important to have a good contact between the MEA and the GDL to ensure even distribution of the reactants to the catalyst and removal of the unwanted products, such as carbon dioxide, from the catalyst.

The next components are the gaskets, which secure a seal between the bipolar plates and the membrane. Typical gasket materials are PTFE or silicone rubber. The thickness of the gasket is crucial, since it has to be thick enough to prevent leaks; however, it cannot be too thick as that would hinder electrical contact between the plate and the MEA.

The gaskets rest on the bipolar plates. The bipolar plates are made of graphite and have a serpentine channel network etched on their surface. The channel network is the activate area of the fuel cell since it regulates the amount of fuel in contact with the catalyst; the serpentine channel ensures proper distribution of fuel across the cell. Some essential properties of the bipolar plates include chemical stability, electrical conductivity, and impermeability to gases.

The last components are the current collectors. The current collectors collect current and transport the electrons via the external circuit from the anode to the cathode providing electrical power to the external device.

All of these components were assembled in the order as shown in Figure 26 and then sealed with bolts. A torque of 60 in-lb and then 65 in-lb was applied to every nail in order to have uniform pressure across the cell.

### ***Fuel Cell Test Station Description***

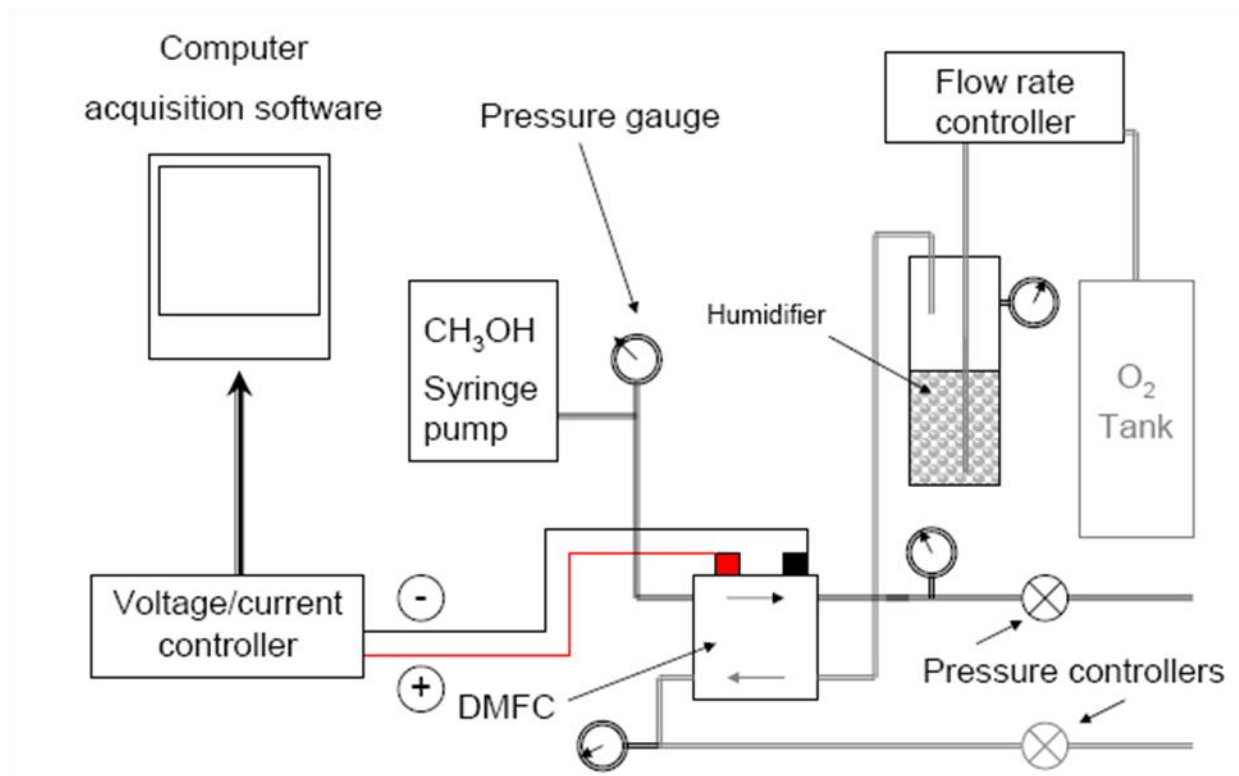


**Figure 27: Schematic of DMFC Test Station**

A sketch of the DMFC station is shown in Figure 27 (Hackquard, 2005), while a photograph is shown in Figure 28. A photograph of the cell is shown in Figure 29.



**Figure 28: DMFC Test Station**

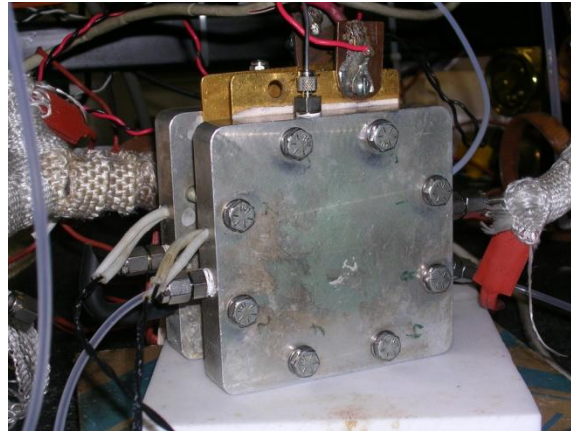


**Figure 29: Fuel Cell in Test Station**

The DMFC station consists of the cathode humidifier, syringe pump (ISCO 1000D), voltage and current controller, oxygen flow rate controller, thermocouples, and temperature controller. The thermocouples are located at the bottom of the humidifier and the cell to detect the humidification temperature and the cell operating temperature respectively. The cell is heated

to the cell operating temperature by placing the heating rods into the side of the cell. The operating temperature is monitored by the temperature controller. Pure oxygen is fed continuously through the cathode humidifier. The cathode humidifier is used to maintain moisture in the oxygen stream in order to keep the membrane humidified. At the cathode outlet, water and oxygen flow out to a beaker filled with water. A dilute methanol solution is continuously fed at a certain feed flow rate via the syringe pump (to the DMFC and it flows out with carbon dioxide produced at the anode to a beaker where it is collected. The current is monitored and recorded as a function of voltage by directly reading from the voltage and current controller (load box). The voltage and current density were plotted in polarization curves.

### ***Fuel Cell Activation***

Activation of the prepared MEA is necessary before testing in order to provide enough hydration to the membrane and activate the anode catalyst to optimize the performance of the cell. It is necessary to activate the anode catalyst because of the slow reaction kinetics of the methanol oxidation reaction at the anode and it was found in the study of Chakraborty et al. that performance increased with time as the anode catalyst was exposed to methanol (Chakraborty, et al., 2007). The first step was to set the cathode humidifier temperature to 85°C (later 35°C) and the fuel cell temperature to 70°C. The oxygen tank and the syringe pump were immediately turned on to feed oxygen and methanol respectively to the fuel cell. The flow rate of oxygen was set and monitored at 70 mL/min using the oxygen flow rate controller. Refer to Appendix 2 for the oxygen flow rate controller's calibration curve. The flow rate of methanol was set at 1ml/min. Once the DMFC and the cathode humidifier reached the desired temperatures, a voltage of 0.3 V was applied across the cell via the load box for at least 6 hours or until the current profile reached steady state.

## ***Fuel Cell Test Conditions***

Once the MEA was activated, the operating conditions were set. The initial operating conditions used were based on Alexander Hacquard's M.S. thesis (Hacquard, 2005). The cell temperature used was 70° C, and the cathode humidifier was at 85° C. The anode flow rate was set to 1 mL/min of 1 M of methanol solution and the cathode flow rate was 70 mL/min of pure oxygen. The anode feed conditions used are also fairly common in literature. These operating conditions were modified later to obtain optimal performance.

After stabilization, a potential difference of 0.6 or 0.7 V was applied across the cell. The resulting current was allowed to stabilize and then the reading was recorded. This way the cell voltage was changed manually via voltage and current controller from open circuit potential value to 0.2 V, with a step of 0.1. The corresponding current values were measured. The open circuit potential was determined by setting the load box to no current.

## **Bilayer Membrane**

As mentioned before, the bilayer membrane is composed of two different equivalent weight Nafion layers. The chemical properties of the membrane are the same as Nafion 115 so the same pretreatment, catalyst deposition, and post-treatment (if needed) procedures were followed. See Appendix 1 for more details.

## **Carboxylic Acid Membrane**

The as-received Nafion 982 membrane is in dry sodium form. It has to be converted to proton form prior to use in DMFCs. But since one side of the membrane has carboxylic acid groups, sulfuric acid could not be used during pretreatment. Instead 0.5 M nitric acid was used. The membrane was boiled in the acid for 1.5 hours, followed by heating in DI water for 1 hour.

This treatment procedure was used either before hotpressing the ElectroChem GDLs onto the membrane, or after spraying the membrane with catalyst. See Appendix 1 for more details.

Upon contact with liquid, Nafion 982 became extremely warped as shown in Figure 30. Therefore, flattening the membrane prior to hotpressing was necessary to ensure accurate GDL alignments. The membrane was flattened by placing it in the hotpress machine between Kim<sup>®</sup> wipes without heat or pressure.



**Figure 30: Photo of a warped carboxylic acid membrane (N982)**

In the case of hotpressing the catalyzed ElectroChem GDE to the membrane, a longer hotpressing duration (2 metric tons for 5 minutes) was required in order to transfer the catalyst from the GDE onto the membrane.

## **Silica Membrane**

Silica membranes were prepared by impregnating silica particles into the pores by the Sol-Gel method, adapted from Nikhil Jalani's dissertation (Jalani, 2006). A detailed procedure for the preparation of the membrane and membrane pre-treatment/post treatment is provided in Appendix 3.

Silica membrane Preparation was divided into three parts: Cleaning and Converting to Sodium Form, Silica Impregnation, and Cleaning Surface Silica & Converting Back to Proton Form.

### ***Part 1: Cleaning & Converting to Sodium Form***

The as-received Nafion 115 membrane was cut into a 2.0 inches x 2.0 inches square and purified in 3 wt% hydrogen peroxide followed by water. It was then converted to sodium form by boiling in 1 M sodium hydroxide for 4 hours to increase mechanical strength for further steps. It was rinsed in water for 30 minutes prior to placing the membrane in the vacuum oven for 12 hours at 110°C. Just before placing the membrane in the oven it was blotted gently with Kim<sup>®</sup> wipes to wipe off excess water. This decreases the warping of the membrane in the oven. The mass of the dry membrane recorded.

The vacuum oven and the vacuum pump used were Precision Instruments Model 19 and Duo Seal Vacuum Pump respectively. The oven has an analogue scale for temperature; see Appendix 4 for the temperature calibration. Extrapolating from the calibration data, a setting of 3.75 was determined for 110°C.

### ***Part 2: Silica Impregnation***

Immediately after completion of Part 1 the membrane was immersed in a 2:1 methanol/water solution for one hour to swell the pores of the membrane in order to maximize absorption of the precursor solution. The membrane was then immersed in a precursor solution of 3:2 tetraethyorthosilicate/methanol solution. The silica content of the membrane was found to vary with the duration of immersion in the precursor solution; the longer the immersion, the greater the silica content obtained, but it was difficult to achieve more than 4% silica absorption.

The length was varied from 2 – 8 hours. The membrane was removed from the solution after the prescribed time and again wiped lightly with Kim wipes to remove excess solution so that the surface of the dried membrane is free from excess silica. It was placed in the oven for 24 hour at 110°C to complete the condensation reactions. The mass of the dry membrane was recorded and the wt % silica was calculated from the weight change.

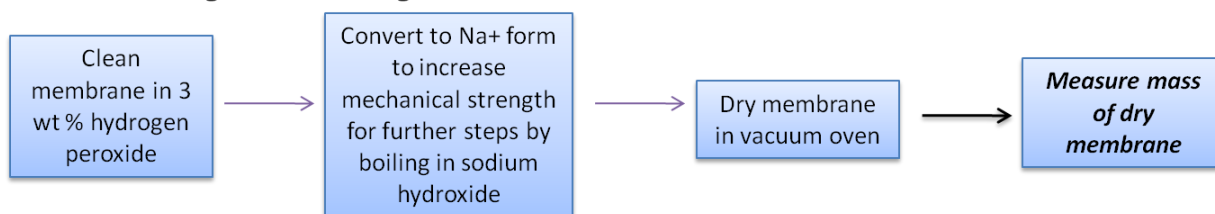
### ***Part 3: Cleaning Surface Silica and Sulfation***

The surface of the membrane was cleaned by heating in water followed by acetone to remove excess silica. The next step was to boil the membrane in 0.5 M sulfuric acid for 1.5 hours. This step sulfates the silica, i.e.  $\text{SiO}_2/\text{SO}_4^{2-}$  is formed in the pores of the membrane. It should also convert the membrane back to proton form. After rinsing in water the membrane is ready for catalyst application, either directly on the membrane, or for hotpressing to a catalyzed GDL.

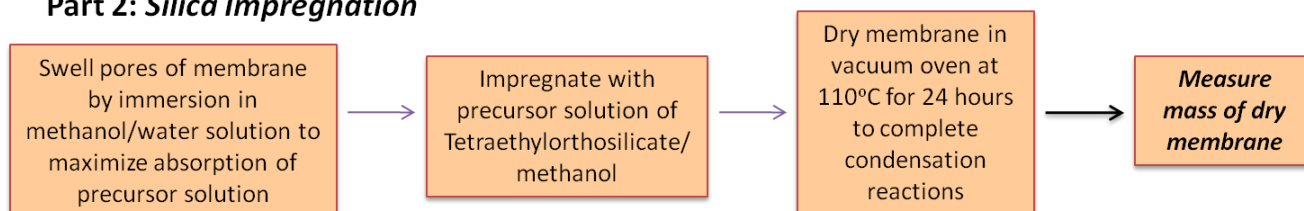
For some homemade silica MEAs, the sulfuric acid step was moved to *after* spraying catalyst on the membrane. This was referred to as ‘Post-treatment’ of silica membranes. It was done to find out the effect of converting the membrane back to proton form *after* catalyst application (like unmodified Nafion 115 and bilayer membranes).

The schematic presented in Figure 31 summarizes the most important steps for making silica membranes.

### Part 1: Cleaning & Converting to Na<sup>+</sup> Form



### Part 2: Silica Impregnation



### Part 3: Cleaning Surface Silica & Sulfation

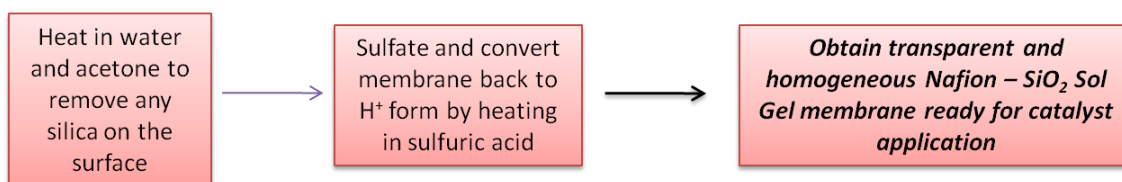


Figure 31: Silica-Nafion Membrane Preparation

## Aldrich Silica

The Aldrich silica membrane is different from all other membranes, in that it is not composed of Nafion. It's chemical and physical properties are thus different. The membrane could not be purified using 3 wt % hydrogen peroxide as it dissolved. The manufacturer does not specify any pretreatment procedure so it was just cleaned in water prior to catalyst application.

Catalyst could not be directly deposited on the membrane because it was much thinner than Nafion 115. The lack of thickness caused the catalyst to penetrate the membrane so catalyst could only be applied on the GDL. The glass transition temperature of this membrane is much higher than that of Nafion, at 200°C (SigmaAldrich, 2007). When the membrane was hotpressed to the catalyzed ElectroChem GDEs, more pressure was required to transfer the catalyst onto the membrane. So it was hotpressed at 205°C and 2.5 metric tons for 5 minutes.

## **Chapter 4: Results & Discussion**

Through our results and discussion we show the analysis involved in developing an optimal MEA and a high-performing PEM. First, a baseline for performance and best operating conditions were established using the commercial E-TEK MEAs. Then the results obtained from varying the different parameters involved in MEA fabrication techniques were analyzed to determine optimal fabrication conditions. Finally the membranes most effective at blocking methanol crossover are presented.

### **Establishing Base Operating Conditions using E-TEK MEAs**

The E-TEK MEA was used to establish the optimum base operating condition such as methanol feed concentration, fuel cell temperature, and cathode humidification temperature for DMFCs.

#### ***Effect of Methanol Feed Concentration***

The optimal operating methanol feed concentration is essential to determine because the performance of the DMFC varies with the fuel concentration. From Figure 32, in the region of interest ( $>0.3V$ ), 1M methanol solution delivered the highest performance. As expected, the performance dropped as methanol concentration increased. This is due to increased methanol cross-over to cathode.

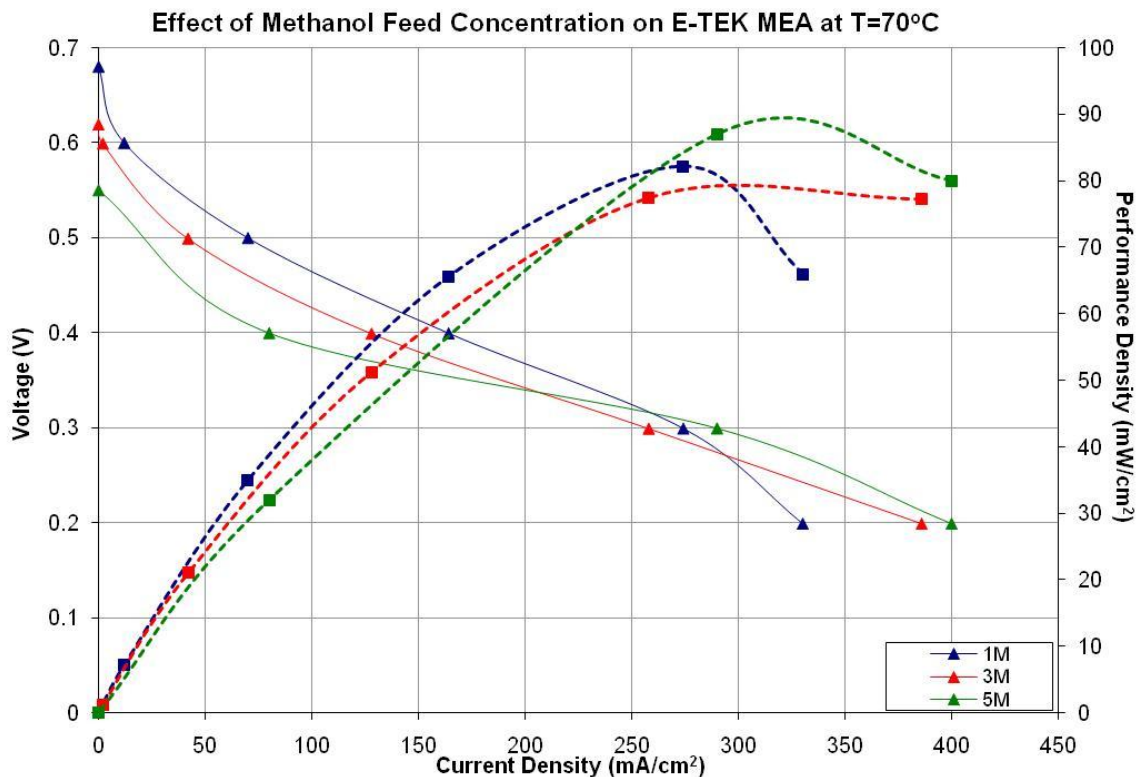


Figure 32: Effect of Methanol Feed Concentration on E-TEK MEA, Cathode humidifier at 85°C

Although most fuel cells operate at 1M concentration to optimize performance, higher methanol concentrations are desirable to maximize the energy density of the fuel. Therefore 3M methanol solution was determined as the optimal operating feed concentration. Also, operating at 1M produced considerable oscillations, which makes the data less reliable.

### *Effect of Cell Temperature*

The recommended operating temperature range for the E-TEK MEA was 25°C - 80°C. An operating cell temperature within that range needed to be established as a base condition. From Figure 33, the cell performed better at a temperature of 80 °C than 70°C except at lower current densities, although this difference is relatively small.

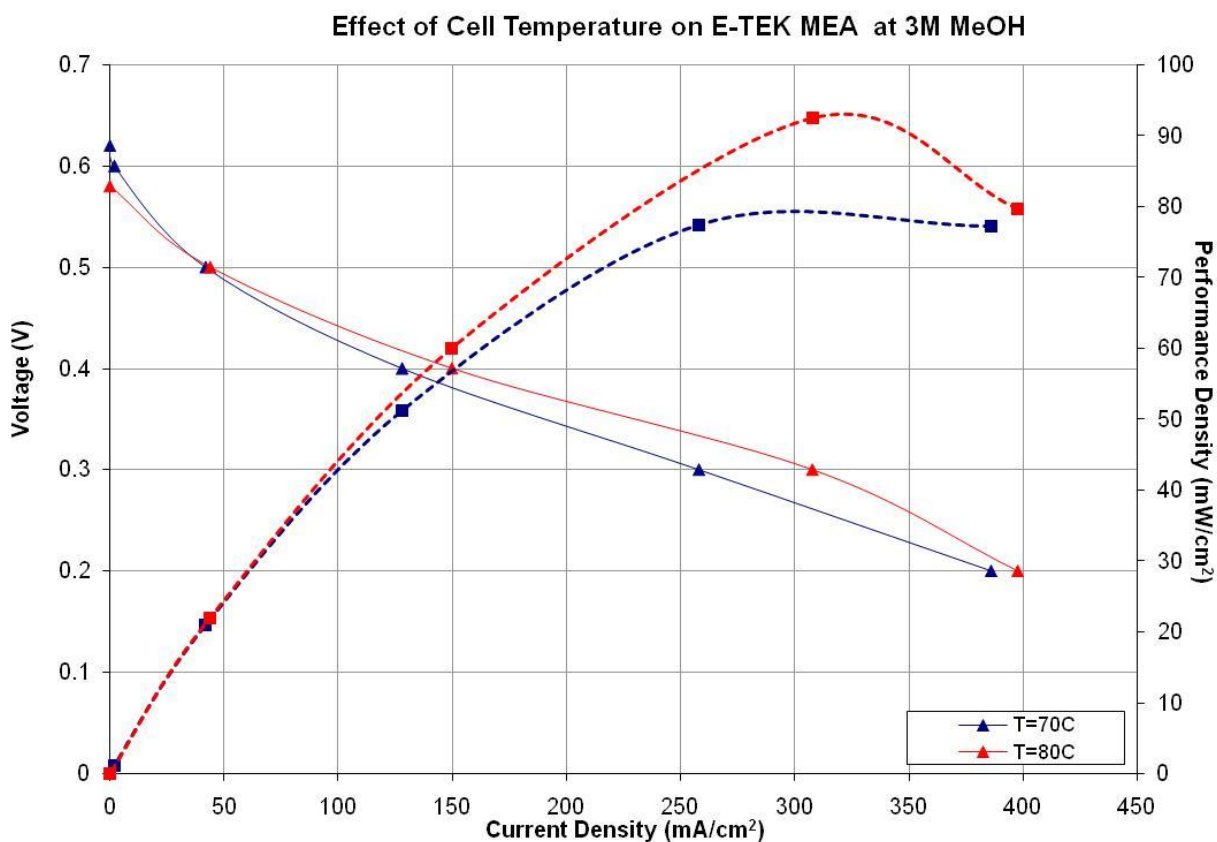


Figure 33: Polarization and Performance Density Curves on Effect of Cell Temperature on E-TEK MEA

DMFCs perform better at higher temperatures because the kinetics at the electrodes are promoted at higher temperatures. Although 80°C yields a higher cell performance, a cell temperature of 70°C was set as the base condition because of the considerable oscillations at the higher temperature, which makes it difficult to quantify data.

### ***Vapor Methanol Feed***

Vapor methanol feed is of interest for passive DMFCs. The humidification at the cathode should be sufficient to maintain moisture in the cell; the anode feed was set at 1 mL/min of 1 M methanol/water solution. The anode feed tube was heated with heating tape to vaporize the methanol.

When a potential difference was applied across the cell there were huge fluctuations in the current readings though. The OCP also fluctuated. The fluctuations were of a significant magnitude and no data could be taken. Perhaps the feed was not sufficiently vaporized and the methanol was a two-phase mixture. More residence time might be needed to vaporize the feed.

### ***Effect of Cathode Humidifier Conditions***

Since the feed fuel in DMFCs is dilute liquid methanol, there is no need for humidification at the anode. It was hypothesized that due to dilute anode feed, there is enough humidification in the entire cell to operate without a cathode humidifier as well. Figure 34 below shows the results for two cathode humidification temperatures, 85° and 35°C. At a cathode humidification temperature of 35°C the humidification is fairly low and negligible.

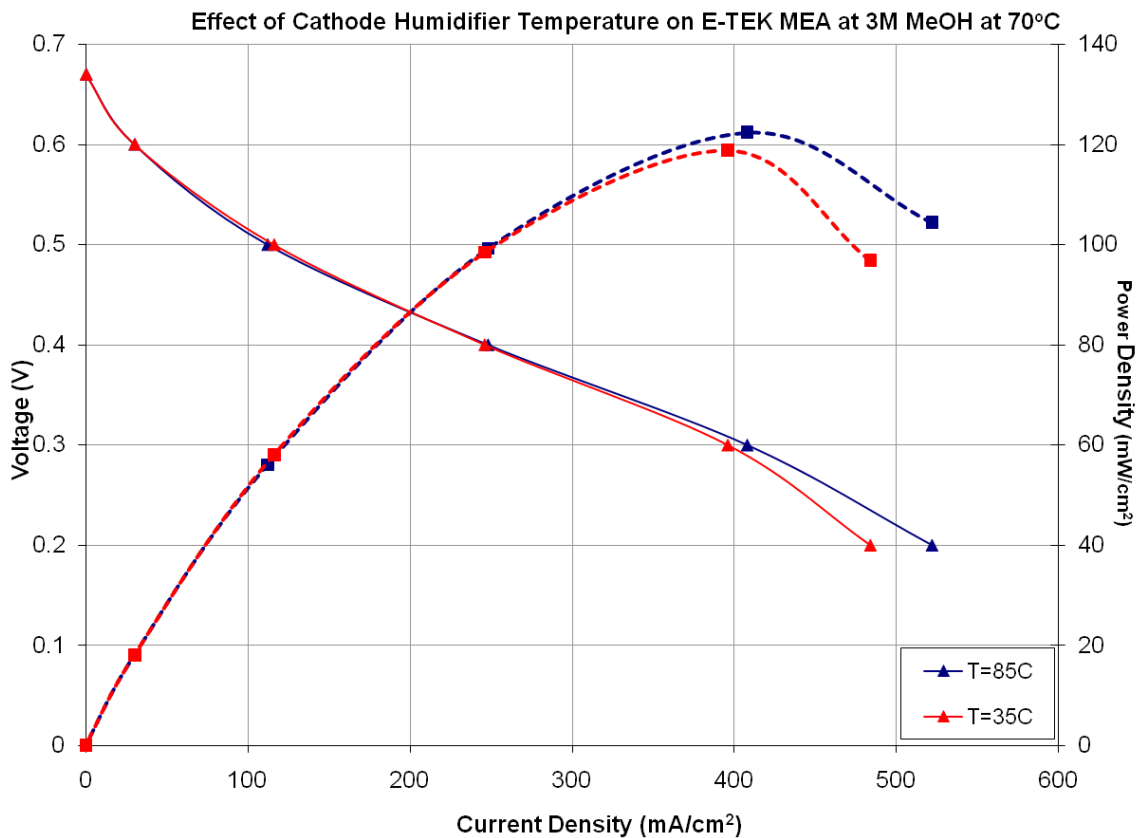


**Figure 34: Effect of Cathode Humidifier Conditions**

Especially, in the lower current density region the MEA performed the same under both humidification conditions. Hence further experiments were conducted at a cathode humidification temperature of 35°C.

### ***Base Operating Conditions***

Based on the above, the best operating conditions were determined to be:

<b>Cell Conditions</b>	<b>Anode Conditions</b>	<b>Cathode Conditions</b>
Cell Temperature: 70°C	Concentration of feed Methanol = 3M	Oxygen flow rate = 70 mL/min
	Flow rate of feed Methanol = 1 mL/min	Humidification temperature = 35°C

Figure 35 below shows the performance of the E-TEK MEA at the above conditions.

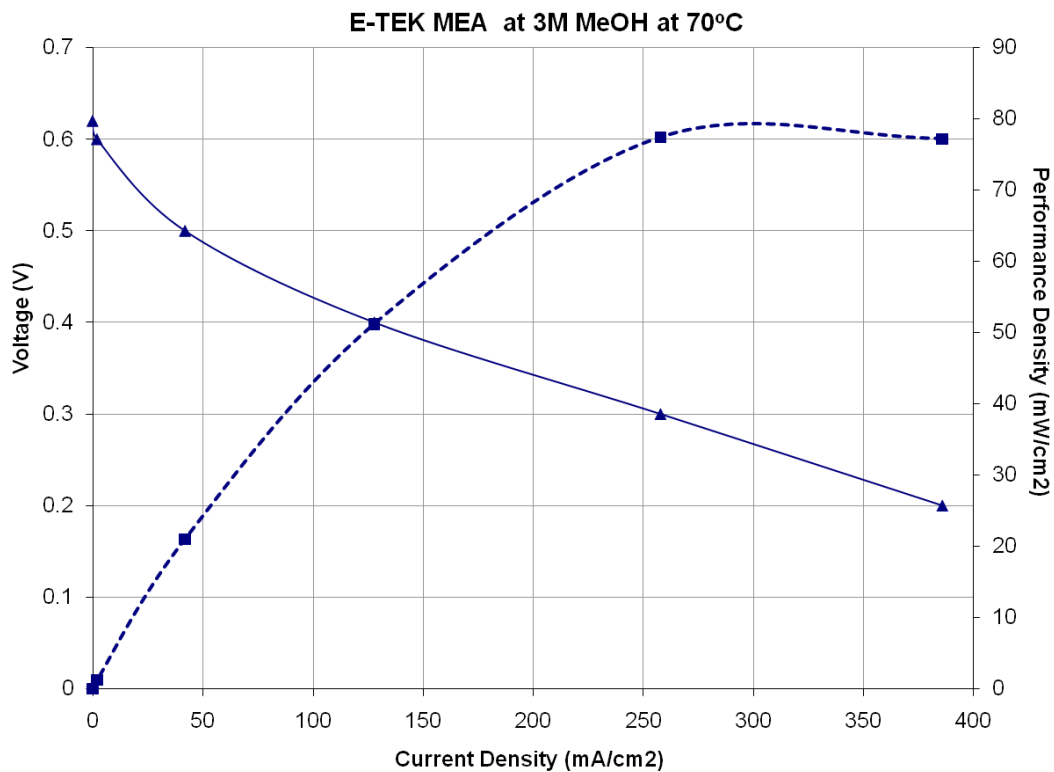


**Figure 35: E-TEK MEA Performance at Base Operating Conditions**

The OCP was 0.62V and the current density at 0.3V was 258 mA/cm<sup>2</sup>.

# Optimizing Nafion 115 MEA Fabrication

## Catalyst Ink Deposition: GDL-Application and Membrane-Application

Catalyst deposition methods primarily affect the resistances of the interfaces between the membrane, the catalyst, and the GDL. When analyzing interfacial resistance, the constant slope region (Ohmic region) of the V-I curve is of high interest since the slope of this region is proportional to the combined resistance of the proton exchange membrane, the catalyst-membrane interface, and the catalyst-GDL interface. Figure 36 shows that there are considerable differences in the slopes of the Ohmic region for MEAs fabricated with commercial electrodes, catalyzed GDLs, and catalyzed membranes.

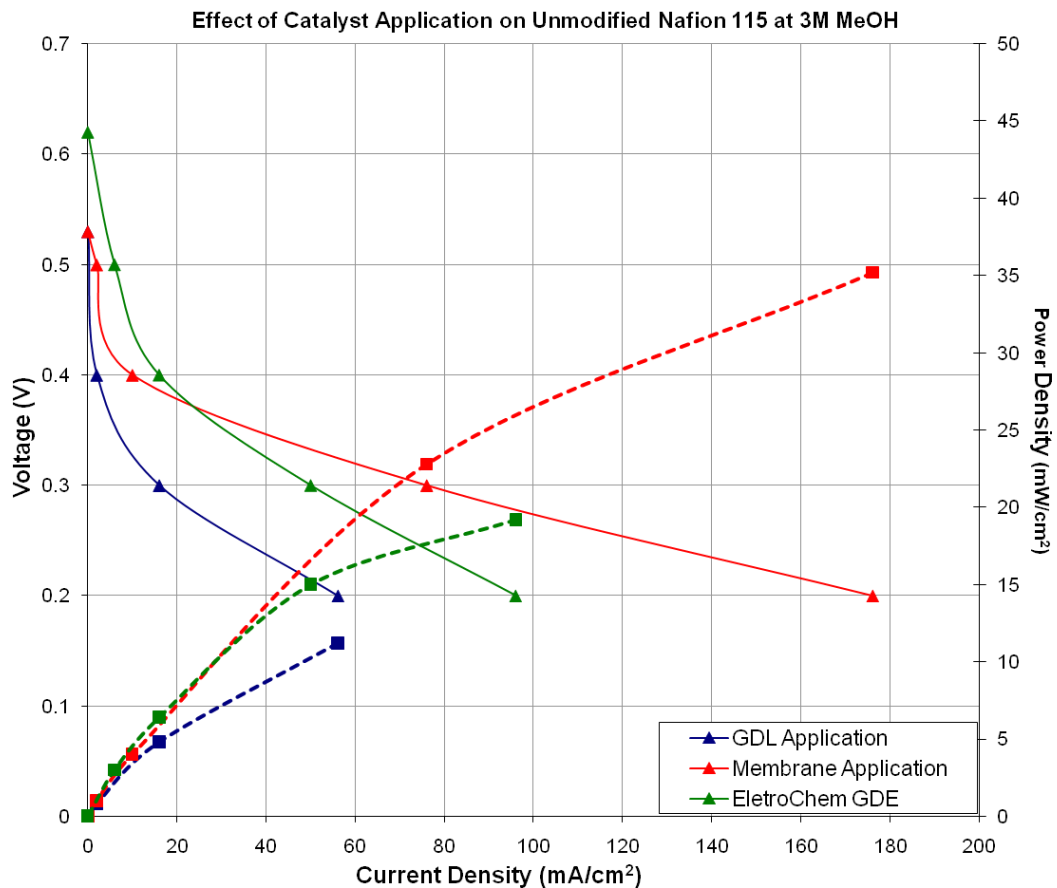


Figure 36: Effect of Methods of Catalyst Application

The resistances for the MEAs with the commercial electrode and the catalyzed GDLs are relatively the same. This is expected since both MEAs had catalyst applied directly onto the GDL, and both of these electrodes were hot-pressed onto unmodified Nafion 115 with the same hot-pressing protocol (2 minutes at 135°C and 2 metric tons of pressure). Since resistances are a product of the MEA fabrication procedure, then the ElectroChem electrode and the home-made catalyzed GDL had the same resistance, and parallel Ohmic regions in the I-V curve, since they were both fabricated the same way.

Membrane Electrode Assemblies (MEAs) with catalyst sprayed directly on the membrane performed better than MEAs with catalyst sprayed on GDLs and MEAs fabricated with ElectroChem GDEs. MEAs with catalyzed membranes had slopes in the Ohmic region that were half that of the MEAs with GDL application. The electrical conductivity of carbon cloth is 200  $\text{Scm}^{-1}$  while the protonic conductivity of Nafion is 0.1  $\text{Scm}^{-1}$ . This means that electrons are conducted at 2000 times the rate of protons and that protonic transport limits fuel cell performance. Therefore, a close contact between the membrane and the catalyst is more important than close contact between the GDL and the membrane since access of catalytic reaction sites to the proton transporter (Nafion membrane) is more important than their access to the electron transporter (GDL). This close contact between the membrane and the catalyst was best achieved when catalyst was sprayed directly onto the membrane.

The open circuit potential (OCP) is highest for the MEA fabricated with ElectroChem GDEs. OCP is highly dependent on the integrity of the catalyst layer, which depends on the catalyst deposition technique. If catalyst is applied directly onto the membrane, then it is more likely to develop cracks due to swelling and contraction of the membrane during spraying and drying. Catalyst layers of catalyzed membranes are also more susceptible to cracking upon hot-

pressing. Cracks in the catalyst layer reduce the amount of overall reaction. At the anode, cracks form a conduit for methanol to directly access the membrane, thus, increasing methanol crossover and decreasing the OCP due to oxidation of methanol at the cathode. Therefore, Figure 36 shows that MEAs fabricated with ElectroChem GDEs exhibit a higher OCP than those with fabricated by the direct spray method on the membrane.

### ***Nafion Loading***

Nafion is a necessity in catalyst ink in order to produce a three-phase interface where redox reactions occur. The triple-phase contact provides separate transport media for protons and electrons. Although, Nafion is required for protonic conduction in the catalyst layer, the trade off is that excess Nafion engulfs catalyst sites to prevent electronic conduction as the electronic medium is blocked access to the loci of reaction. Figure 37 shows three schematics of catalyst layers with different Nafion loading.

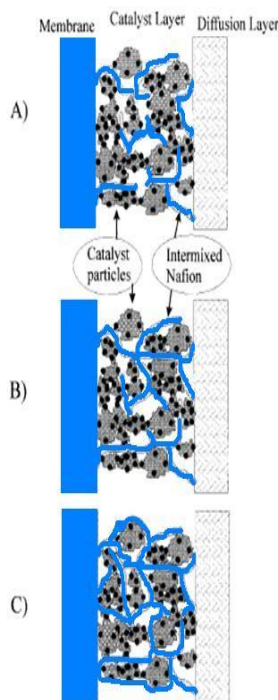


**Figure 37: Effect of Nafion Loading in Catalyst Area**

Schematic *a* in Figure 37 shows a catalyst layer that is limited by low proton transport since there is not enough Nafion ionomer to transport protons from reaction sites to the membrane. Schematic *b* shows an optimum Nafion loading where there is a high level of three-phase interface, but not too much Nafion as to block electronic conductivity. Schematic *c* represents a catalyst layer where catalytic sites are engulfed by excess Nafion that block the path from reaction sites to any electronic transport medium.

Catalyst inks with Nafion loading of  $0.7\text{mgcm}^{-2}$  performed better than inks with Nafion loading of  $1.2\text{mgcm}^{-2}$ . Figure 38 shows that the  $1.2\text{mgcm}^{-2}$  Nafion loading blocked electronic conductivity, since the slope of the corresponding I-V curve in the Ohmic region was much higher than that of  $0.7\text{mgcm}^{-2}$ . This showed that there was a higher resistance within the entire MEA for a Nafion loading of  $1.2\text{mgcm}^{-2}$ . This resistance can be attributed to blocked electronic conduction as excess Nafion displaces carbon particles that would otherwise contact catalytic sites to form a three-phase interface, which is conducive to the amount of charge transport.

Additionally, catalytic sites that are completely engulfed by Nafion are inactive sites and reduce the total amount of reaction. Therefore, not only is the resistance higher with a Nafion loading of  $1.2\text{mgcm}^{-2}$ , but the open circuit potential is also lower also as less reaction occurs. Figure 38 shows that a Nafion loading of  $0.7\text{mgcm}^{-2}$  provides a higher OCP and exhibits less activation losses than a loading of  $1.27\text{mgcm}^{-2}$ . The two values for Nafion loading were chosen based on literature, and results show that a loading of  $0.7\text{mgcm}^{-2}$  is better.

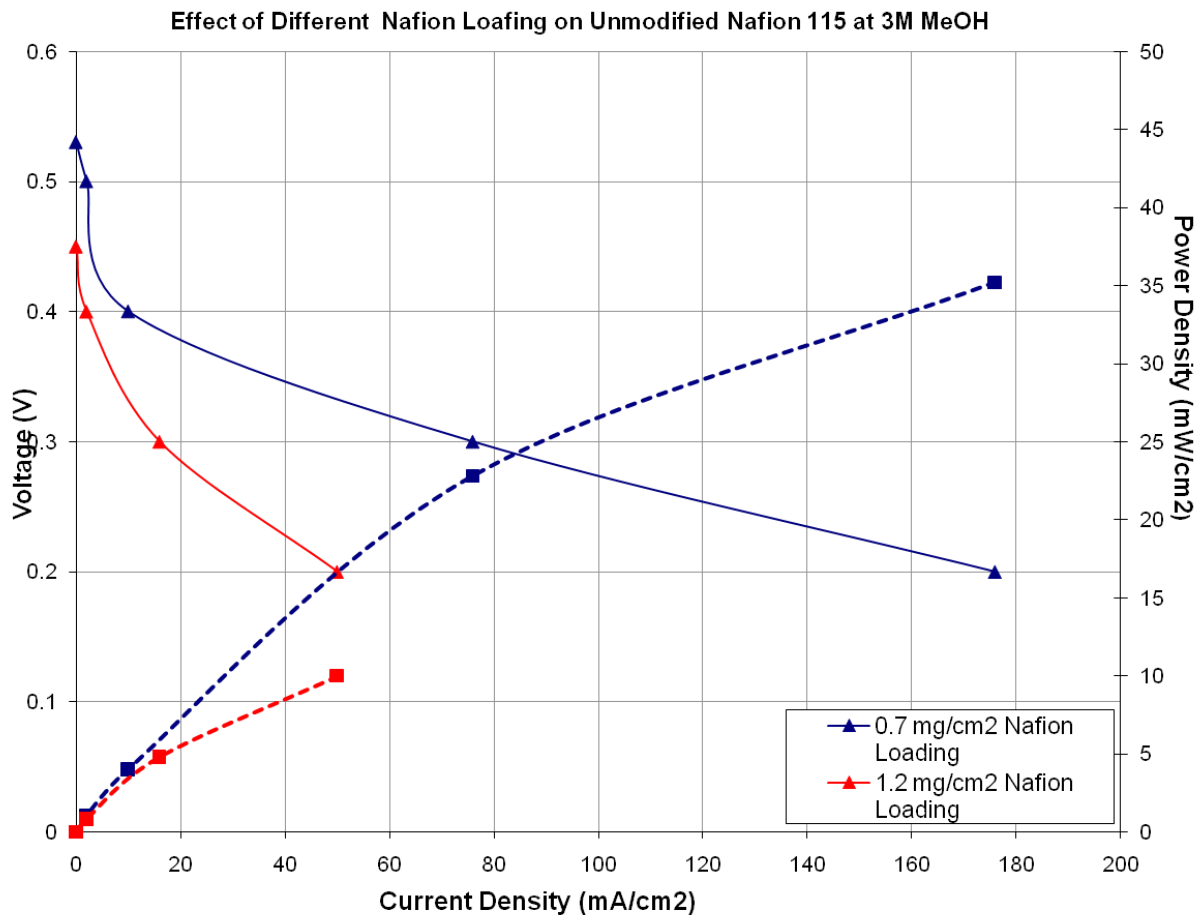
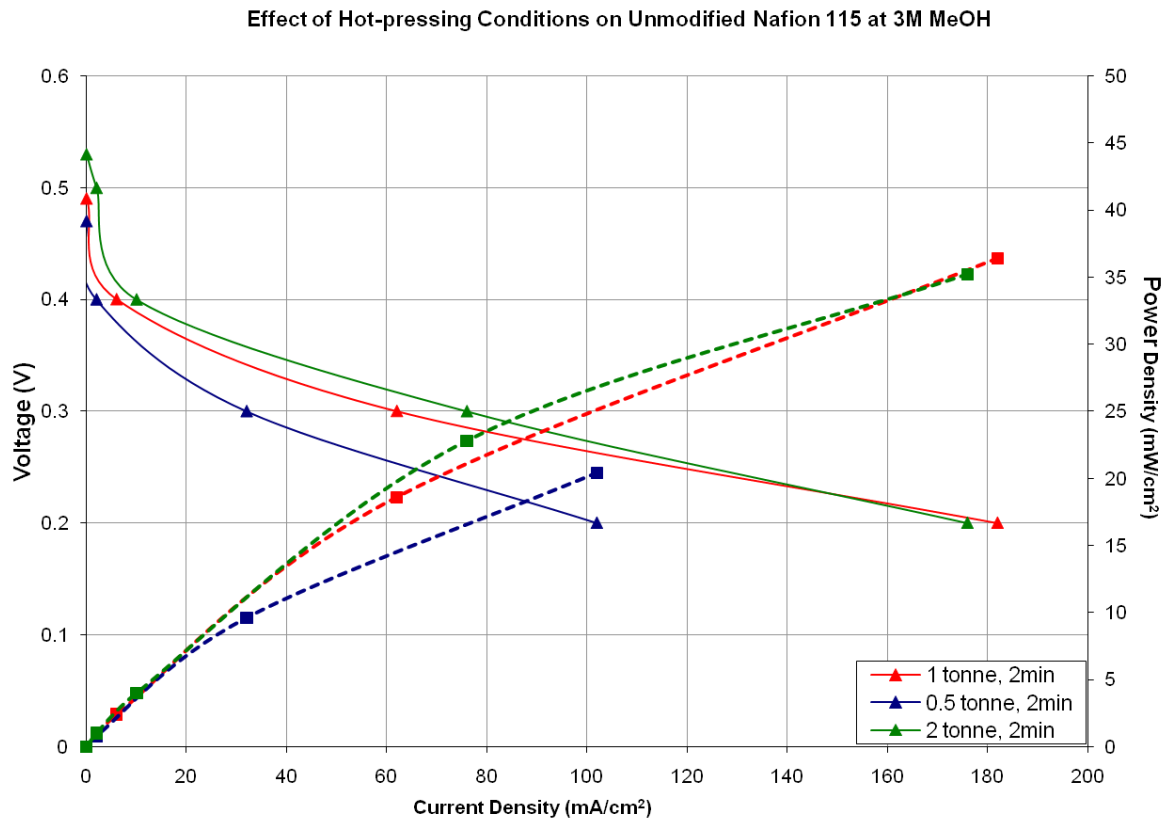


Figure 38: Effect of Nafion Loading in Catalyst Slurry for Homemade MEAs

### *Effects of Hot-Pressing*

Hot-pressing should be performed at the lowest possible pressure that provides sufficient contact between the membrane and the catalyst. Open Circuit Potential (OCP) is highly dependent on the integrity of the catalyst layer. Therefore, cracks in the catalyst layer reduce the amount of overall reaction. At the anode, cracks form a conduit for methanol to directly access the membrane, thus, increasing methanol crossover and decreasing the OCP due to oxidation of methanol at the cathode (over potential). Additionally, the interfacial contact between the membrane and the catalyst layer is supremely important to produce a small slope in the Ohmic

region of the polarization curve. During hot-pressing, Nafion is heated to above its glass transition temperature so that it intersperses throughout the catalyst to form close contact. The goal is an intact catalyst layer that is well-stuck to the membrane. Achieving this goal involves utilizing the minimum hot-pressing pressure (to prevent cracking of the catalyst layer) that provides sufficient catalyst-membrane contact (to reduce the interfacial resistance).



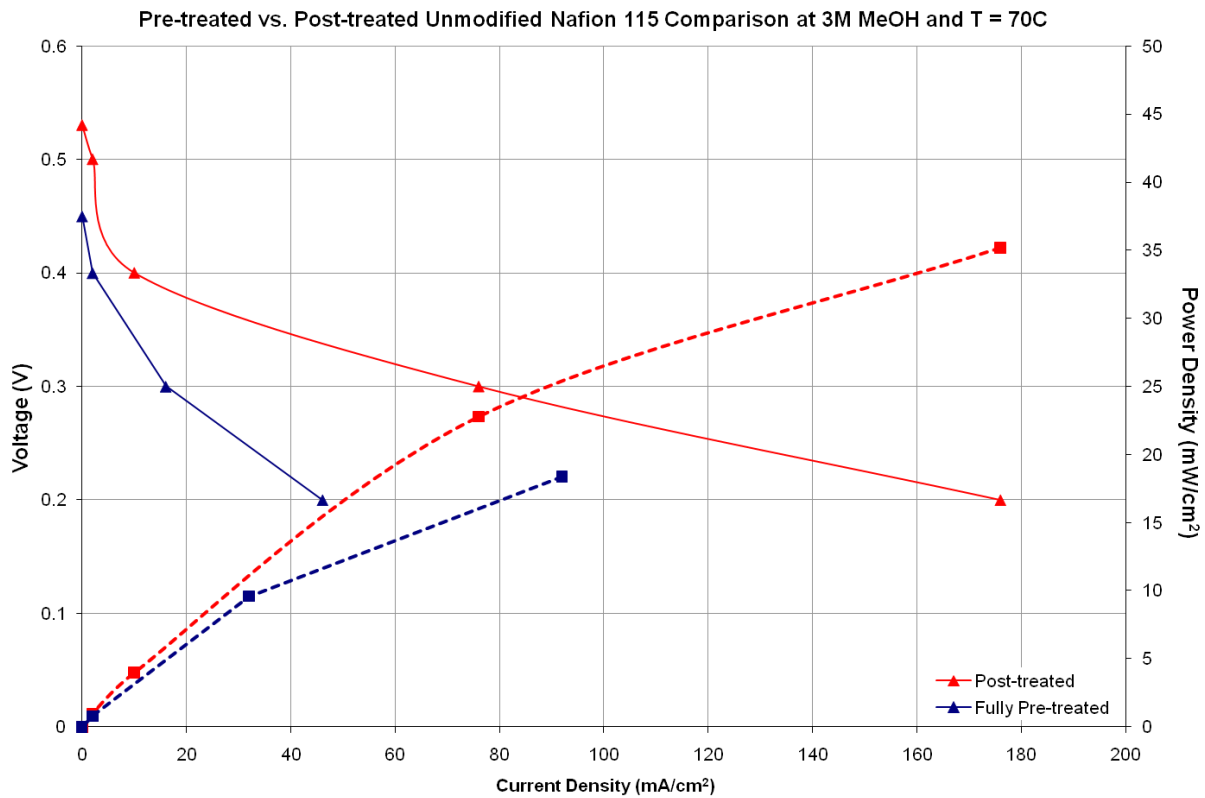
**Figure 39: Effect of Hotpressing Conditions**

Figure 39 shows that 2 metric tons of pressure provided the best performance since it did not crack the catalyst layer to the extent expected. The highest pressure provided a strong contact between the GDL and the membrane, thus, limiting losses from insufficient electronic conductivity and demonstrating high current densities between 0.3-0.4V. However, the slope of the MEA hot-pressed at 1 metric ton in the Ohmic region was less steep than that of the 2 ton

MEA implying that it had a slightly lower PEM resistance. At 2 tons, the porosity and structure of the GDL can be affected and increase the layer's resistance to electronic conductivity (hotpressing). However, a pressure of 1 ton is insufficient to compromise the GDL in the same way, and therefore, less resistance results as shown in Figure 39.

### ***Effects of Pre-Treatment or Post-Treatment of Catalyzed Membranes***

Freshly protonating the sulfonic acid sites in Nafion 1100EW of the catalyst ink through post-treatment provided a greater facility for proton transport, and provided better overall fuel cell performance. However, there was a trade off. Post-treatment expanded the catalyst layer that was sprayed onto the membrane directly. Since the active area used in testing was only 5 cm<sup>2</sup>, then the expansion of the deposited catalyst resulted in a less dense active catalyst layer.



**Figure 40: Effect of Full Pretreatment vs. Post-treatment on Nafion 115**

Figure 40 shows that treating an MEA in sulfuric acid solution after the catalyst application (post-treatment) step exhibited higher power densities than MEAs with pre-treatment.

***Comparison of Homemade Nafion 115 MEA with E-TEK MEA***

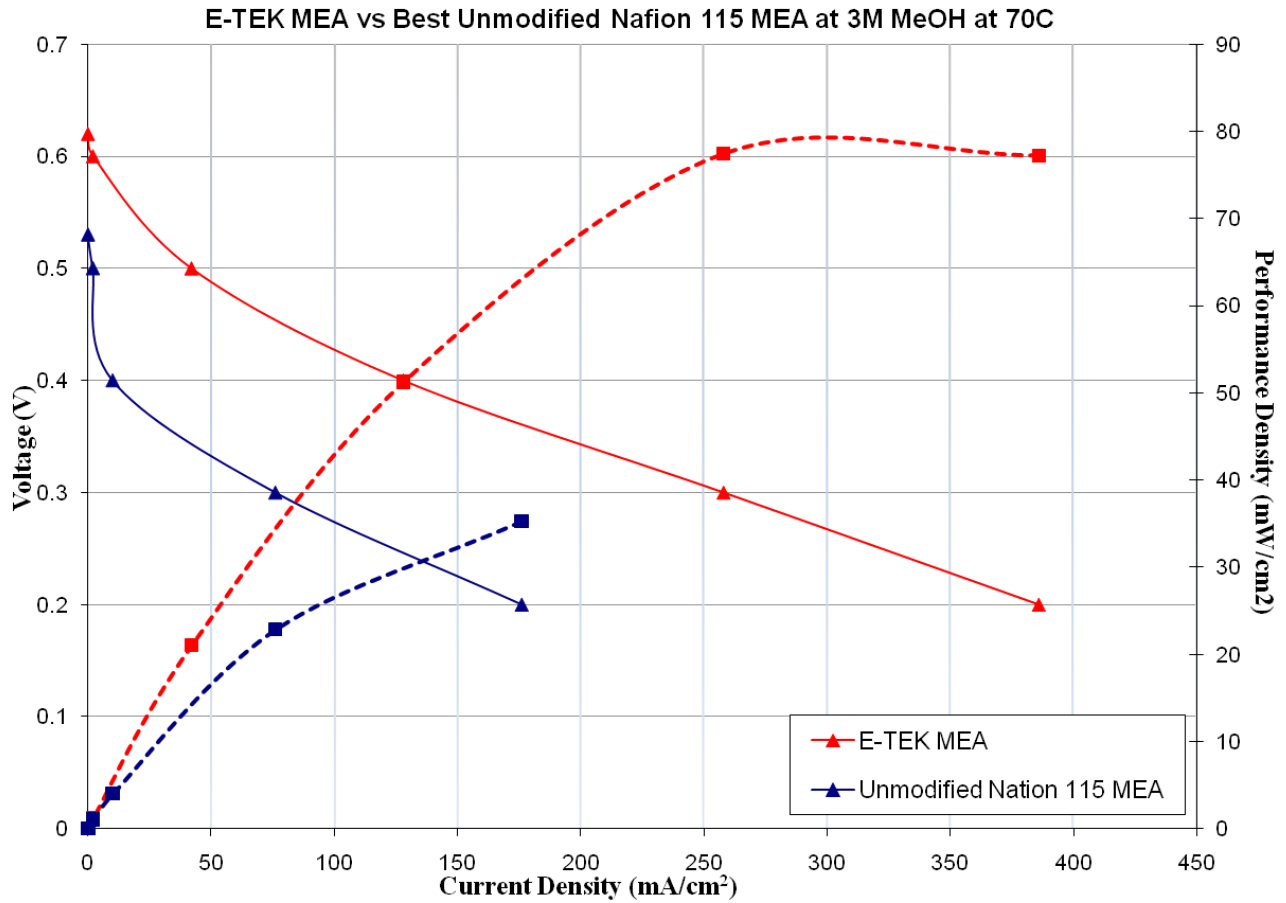


**Figure 41: E-TEK MEA Performance vs. Optimal Home-made Nafion 115 MEA Performance**

Figure 41 compares the performance of a commercial MEA manufactured by E-TEK<sup>®</sup> with that of a home-made MEA with catalyst sprayed directly on unmodified Nafion 115 (the same membrane used by the E-TEK MEA). The E-TEK MEA thoroughly outperforms the homemade MEA due to different fabrication protocol. E-TEK uses a different technique for

catalyst deposition, since the Energy Dispersive X-Ray (EDX) analysis in Figure 42 shows that platinum is not present at the catalyst-GDL interface in the E-TEK MEA as it is in ElectroChem catalysts (Figure 43). Instead Nafion dominates implying that Nafion is well-mixed and interspersed throughout the catalyst. Therefore, it is concluded that platinum is embedded directly on the membrane.

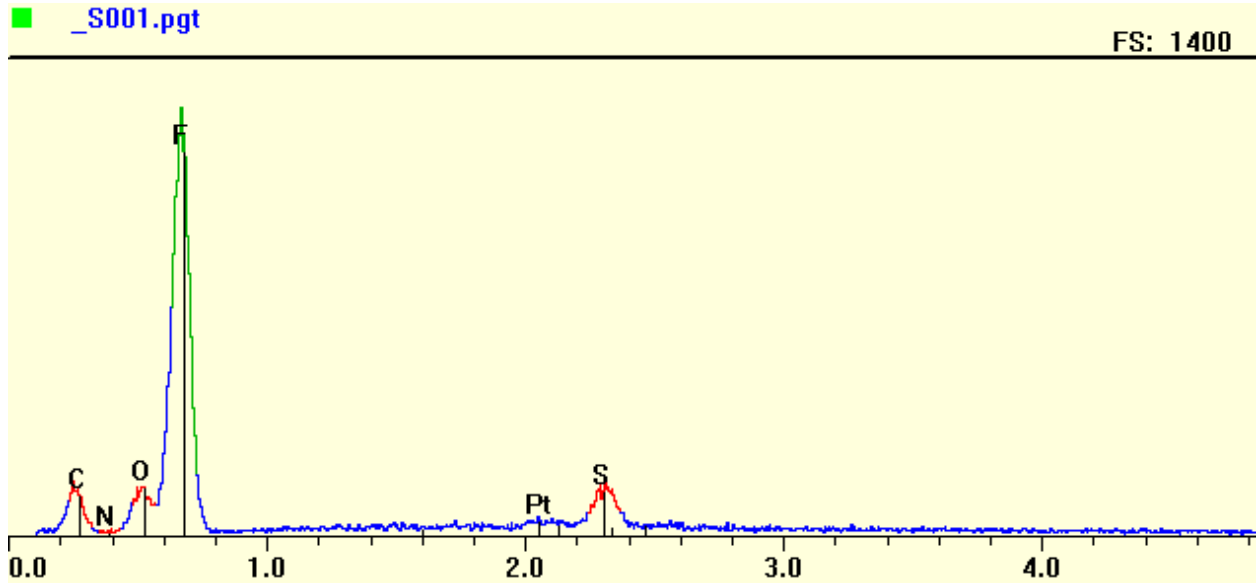


Figure 42: EDX spectrum for a catalyst layer from an E-TEK MEA.

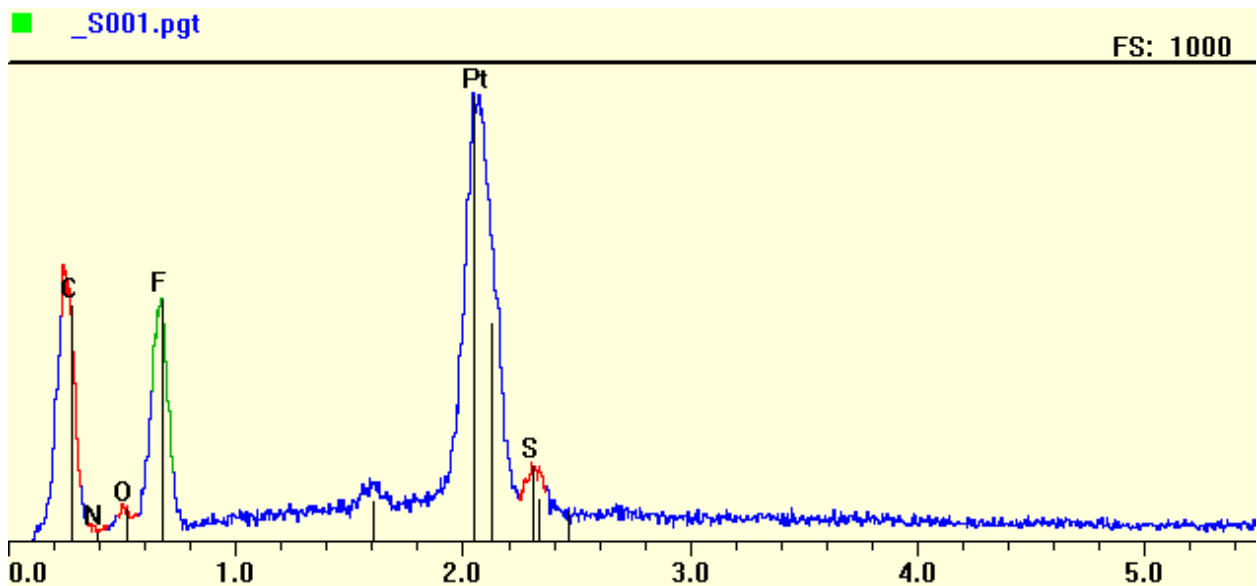
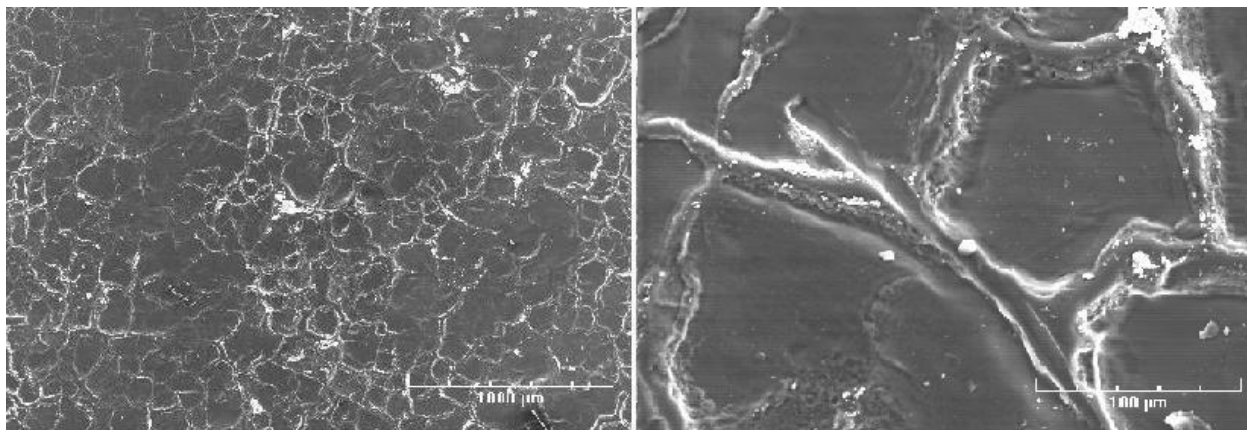
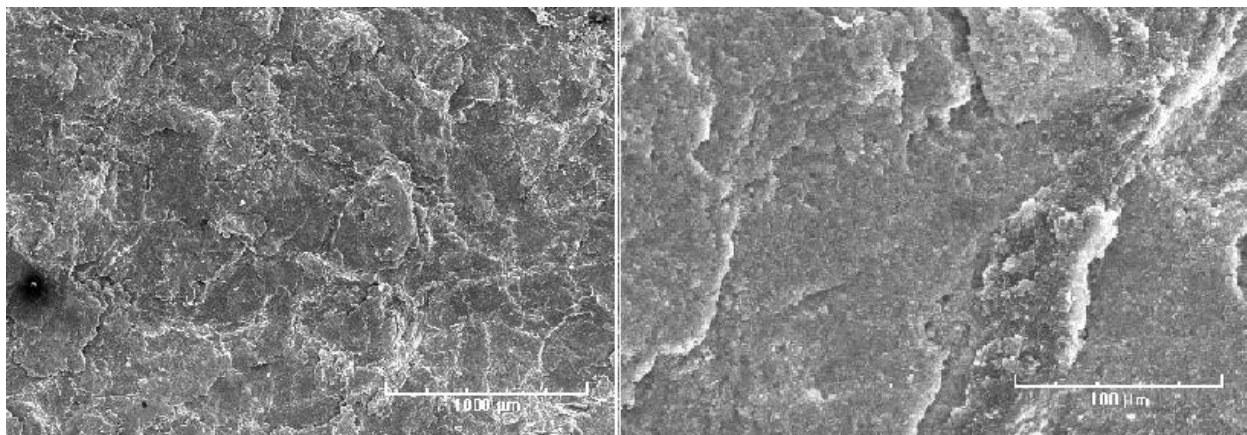


Figure 43:EDX spectrum for the catalyst layer from an Electrochem electrode.

Figure 44 also shows that Nafion (white lines) is uniformly dispersed throughout the entire catalyst layer of the E-TEK MEA. There are no cracks on the catalyst surface and the structure of the catalyst of the E-TEK MEA is more uniform than the ElectroChem catalyst surface shown in Figure 45. The images on the left sides of Figures 44 and 45 are at a magnification of 50x and the ones of the right sides are at 500x.



**Figure 44: SEM image of a catalyst layer from an E-TEK MEA: 50x and 500x**



**Figure 45: SEM image of a catalyst layer of an MEA hot-pressed with Electrochem GDLs.: 50x and 500x**

## Membrane Comparisons

As mentioned previously, in order to accurately compare the performance of the various membranes, the number of variables involved during the fabrication of the MEAs had to be minimized. Spraying catalyst on the membrane or gas diffusion layer by its very nature involves variables. Slight variations during catalyst ink preparation and spraying could affect the Voltage-Current data and would result in an inaccurate comparison. For this reason, the different membranes were hotpressed with catalyst coated gas diffusion layers purchased from ElectroChem<sup>®</sup>, and then tested.

### *Membranes Tested with ElectroChem<sup>®</sup> Gas Diffusion Electrodes*

Figure 46 and Figure 47 below display the polarization curves and the power density curves for the different membranes. Hotpressing pressures were kept constant for all membranes at 2 metric tons applied for 2 minutes. There are two sets of curves for the bilayer membrane. The one labeled 'Bilayer' had the cathode side as the 1500 equivalent weight side, and the one labeled 'Bilayer switched' had the anode side as the 1500 equivalent weight side.

The 'bilayer switched' membrane performed much lower than all other membranes, thus confirming that the higher equivalent side (less acidic side) should be the cathode side. Recalling the schematic of the bilayer membrane in the *Goals, Hypothesis, and Plan of Work* section, when the cathode side is the more acidic side, the concentration gradient for methanol is reversed. Unfortunately, creating a negative concentration gradient for protons impeded proton conductivity more than methanol crossover was. This resulted in a drop in performance.

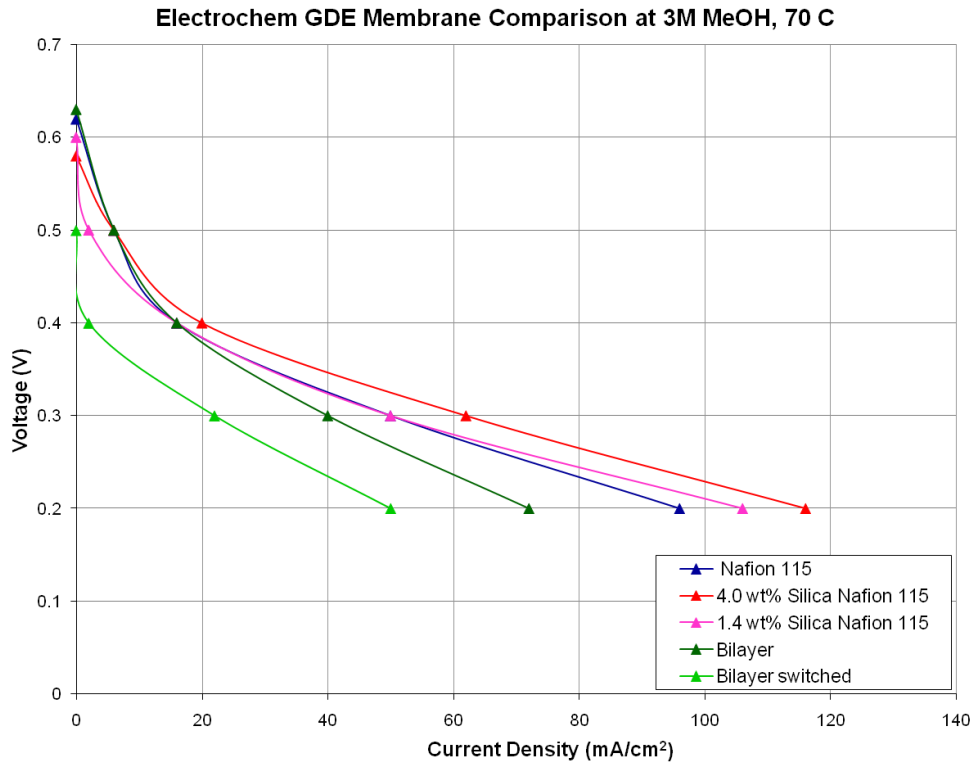


Figure 46: Electrochem GDE Membrane Comparison – Polarization Curves

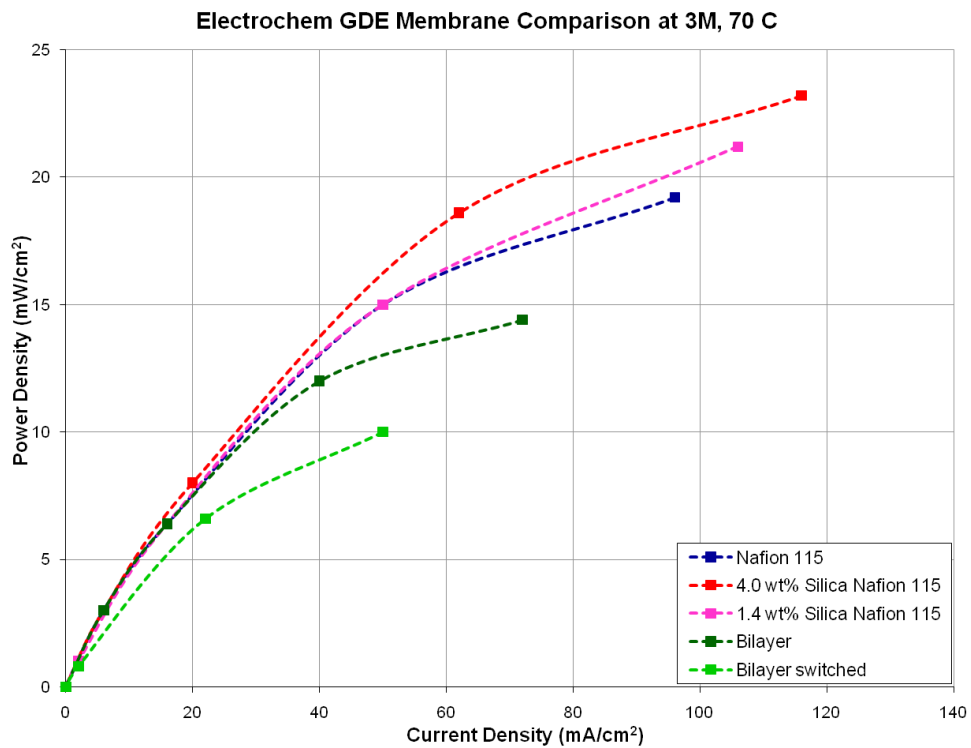
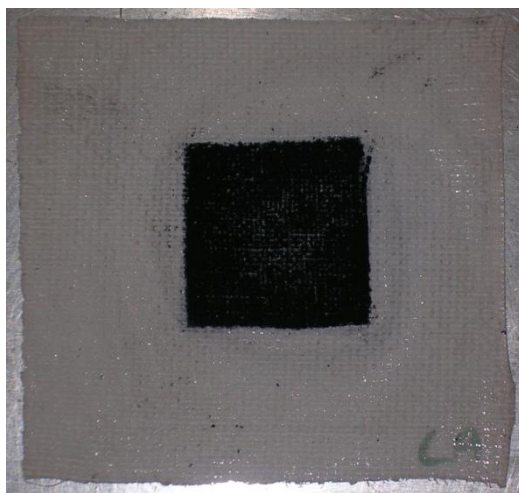


Figure 47: Electrochem GDE Comparison – Power Density

In the high current density region the bilayer membrane performs worse than other membranes. But in the region of interest, that is, in the lower current density region, the bilayer membrane performs the same as Nafion 115. While hotpressing the GDEs to the bilayer membrane it was observed that possibly not all of the catalyst was transferred to the membrane. As the membrane is somewhat thicker than Nafion 115, and since it has a PTFE grid that further enhances the thickness, a higher hotpressing pressure may have been necessary. So it was determined that despite the similar performance, the bilayer membrane has potential advantages over unmodified Nafion 115.

The 4.0 wt % silica membrane performed considerably better than the 1.4 wt % silica membrane. This could be because the higher silica content membrane has more acidic sites (refer to Literature Review) and so provides greater proton conductivity. The former has more silica in its pores and is more effective in blocking methanol crossover.

In addition to the bilayer and the silica membranes, carboxylic acid and Aldrich silica membranes (refer to the *Goals, Hypothesis, and Plan of Work* section) were fabricated. The results are not displayed in the graphs above because performance was very low and no data could be taken. A photo of the carboxylic acid MEA is displayed in Figure 48 below.



**Figure 48: Photo of a Carboxylic Acid MEA (Nafion 982)**

As can be seen from the image, the catalyst layer is not fully intact. White threads, belonging to the membrane, are plainly visible. This membrane is much thicker than Nafion 115, and unlike Nafion 115 has macroscopic roughness. Additionally, this membrane was manufactured to be used for the electrolysis of brine, which is a very different application. All these factors might explain why negligible current was generated when a potential difference was applied across this MEA. Even after the sides were switched (the anode side was the carboxylic acid side) no current was generated.

Figure 49 below is a photo of an Aldrich silica MEA. The Aldrich silica membrane looks very different from Nafion and is much thinner, at 60 micrometers compared to 125 micrometers. This could be one of the reasons for its poor performance, as a thinner membrane should have more methanol crossover.

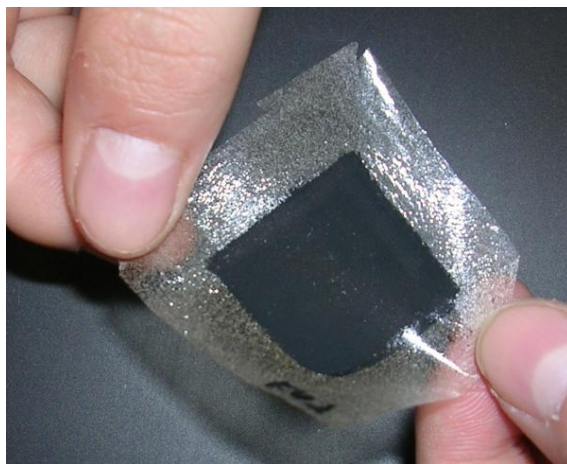


**Figure 49: Aldrich Silica MEA**

Based on the polarization curves and the power density curves in Figures 46 and 47, it was determined that the following membranes were of interest:

- Higher silica content Nafion membranes, wt % silica > 3%
- Bilayer membrane with the cathode as the 1500 equivalent weight side.

## *Fabrication of Homemade Bilayer and Silica Membranes*

For Nafion 115 membranes it was already determined that post-treating the membrane in sulfuric acid *after* catalyst application was better than fully pre-treating the membrane and then spraying catalyst. But for the bilayer membrane the opposite was found to be true, as Figure 50 below shows.

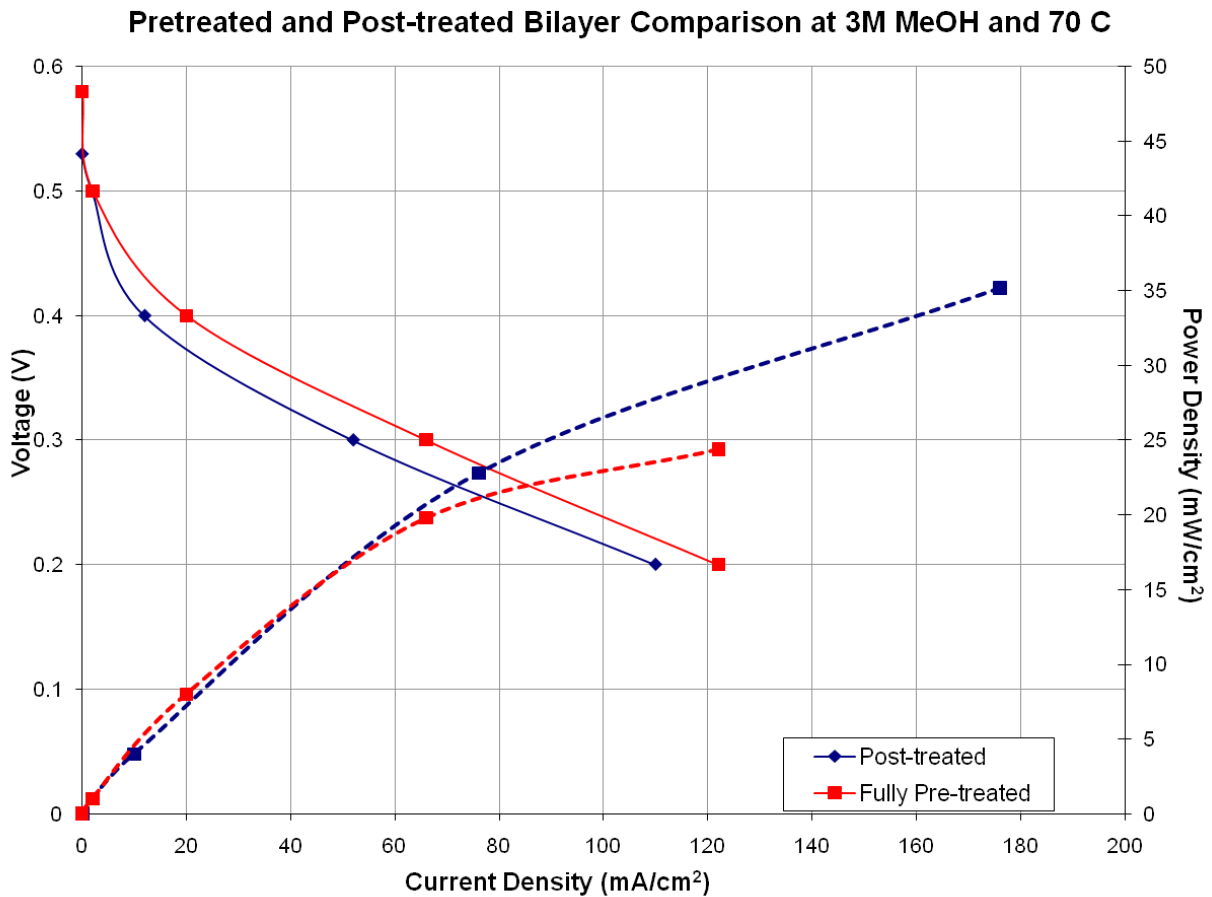


**Figure 50: Homemade Bilayer MEA - Fully Pretreated vs. Post-treated**

The fully pre-treated membrane performed better than the post-treated one almost uniformly. So the full pre-treatment method was adopted for further MEA fabrication of bilayer membranes. The reasons for this are somewhat unclear though. Boiling the membrane in sulfuric

acid after catalyst application ensures the protonation of the Nafion in the catalyst ink. But it seems that for the bilayer membrane other factors are important. The membrane contains a PTFE grid and it is possible that boiling it in acid after catalyst application disturbs the membrane-catalyst interface and the catalyst surface. The PTFE grid should prevent the expansion of the membrane in the x and y directions, but the membrane is still allowed to expand in the z-direction. This might have adverse effects on the catalyst integrity.

The silica Nafion 115 membranes were also treated in sulfuric acid prior to catalyst application in order to sulfate. Treating it in sulfuric acid after catalyst application did not work as it caused the catalyst surface to flake off the membrane while boiling in the sulfuric acid. It seems that the silica impregnation changes the surface morphology of the membrane, despite cleaning the surface of the membranes with acetone and water.

The next section compares the best membranes. A note should be made of the differences in the treatment procedure though, as follows:

Nafion 115: Boil in sulfuric acid after catalyst application

Bilayer: Boil in sulfuric acid before catalyst application

Silica: Boil in sulfuric acid before catalyst application

## ***Home-made Membrane Comparison – Best Membranes***

### **Membrane Comparison at 3M Concentration**

For Nafion 115 membrane, it has already been established that applying catalyst on the membrane is better than applying catalyst on the GDL. Catalyst was applied on the surfaces of the bilayer membrane and a 3.5 wt% silica membrane, and the MEAs were tested at the same conditions as listed under *ElectroChem GDE Comparison* section (3M methanol feed at a cell

temperature of 70°C). Figure 51 displays the polarization curves and the power density curves. The Bilayer membrane had the highest performance in the low current density region because the difference in the equivalent weights created a non-uniform proton concentration gradient that facilitated proton transport while decreasing the methanol flux, which consecutively reduced the cathode resistance, and hence increased the performance.

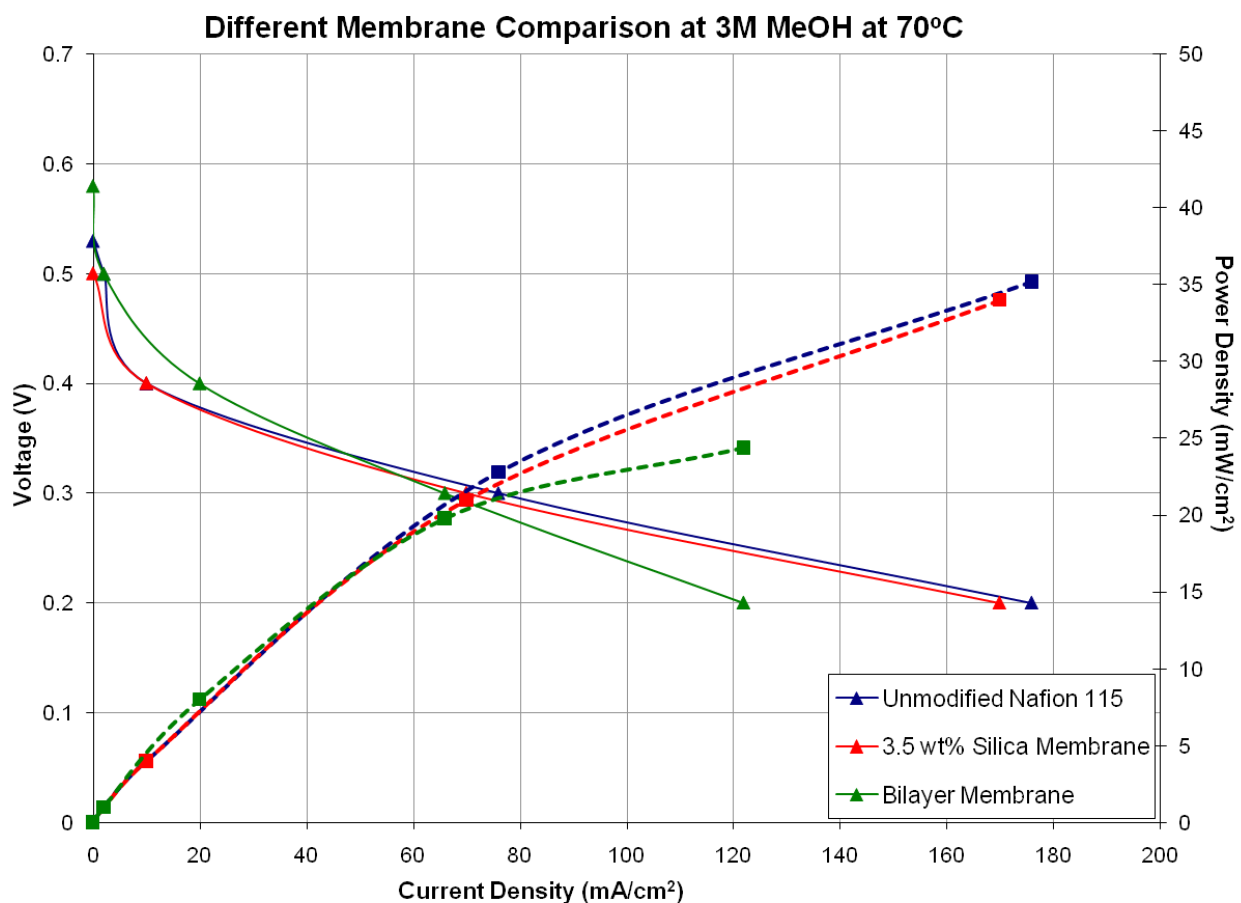


Figure 51: Membrane Comparison at 3M

The silica membrane performed more or less the same as the Nafion 115 membrane; and they both performed lower than Bilayer in the low current density region. Nafion 115 and silica

have uniform concentration gradients so the methanol flux is higher than for the Bilayer. The silica membrane also has a higher methanol flux because of its acidity.

In the high current density region, the silica membrane and Nafion 115 have similar performance. Bilayer performed worse than the other membranes in this region. It had a steeper slope than the other membranes, which indicates that the PEM resistance is higher. This might be due to the interface between the two different equivalent weight sides. This decreases the proton conductivity, thus decreasing performance.

### Membrane Comparison at 5M and 7M Concentration

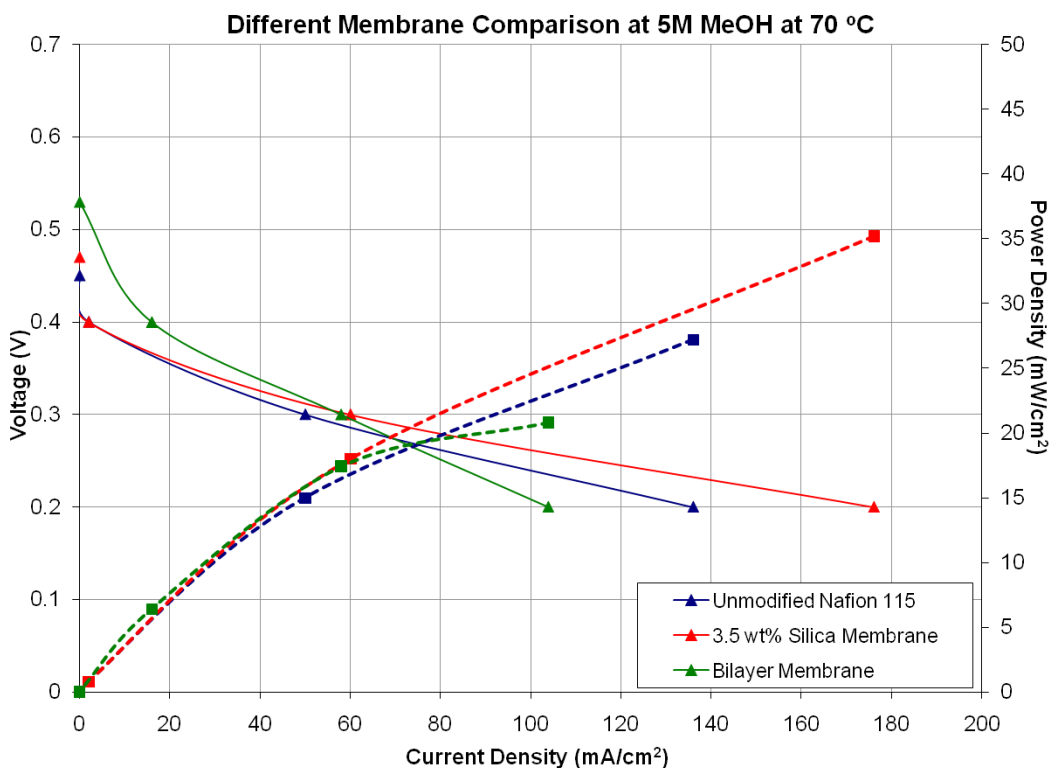


Figure 52: Different Membrane Comparison at 5M MeOH

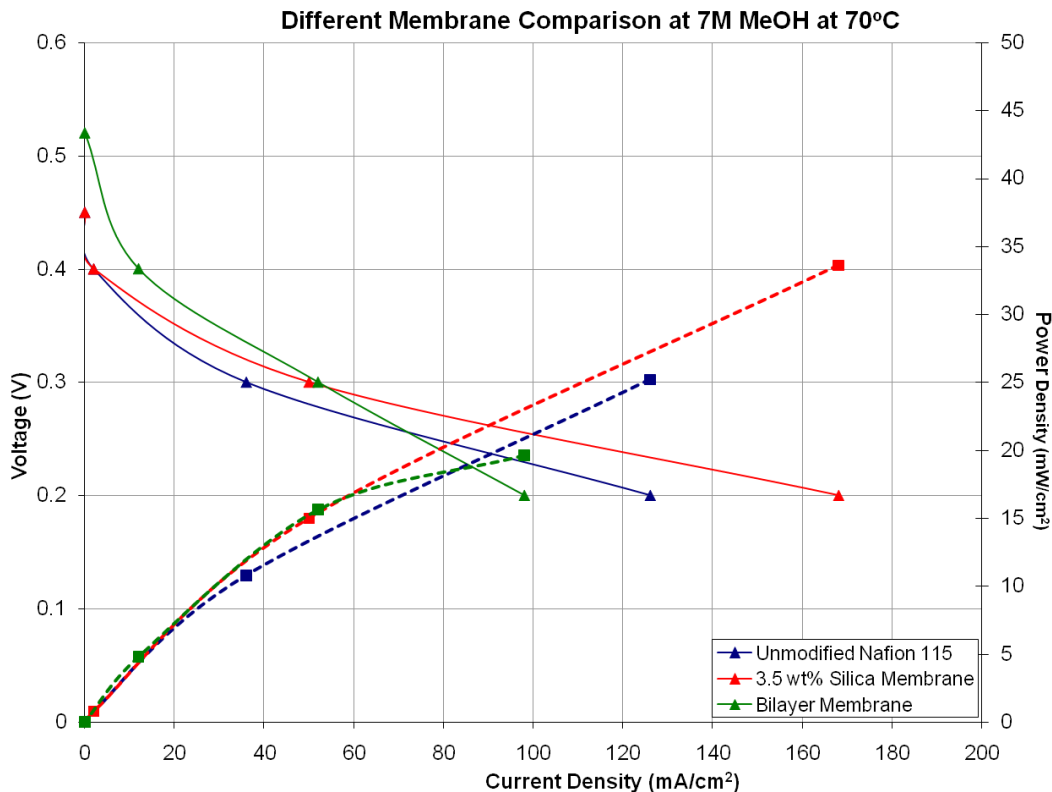


Figure 53: Different Membrane Comparison at 7M MeOH

The same three MEAs were next tested at higher methanol concentrations, 5M and 7M respectively, to determine the effects of concentration on performance. Figure 52 and 53 show polarization and performance density curves for when the MEAs were tested at 5M and 7M methanol concentration respectively.

Performance of all three membranes dropped as the methanol concentration increased due to the increase in the methanol flux. The drop in performance is less significant for the silica and bilayer membranes; however, as compared to Nafion 115. Both Figure 52 and Figure 53 show the same trend.

In the low current density region, Bilayer performed the best, followed by the 3.5 wt% silica membrane. Nafion 115 had the lowest performance. The silica membrane performed better than unmodified Nafion 115 because it is more effective in blocking methanol crossover.

It was hypothesized (refer to Literature Review) that silica membranes block vehicular diffusion, while increasing Grothuss diffusion. So methanol crossover does not increase as much as proton conductivity does, resulting in greater performance.

In the high current density region the silica membrane has a flatter slope, indicating that it has less PEM resistance and is more conductive. This is why it performs much better than Nafion 115 in this region.

### Determining the Optimal Membrane

As mentioned earlier in the report, it is desirable to have a concentrated methanol feed. The performance drops across various voltages when increasing the concentration from 3M to 7M were analyzed to find the best membrane that obstructed methanol crossover.

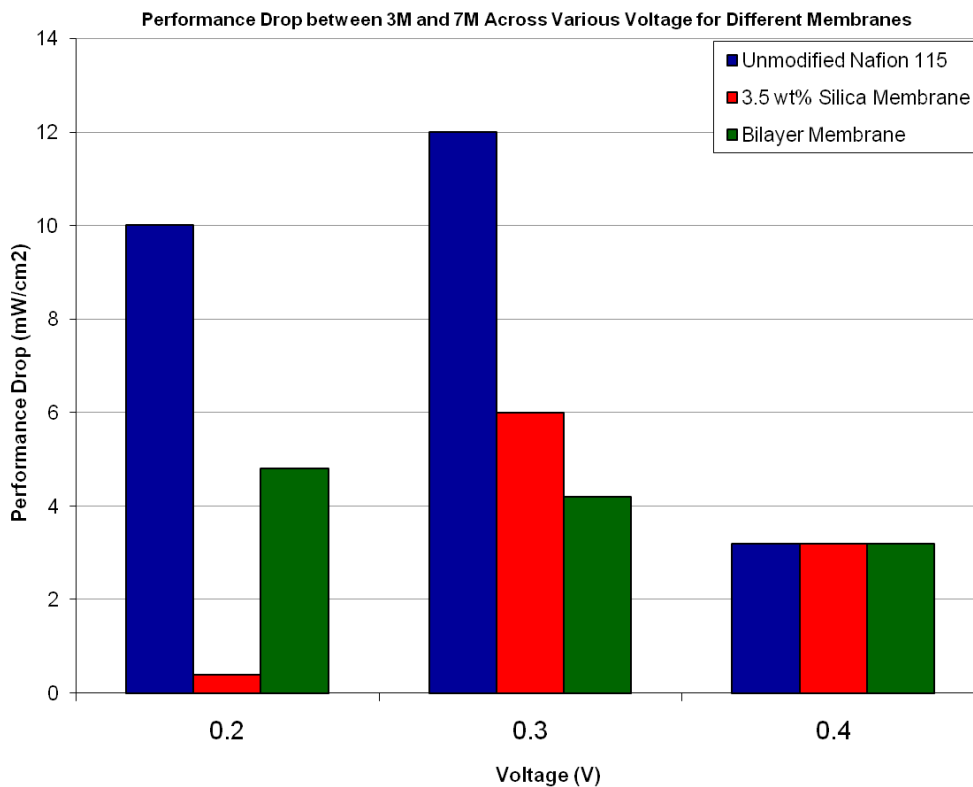


Figure 54: Performance Drop between 3M and 7M across Various Voltages for Different Membranes

Figure 54 shows power density drop for each membrane (Nafion 115, Bilayer, and 3.5 wt% silica) at the voltages of 0.2, 0.3, and 0.4, when the methanol concentration was increased from 3M to 7M. When methanol feed concentration increased, methanol crossover increased as well; therefore, it is desirable to have the lowest performance drop when the methanol feed concentration is increased to indicate the membrane that is most effective at blocking methanol crossover. Since the efficiency for the DMFC is highest at 0.3 and 0.4V, low performance drops are desirable at these voltages. As seen in Figure 54, all three membranes had the same performance drop across 0.4V.

However, at 0.3V the performance drops for Bilayer and silica membranes were approximately 70% and 50% lower than for unmodified Nafion 115. This indicates that bilayer and silica membranes are both more effective at obstructing methanol crossover than unmodified Nafion 115. Moreover, Bilayer had the lowest performance drop; therefore it is most effective at blocking methanol crossover in the region of interest. The silica membrane showed less than 1 mW/cm<sup>2</sup> in performance drop at 0.2V, which is an indication of its high conductivity.

As the methanol concentration increases, the silica membrane shows less methanol crossover than Nafion 115. So despite the high conductivity it has potential for uses in DMFCs at higher methanol feed concentrations.

## Chapter 5: Conclusions & Future Work

This section will summarize optimal MEA fabrication techniques and describe which membranes have potential advantages over Nafion 115 for DMFCs. According to the results of this research, recommendations for future work were made.

### Conclusion

An intensive study of MEA fabrication was conducted in this research. There were several factors in MEA fabrication that affected fuel cell performance, and this research found optimal ways to confront these issues. Firstly, spraying catalyst directly on the membrane was the best deposition technique since it produced close contact between the catalyst and the membrane. Secondly, a Nafion loading of approximately  $0.7\text{mgcm}^{-2}$  was found to be optimum as it maximized the three-phase interface. Thirdly, 2 metric tons of pressure was found to be optimum during hot-pressing as it provided a strong contact between the GDL and the membrane without compromising the integrity of the catalyst layer. Fourthly, MEAs with catalyzed Nafion 115 membranes performed best when sulfuric acid treatment was performed after catalyst application since post-treatment protonated sulfonic acid sites in the Nafion in dispersed throughout the catalyst layer.

Although both the bilayer and silica membranes show potential advantages over Nafion 115 -especially at higher methanol concentrations – they do so for different reasons. The bilayer membrane performed as a lower conducting membrane is expected to (refer to *DMFC Performance* section). It is likely that the interface within the membrane acts as a resistance to proton conductivity as well as to methanol crossover.

The bilayer membrane was effective at reducing methanol crossover, as indicated by the high open circuit potential values. The different equivalent weight within the membrane did not compensate for the increased thickness. The Ohmic region had a high slope due to PEM losses, so the conductivity of the membrane is lower. In the region of interest though (0.3 – 0.4V), the bilayer membrane performs better than either silica or Nafion 115 due to effective blockage of methanol crossover, especially at higher concentrations.

When operating at low methanol concentrations, the silica membrane performs as a higher conducting MEA is expected to. The OCP is relatively low because of high conductivity and high methanol crossover. This is due to the acidic nature of the sulfated silica particles in the membrane. In the high current density region it performs much better than either Nafion 115 or Bilayer, which is proof of the membrane's conductivity.

At higher methanol concentrations the trend, when compared to Nafion 115, is slightly different. The OCP is higher than for Nafion 115 because the silica membrane is more effective at blocking methanol crossover than Nafion 115. It seems that the contribution of the Grotthuss diffusion mechanism increases by impeding vehicular diffusion, this resulting in less methanol crossover. In the high current density region silica membrane continues to perform far better than the other two membranes.

Hence the silica membranes have a potential advantage over Nafion 115 membranes at higher methanol concentrations. Also, higher silica content membranes should reduce methanol crossover even more effectively. But it was difficult to get more than 4% silica absorption in the membrane using the preparation procedure described in this report. A longer duration in the TEOS solution was not fruitful. It just altered the surface morphology of the membrane, making it smoother, which in turn makes it difficult for the catalyst to adhere to the surface.

## Recommendations for Future Work

Testing at higher methanol concentrations is an important aspect for practical applications of DMFCs because of the higher energy density. About 10-15 M of feed methanol solution is desired in the industry. Since both silica and bilayer membranes performed better than unmodified Nafion 115 membranes at higher methanol concentrations, investigating the two membranes is recommended, especially at even higher concentrations.

An increase in the weight percent of silica particles increased the performance of the membrane. Current studies presume that 4-8 wt% of silica particles effectively block methanol crossover without significantly modifying the surface morphology of the membrane. For this, the current silica membrane preparation procedure would have to be modified. One of the key steps is the duration in the vacuum oven after silica impregnation (as condensation reactions take place). Currently the duration in the vacuum oven is 24 hours at 110°C. The extent of acidity of the silica particles after sulfation also plays a role in performance. This should depend on the duration of boiling the membrane in sulfuric acid when sulfating it. Currently the duration in sulfuric acid is 1.5 hours. Modification techniques should also focus on decreasing the water uptake of the membrane, as it is responsible for methanol crossover.

The Bilayer membrane already had fixed equivalent weights when it was bought from the supplier. It would be interesting to see the effects of a different combination of equivalent weights as this would alter the concentration gradient and the resistance of the membrane.

The carboxylic membrane tested for this study was not suitable for DMFCs. Exploration of suitable carboxylic membranes has some potential according to literature. One recommendation would be to investigate methods that exchange sulfonic acid sites of in commercial Nafion membranes for carboxylic acid sites.

Due to limitations of time, passive-mixing in DMFCs could not be further explored. As passive DMFC generally show better performance than active DMFC, this can be further looked into. When vaporizing the methanol feed, more residence time in the heating lines may be provided by reducing the flow rate of methanol below 1 mL/min.

# References

Chakraborty Debasish, Chorkendorff Ib and Johannessen Tue Metamorphosis of the mixed phase PtRu anode catalyst for direct methanol fuel cells after exposure of methanol: In situ and ex situ characterizations [Journal]. - Lyngby : Journal of Power Sources, 2007. - 1 : Vol. 173.

Chen R. and Zhao T. S. A novel electrode architecture for passive direct methanol fuel cells [Journal]. - Hong Kong SAR : Electrochemistry Communications, 2007. - Vol. 9.

Chen R. and Zhao T. S. Performance characterization of passive direct methanol fuel cells [Journal]. - Hong Kong : Journal of Power Sources, 2007. - 1 : Vol. 167.

Chen R. and Zhao T. S. Porous current collectors for passive direct methanol fuel cells [Journal]. - Hong Kong : Electrochimica Acta, 2007. - Vol. 52.

Choi Pyoungho, Jalani Nikhil H and Datta Ravindra Thermodynamics and Proton Transport in Nafion [Journal] // Journal of The Electrochemical Society. - 2005. - pp. E123-E130.

Choi Pyoungho, Jalani Nikhil H and Datta Ravindra Thermodynamics and Proton Transport in Nafion - Proton Transport in Nafion/Sulfated ZrO<sub>2</sub> Nanocomposite Membranes [Journal]. - Worcester : Journal of The Electrochemical Society, 2005. - A1548 : Vol. 152.

Choi Pyoungho, Jalani Nikhil H and Datta Ravindra Thermodynamics and Proton Transport in Nafion - Proton Diffusion Mechanisms and Conductivity [Journal] // Journal of The Electrochemical Society. - Worcester : Journal of The Electrochem Society, 2005. - 3 : Vol. 152. - pp. E123-E130.

Dyck A., Fritsch D. and Pereira Nunes S.P. Proton-conductive membranes of sulfonated polyphenylsulfone [Journal]. - [s.l.] : Journal for Applied Polymer Science, 2002. - 11 : Vol. 86.

Elias Quincy Quincy and Kurek Kathrin H Principles of High Performance Membrane Electrode Asseby Fabrication [Report]. - Worcester : Worcester Polytechnic Institute, 2007.

Farhat T.R. and Hammond P.T. Fabrication of a "soft" membrane electrode assembly using layer-by-layer technology [Journal]. - [s.l.] : Advanced Functional Materials, 2006. - 3 : Vol. 16.

Hackquard Alexandre Improving and Understanding Direct Methanol Fuel Cell Performance [Report]. - Worcester, MA : Worcester Polytechnic Institute, 2005.

Han Sangil, Lee Jang Woo, Kwak Chan, Chai Geun Seok, Son In Hyuk, Jang Moon Yup, An Sung Guk, Cho Sung Yong, Kim Jun Young, Kim Hyung Wook, Serov Alexey Alexandrovych, Yoo Youngtai, Nam Kie Hyun High performance membrane-electrode assembly

based on surface-modified membrane [Journal]. - [s.l.] : Journal of Power Sources, 2007. - 74-78 : Vol. 167.

Heitner-Wirguin C. Recent advances in perfluorinated ionomer membranes: structure, properties and applications [Journal]. - [s.l.] : Journal of Membrane Science, 1996. - 1-33 : Vol. 120.

Hensley Jesse E and Way Douglas J The relationship between proton conductivity and water permeability in carboxylate/sulfonate perfluorinated ionomer membranes [Journal]. - Golden, CO : Journal of Power Sources, 2007. - 1 : Vol. 172.

Hickner Michael A., Ghassemi Hossein, Kim Yu Seung, Einsla Brian R., McGrath James E. Alternative Polymer Systems for Proton Exchange Membranes (PEMs) [Journal]. - [s.l.] : American Chemical Society, 2004. - 4587-4612 : Vol. 104.

Iojoiu C., Marechal M., Chabert F., Sanchez J.-Y.

Mastering Sulfonation for Aromatic Polysulfones: Crucial for Membranes for Fuel Cell Applications [Journal]. - Weinheim : Fuel Cells, 2005. - 3 : Vol. 5.

Jalani Nikhil Development of Nanocomposite Polymer Electrolyte [Report]. - Worcester, MA : Worcester Polytechnic Institute, 2006.

Jalani Nikhil Development of Nanocomposite Polymer Electrolyte Membranes for Higher Temperature PEM Fuel Cells [Report]. - Worcester : Worcester Polytechnic Institute, 2006.

Jewett Gregory, Guo Zhen and Faghri Amir Water and air management systems for a passive direct methanol fuel cell [Report]. - Storrs : Journal of Power Sources, 2007.

Jiang Ruichun, Kunz Russell and Fenton James Composite silica/Nafion membranes prepared by tetraethylorthosilicate sol-gel reaction and solution casting for direct methanol fuel cells [Journal]. - Storrs, CT : Journal of Membrane Science , 2005. - 116 - 124 : Vol. 272.

Ladewig Bradley, Knott Robert, Martin Darren, Diniz da Costa Joao, Lu Gao Nafion-MPMDMS nanocomposite membranes with low methanol permeability [Journal]. - Menai, Australia : Electrochemistry Communications, 2006. - 4 : Vol. 9.

Liu J. G., Zhao T. S., Liang Z. X., Chen R. Effect of membrane thickness on the performance and efficiency of passive direct methanol fuel cells [Journal]. - Hong Kong : Journal of Power Sources, 2005. - 1 : Vol. 153.

Liu Jianguo, Zhao Tian-Shou, Chen Rong, Wong Chung Wai Effect of methanol concentration on passive DMFC performance [Journal]. - Hong Kong SAR : Fuel Cells Bulletin, 2005.

Lobato J., Rodrigo M.A., Linares J.J., Scott K. Effect of the catalytic ink preparation method on the performance of high temperature polymer electrolyte membrane fuel cells [Journal]. - [s.l.] : Journal of Power Sources, 2006. - 284-292 : Vol. 157.

Mauritz K.A. and Moore R.B. State of Understanding of Nafion [Journal]. - [s.l.] : Chemical Reviews, 2004. - 4535-4585 : Vol. 104.

O'Hayre Ryan, Cha Suk-Won, Colella Whitney, Prinz Fritz B. Fuel Cell Fundamentals [Book]. - Hoboken, NJ : John Wiley & Sons, Inc., 2006.

Rajendran Raj G. Polymer Electrolyte Membrane Technology for Fuel Cells [Journal]. - [s.l.] : MRS Bulletin, 2005. - Vol. 30.

Ren Suzhen, Sun Gongquan, Li Chennan, Song Shuqin, Xin Qin, Yang Xuefang Sulfated zirconia-Nafion composite membranes for higher temperature direct methanol fuel cells [Journal]. - Dalian, China : Journal of Power Sources, 2006. - 724 - 726 : Vol. 157.

Schultz Thorsten, Zhou Su and Sundmacher Kai Current Status of and Recent Developments in the Direct Methanol Fuel Cell [Journal]. - [s.l.] : Chemical Engineering Technology, 2001. - 12 : Vol. 24.

SigmaAldrich Silica-Polymer Composite Proton Exchange Membrane [Online] // sigmaaldrich. - Sigma Aldrich, 2007. - April 17, 2008. - <http://www.sigmaaldrich.com/catalog/search/ProductDetail/ALDRICH/596329>.

SigmaAldrich Silica-Polymer Composite Proton Exchange Membrane [Online] // sigmaaldrich. - Sigma Aldrich, 2007. - April 17, 2008. - <http://www.sigmaaldrich.com/catalog/search/ProductDetail/ALDRICH/596329>.

Silica-Polymer Composite Proton Exchange Membrane [Online] // sigmaaldrich. - Sigma Aldrich, 2007. - April 17, 2008. - <http://www.sigmaaldrich.com/catalog/search/ProductDetail/ALDRICH/596329>.

Song S.Q., Liang Z.X., Zhou W.J., Sun G.Q., Xin Q., Stergiopoulos V., Tsiakaras P. Direct methanol fuel cells: The effect of electrode fabrication procedure on MEAs structural properties and cell performance [Journal]. - [s.l.] : Journal of Power Sources, 2005. - 495-501 : Vol. 145.

Sun Liangliang, Ran Ran, Wang Guixing, Shao Zongping Fabrication and performance test of a catalyst-coated membrane from direct spray deposition [Journal]. - [s.l.] : Solid State Ionics, 2008. - Vol. doi:10.1016/j.ssi.2008.01.081.

Walker M. and Baumgartner K.-M. Proton-Conducting Polymers with Reduced Methanol Permeation [Journal]. - [s.l.] : Journal of Applied Polymer Science, 1999. - 67-73 : Vol. 74.

Wilson Mahlon S. and Gottesfeld Shimshon High Performance Catalyzed membranes of Ultra-low Pt Loadings for Polymer Electrolyte Fuel Cells [Journal]. - [s.l.] : Journal of the Electrochemical Society, 1992. - 2 : Vol. 139.

Yang Y. and Holdcroft S. Synthetic Strategies for Controlling the Morphology of Proton Conducting Polymer Membranes [Journal]. - [s.l.] : Fuel Cells, 2005. - 2 : Vol. 5.

Zhang Jian, Yin Ge-Ping, Wang Zhen-Bo, Lai Qin-Zhi, Cai Ke-Di  
Effects of hot pressing conditions on the performances of MEAs for direct methanol fuel cells [Journal]. - [s.l.] : Journal of Power Sources, 2007. - 73-81 : Vol. 165.

# Acknowledgements

We would like to thank Professor Datta for advising us and providing insightful analysis, in addition to his support. We would like to thank Saurabh Vilekar for his diligent guidance both in lab and out of lab, especially with troubleshooting and analysis. Jack Ferraro and Doug White helped us with troubleshooting in lab. Finally we would like to thank Natalie Pomerantz for helping us with the Scanning Electron Micrograph imaging.

# Appendices

## Appendix 1: Membrane Treatment Procedures

### *Unmodified Nafion 115 Membranes & Bilayer Membranes*

#### Full Pre-treatment Method

To be used when:

- Spraying catalyst onto GDLs for Nafion or Bilayer membranes
- Using EletroChem GDEs for Nafion or Bilayer membranes
- Spraying catalyst on membrane surface of Bilayer membranes.

Duration	Step
1 hour	Boil (low) in DI water
1.5 hours	Low boil in 3% H <sub>2</sub> O <sub>2</sub>
1 hour	Low boil in DI water
1 hour	Low boil in 0.5M H <sub>2</sub> SO <sub>4</sub>
1 hour	Low boil in DI water
N/A	Store the membrane in DI water until hotpressing to GDL (with catalyst layer already on it)

#### Post-treatment Method

To be used when spraying catalyst directly onto the Nafion membrane.

Phase	Duration	Step
<b>Pre-treatment</b>	1 hour	Boil (low) in DI water
	1.5 hours	Low boil in 3% H <sub>2</sub> O <sub>2</sub>
	1 hour	Low boil in DI water.
	N/A	Store in DI water until catalyst application
<b>Catalyst App</b>	5 min.	Dry in hot-press at 0 tons pressure and no heat
	N/A	Immediately afterward apply catalyst
	1.5 hours	Dry in oven at 80 C
<b><i>SPRAY CATALYST ON MEMBRANE</i></b>		
<b>Post treatment</b>	1.5 hours	Low boil in 0.5M H <sub>2</sub> SO <sub>4</sub>
	1 hour	Low boil in DI water
	N/A	Store in water until MEA assembly
	5 min.	Just before assembly dry in hot press at 0 lbs pressure and no heat.

## *Carboxylic Acid Membranes*

<b>Duration</b>	<b>Step</b>
1.5 hour	Low boil in 0.5M HNO <sub>3</sub>
1 hour	Heat in DI water

### *Aldrich Silica Membrane*

If needed, heat gently in water for 1 hour prior to catalyst application.

### *Preparation of Solutions*

#### 1000mL of 3 wt % H<sub>2</sub>O<sub>2</sub>:

- In a 600 mL beaker, measure 85.7 mL of 35 wt % H<sub>2</sub>O<sub>2</sub>
- Add 914 mL water

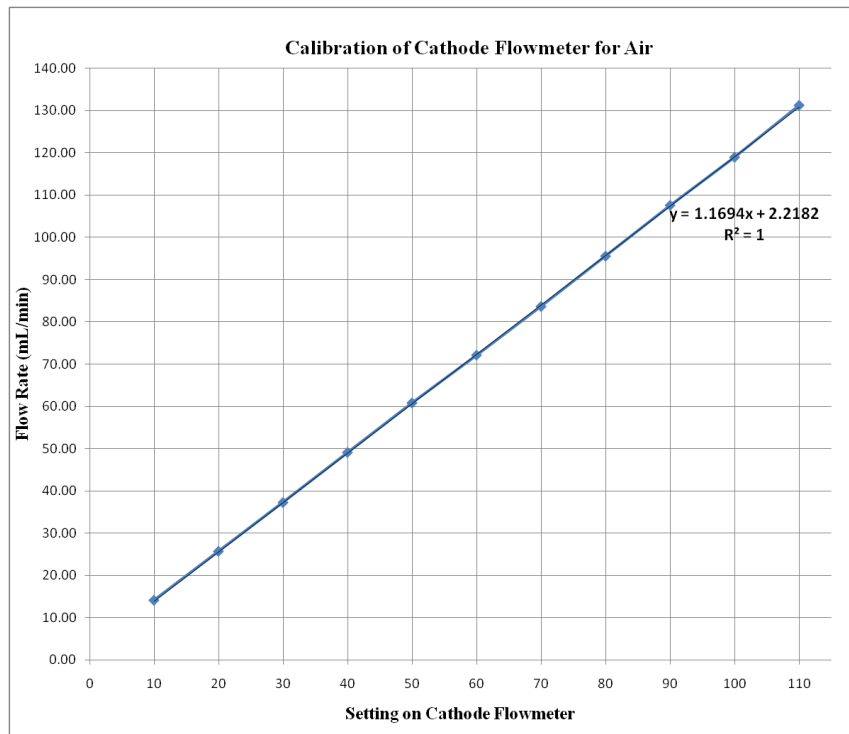
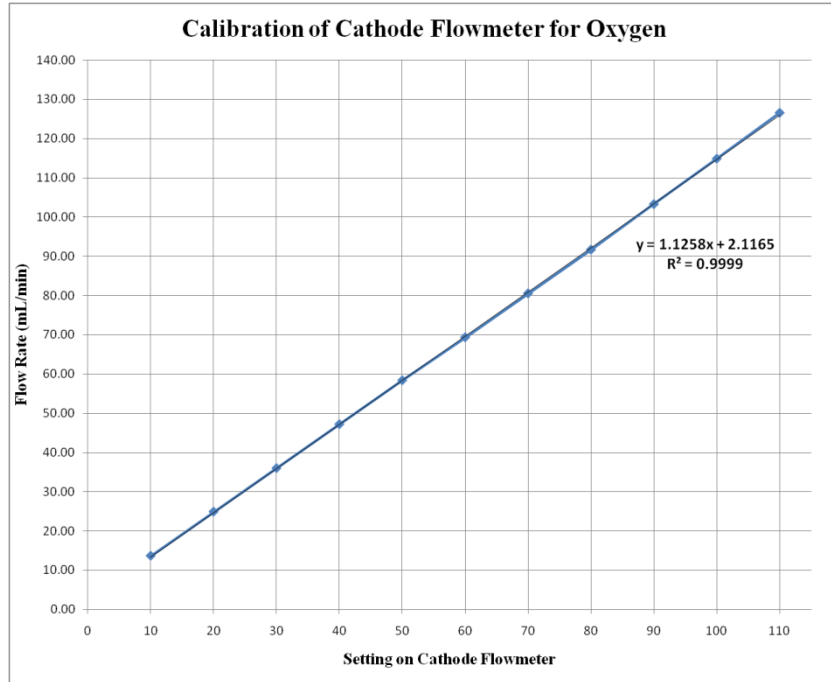
#### 1000 mL of 0.5M H<sub>2</sub>SO<sub>4</sub>:

- In a 600 mL beaker, measure 27 mL of 98 wt % H<sub>2</sub> SO<sub>4</sub>
- Add 973 mL water

#### 100 mL of 0.5M HNO<sub>3</sub>:

- In a 600 mL beaker, measure 97.1 mL water
- Add 2.86 mL of 70 wt % HNO<sub>3</sub>

## Appendix 2: Calibration of Cathode Flow Meter for Oxygen and Air



## Appendix 3: Synthesis Procedure for Nafion-SiO<sub>2</sub> Sol-Gel Membrane

### Membrane Synthesis

Phase	Duration	Step
1	N/A	Cut a 2.0 in. x 2.0 in. square of a Nafion 115 membrane
	1 hour	Boil membrane in 150mL of 3 wt % H <sub>2</sub> O <sub>2</sub>
	4 hours	Boil in 600mL of 1 M NaOH solution. (Important to monitor.)
	30 min	Heat in 100mL DI water at 60 C
	N/A	Remove from water beaker. Lightly wipe with Kim wipes before placing membrane on watch glass
	12 hours	Place watch glass in vacuum oven at 110 C (3.75) under 30 in. Hg vacuum.
	N/A	Measure mass of dry membrane (M <sub>1</sub> )
2	1 hour	Heat in 100mL DI water
	1 hour	Immerse in 150mL of 2:1 MeOH : H <sub>2</sub> O solution
	Varies	Remove and immerse in 150mL 3:2 TEOS : MeOH solution (2 – 8
	N/A	Remove from solution. Lightly wipe with Kim wipes before placing membrane on watch glass
	24 hours	Place watch glass in vacuum oven at 110 C (3.75) under 30 in. Hg vacuum.
	N/A	Measure mass of dry membrane (M <sub>2</sub> )
3	30 min	Heat in 100mL DI water
	30 min	Heat in 100mL acetone
	1.5 hours	Boil in 150mL 0.5M H <sub>2</sub> SO <sub>4</sub>
	1 hour	Heat in 100mL DI water
	N/A	Store in 200mL DI water
<b>TRANSPARENT AND HOMOGENEOUS NAFION – SiO<sub>2</sub> SOL GEL MEMBRANE READY FOR HOTPRESSING TO CATALYZED GDL OR CATALYST APPLICATION</b>		

$$\text{Wt \% silica} = [(M_2 - M_1)/M_1]*100$$

### Materials Required

- Sodium hydroxide flakes
- Methanol – 200 proof
- Tetraethylorthosilicate (TEOS) solution
- Acetone
- Sulfuric acid

## *Preparation of Solutions*

### 800mL of 1 M NaOH Solution:

- Weigh 32.0 g of sodium hydroxide flakes in a 1400 mL beaker
- Add 800 mL of DI water
- Stir to dissolve. The remaining solid will dissolve under heat

### 150 mL of 2:1 MeOH : H<sub>2</sub>O solution:

- Measure 100.0 mL of pure methanol in a beaker
- Add 50.0 mL of water

### 150 mL of 3:2 TEOS : MeOH solution:

- Measure 90.0 mL of TEOS solution into a beaker.
- Add 60.0 mL of pure methanol

### 100mL of 3 wt % H<sub>2</sub>O<sub>2</sub>:

- In a 600 mL beaker, measure 8.6 mL of 35 wt % H<sub>2</sub>O<sub>2</sub>
- Add 91.4 mL water

### 100 mL of 0.5M H<sub>2</sub>SO<sub>4</sub>:

- In a 600 mL beaker, measure 2.7 mL of 98 wt % H<sub>2</sub> SO<sub>4</sub>
- Add 97.3 mL water

## Appendix 4: Temperature Calibration for Vacuum Oven

Vacuum Oven: Precision Vacuum Oven Model 19

Setting	Temperature	
	°F	°C
0.5	122	50
1.0	142	61
1.5	159	71
2.0	178	81
2.5	190	88
3.0	210	99

Calibration could only be performed up to 99°C due to the thermometer scale restrictions. From extrapolation, a setting of 3.75 would yield 110°C.

## Appendix 5: Raw Data

### *E-TEK Commercial MEA*

#### MEA 001

<b>E-TEK MEA</b>	Anode: Pt/Ru black 5mg/cm <sup>2</sup> , Cathode: Pt black 5mg/cm <sup>2</sup> , 3M 1ml/min MeOH, 70ml/min O <sub>2</sub> , T=70C cathode humidifier =85C		
<b>V (V)</b>	<b>I (A)</b>	<b>I (mA/cm<sup>2</sup>)</b>	<b>P (mW/cm<sup>2</sup>)</b>
0.2	1.93	386	77.2
0.3	1.29	258	77.4
0.4	0.64	128	51.2
0.5	0.21	42	21
0.6	0.01	2	1.2
0.62	0	0	0

#### MEA 001

<b>E-TEK MEA</b>	Anode: Pt/Ru black 5mg/cm <sup>2</sup> , Cathode: Pt black 5mg/cm <sup>2</sup> , 3M 1ml/min MeOH, 70ml/min O <sub>2</sub> , T=80C cathode humidifier = 85C		
<b>V (V)</b>	<b>I (A)</b>	<b>I (mA/cm<sup>2</sup>)</b>	<b>P (mW/cm<sup>2</sup>)</b>
0.2	1.99	398	79.6
0.3	1.54	308	92.4
0.4	0.75	150	60
0.5	0.22	44	22
0.58	0	0	0

### *Catalyst Application on GDL: Catalyzed ElectroChem GDLs and Home-made MEAs*

#### MEA 004

<b>Nafion 115</b>	Anode: Pt/Ru black 4mg/cm <sup>2</sup> , Cathode: Pt black 4mg/cm <sup>2</sup> , (old GDL (ElectroChem)). Hot -pressed: 2 ton & 2min, 3M 1ml/min MeOH, 70ml/min O <sub>2</sub> , T=70C humidifier =85C. 0.7 mg/cm <sup>2</sup> Nafion, Fully-treated		
<b>V (V)</b>	<b>I (A)</b>	<b>I (mA/cm<sup>2</sup>)</b>	<b>P (mW/cm<sup>2</sup>)</b>
0.2		0.15	30
0.3		0.05	10
0.4		0.01	2
0.58		0	0

**MEA 005**

<b>Nafion 115</b>	Anode: Pt/Ru black 4mg/cm <sup>2</sup> , Cathode: Pt black 4mg/cm <sup>2</sup> , (E-TEK microporous GDL). Hot -pressed: 2 tonne & 2min. 3M 1ml/min MeOH, 70ml/min O <sub>2</sub> , T=70C humidifier =85C. 0.7 mg/cm <sup>2</sup> Nafion, Fully-treated		
<b>V (V)</b>	<b>I (A)</b>	<b>I (mA/cm<sup>2</sup>)</b>	<b>P (mW/cm<sup>2</sup>)</b>
0.2	0.28	56	11.2
0.3	0.08	16	4.8
0.4	0.01	2	0.8
0.53	0	0	0

**MEA 020**

<b>Nafion 115</b>	Anode: Pt/Ru black 4mg/cm <sup>2</sup> , Cathode: Pt black 4mg/cm <sup>2</sup> , (ElectroChem GDL). Hot -pressed:2 tonne & 2min, 3M 1ml/min MeOH, 70ml/min O <sub>2</sub> , T=70C humidifier =35C. Fully-treated		
<b>V (V)</b>	<b>I (A)</b>	<b>I (mA/cm<sup>2</sup>)</b>	<b>P (mW/cm<sup>2</sup>)</b>
0.2	0.48	96	19.2
0.3	0.25	50	15
0.4	0.08	16	6.4
0.5	0.03	6	3
0.62	0	0	0

**MEA 021**

<b>4 wt% Silica</b>	Anode: Pt/Ru black 4mg/cm <sup>2</sup> , Cathode: Pt black 4mg/cm <sup>2</sup> , (ElectroChem GDL). Hot -pressed:2 tonne & 2min, 3M 1ml/min MeOH, 70ml/min O <sub>2</sub> , T=70C humidifier =35C. Fully-treated		
<b>V (V)</b>	<b>I (A)</b>	<b>I (mA/cm<sup>2</sup>)</b>	<b>P (mW/cm<sup>2</sup>)</b>
0.2	0.58	116	23.2
0.3	0.31	62	18.6
0.4	0.1	20	8
0.5	0.03	6	3
0.58	0	0	0

**MEA 022**

<b>Bilayer (switch side)</b>	Anode: Pt/Ru black 4mg/cm <sup>2</sup> , Cathode: Pt black 4mg/cm <sup>2</sup> , (ElectroChem GDL). Hot -pressed:2 tonne & 2min, 3M 1ml/min MeOH, 70ml/min O <sub>2</sub> , T=70C humidifier =35C. Fully-treated		
<b>V (V)</b>	<b>I (A)</b>	<b>I (mA/cm<sup>2</sup>)</b>	<b>P (mW/cm<sup>2</sup>)</b>
0.2	0.25	50	10
0.3	0.11	22	6.6
0.4	0.01	2	0.8
0.5	0	0	0

**MEA 025**

<b>1.4 wt% Silica</b>	Anode:Pt/Ru black 4mg/cm <sup>2</sup> , Cathode: Pt black 4mg/cm <sup>2</sup> , (ElectroChem GDL). Hot -pressed:2 tonne & 2min, 3M 1ml/min MeOH, 70ml/min O <sub>2</sub> , T=70C humidifer =35C. Fully-treated		
<b>V (V)</b>	<b>I (A)</b>	<b>I (mA/cm<sup>2</sup>)</b>	<b>P (mW/cm<sup>2</sup>)</b>
0.2	0.53	106	21.2
0.3	0.25	50	15
0.4	0.08	16	6.4
0.5	0.01	2	1
0.6	0	0	0

**MEA 026**

<b>Bilayer</b>	Anode:Pt/Ru black 4mg/cm <sup>2</sup> , Cathode: Pt black 4mg/cm <sup>2</sup> , (ElectroChem GDL). Hot -pressed:2 tonne & 2min, 3M 1ml/min MeOH, 70ml/min O <sub>2</sub> , T=70C humidifer =35C. Fully-treated		
<b>V (V)</b>	<b>I (A)</b>	<b>I (mA/cm<sup>2</sup>)</b>	<b>P (mW/cm<sup>2</sup>)</b>
0.2	0.36	72	14.4
0.3	0.2	40	12
0.4	0.08	16	6.4
0.5	0.03	6	3
0.63	0	0	0

***Catalyst Application on Membrane*****MEA 006**

<b>Nafion 115</b>	Anode:Pt/Ru black 4mg/cm <sup>2</sup> , Cathode: Pt black 4mg/cm <sup>2</sup> , (E-TEK microporous GDL). Hot -pressed:2 tonne & 2min, 3M 1ml/min MeOH, 70ml/min O <sub>2</sub> , T=70C humidifer =35C. 0.7 mg/cm <sup>2</sup> Nafion, Post-treated		
<b>V (V)</b>	<b>I (A)</b>	<b>I (mA/cm<sup>2</sup>)</b>	<b>P (mW/cm<sup>2</sup>)</b>
0.2	0.88	176	35.2
0.3	0.38	76	22.8
0.4	0.05	10	4
0.5	0.01	2	1
0.53	0	0	0

**MEA 006**

<b>Nafion 115</b>	Anode:Pt/Ru black 4mg/cm <sup>2</sup> , Cathode: Pt black 4mg/cm <sup>2</sup> , (E-TEK microporous GDL). Hot -pressed:2 tonne & 2min, 5M 1ml/min MeOH, 70ml/min O <sub>2</sub> , T=70C humidifer =35C. 0.7 mg/cm <sup>2</sup> Nafion, Post-treated		
<b>V (V)</b>	<b>I (A)</b>	<b>I (mA/cm<sup>2</sup>)</b>	<b>P (mW/cm<sup>2</sup>)</b>
0.2	0.68	136	27.2
0.3	0.25	50	15
0.4	0.01	2	0.8
0.45	0	0	0

**MEA 006**

<b>Nafion 115</b>	Anode:Pt/Ru black 4mg/cm <sup>2</sup> , Cathode: Pt black 4mg/cm <sup>2</sup> , (E-TEK microporous GDL). Hot -pressed:2 tonne & 2min, 7M 1ml/min MeOH, 70ml/min O <sub>2</sub> , T=70C humidifer =35C. 0.7 mg/cm <sup>2</sup> Nafion, Post-treated		
<b>V (V)</b>	<b>I (A)</b>	<b>I (mA/cm<sup>2</sup>)</b>	<b>P (mW/cm<sup>2</sup>)</b>
0.2	0.63	126	25.2
0.3	0.18	36	10.8
0.4	0.01	2	0.8
0.45	0	0	0

**MEA 014**

<b>Nafion 115</b>	Anode:Pt/Ru black 4mg/cm <sup>2</sup> , Cathode: Pt black 4mg/cm <sup>2</sup> , (E-TEK microporous GDL). hot -pressed:2 tonne & 2min, 7M 1ml/min MeOH, 70ml/min O <sub>2</sub> , T=70C humidifer =35C. 0.7 mg/cm <sup>2</sup> Nafion, Fully Pre-treated		
<b>V (V)</b>	<b>I (A)</b>	<b>I (mA/cm<sup>2</sup>)</b>	<b>P (mW/cm<sup>2</sup>)</b>
0.2	0.46	92	18.4
0.3	0.16	32	9.6
0.4	0.01	2	0.8
0.45	0	0	0

**MEA 015**

<b>Nafion 115</b>	Anode:Pt/Ru black 4mg/cm <sup>2</sup> , Cathode: Pt black 4mg/cm <sup>2</sup> , (E-TEK microporous GDL). Hot -pressed:2 tonne & 2min, 7M 1ml/min MeOH, 70ml/min O <sub>2</sub> , T=70C humidifer =35C. 1.2 mg/cm <sup>2</sup> Nafion, Post-treated		
<b>V (V)</b>	<b>I (A)</b>	<b>I (mA/cm<sup>2</sup>)</b>	<b>P (mW/cm<sup>2</sup>)</b>
0.2	0.25	50	10
0.3	0.08	16	4.8
0.4	0.01	2	0.8
0.45	0	0	0

**MEA 017**

<b>2.2wt% Silica</b>	Anode:Pt/Ru black 4mg/cm <sup>2</sup> , Cathode: Pt black 4mg/cm <sup>2</sup> , (E-TEK microporous GDL). Hot -pressed:2 tonne & 2min, 3M 1ml/min MeOH, 70ml/min O <sub>2</sub> , T=70C humdifer =35C. 0.7 mg/cm <sup>2</sup> Nafion, Fully-pretreated		
<b>V (V)</b>	<b>I (A)</b>	<b>I (mA/cm<sup>2</sup>)</b>	<b>P (mW/cm<sup>2</sup>)</b>
0.2	0.45	90	18
0.3	0.18	36	10.8
0.4	0.01	2	0.8
0.47	0	0	0

**MEA 017**

<b>2.2wt% Silica</b>	Anode:Pt/Ru black 4mg/cm <sup>2</sup> , Cathode: Pt black 4mg/cm <sup>2</sup> , (E-TEK microporous GDL). Hot -pressed:2 tonne & 2min, 5M 1ml/min MeOH, 70ml/min O <sub>2</sub> , T=70C humdifer =35C. 0.7 mg/cm <sup>2</sup> Nafion, Fully-pretreated		
<b>V (V)</b>	<b>I (A)</b>	<b>I (mA/cm<sup>2</sup>)</b>	<b>P (mW/cm<sup>2</sup>)</b>
0.2	0.45	90	18
0.3	0.13	26	7.8
0.4	0.01	2	0.8
0.45	0	0	0

**MEA 017**

<b>2.2wt% Silica</b>	Anode:Pt/Ru black 4mg/cm <sup>2</sup> , Cathode: Pt black 4mg/cm <sup>2</sup> , (E-TEK microporous GDL). Hot -pressed:2 tonne & 2min, 7M 1ml/min MeOH, 70ml/min O <sub>2</sub> , T=70C humdifer =35C. 0.7 mg/cm <sup>2</sup> Nafion, Fully-pretreated		
<b>V (V)</b>	<b>I (A)</b>	<b>I (mA/cm<sup>2</sup>)</b>	<b>P (mW/cm<sup>2</sup>)</b>
0.2	0.41	82	16.4
0.3	0.11	22	6.6
0.44	0	0	0

**MEA 019**

<b>2.2wt% Silica</b>	Anode:Pt/Ru black 4mg/cm <sup>2</sup> , Cathode: Pt black 4mg/cm <sup>2</sup> , (E-TEK microporous GDL). hot -pressed:2 tonne & 2min, 3M 1ml/min MeOH, 70ml/min O <sub>2</sub> , T=70C humdifer =35C. 0.7 mg/cm <sup>2</sup> Nafion, Fully-pretreated		
<b>V (V)</b>	<b>I (A)</b>	<b>I (mA/cm<sup>2</sup>)</b>	<b>P (mW/cm<sup>2</sup>)</b>
0.2	0.61	122	24.4
0.3	0.33	66	19.8
0.4	0.1	20	8
0.5	0.01	2	1
0.58		0	0

**MEA 019**

<b>2.2wt% Silica</b>	Anode:Pt/Ru black 4mg/cm <sup>2</sup> , Cathode: Pt black 4mg/cm <sup>2</sup> , (E-TEK microporous GDL). hot -pressed:2 tonne & 2min, 5M 1ml/min MeOH, 70ml/min O <sub>2</sub> , T=70C humidifer =35C. 0.7 mg/cm <sup>2</sup> Nafion, Fully-pretreated		
<b>V (V)</b>	<b>I (A)</b>	<b>I (mA/cm<sup>2</sup>)</b>	<b>P (mW/cm<sup>2</sup>)</b>
0.2	0.52	104	20.8
0.3	0.29	58	17.4
0.4	0.08	16	6.4
0.53	0	0	0

**MEA 019**

<b>2.2wt% Silica</b>	Anode:Pt/Ru black 4mg/cm <sup>2</sup> , Cathode: Pt black 4mg/cm <sup>2</sup> , (E-TEK microporous GDL). hotpressed:2 tonne & 2min, 7M 1ml/min MeOH, 70ml/min O <sub>2</sub> , T=70C humidifer =35C. 0.7 mg/cm <sup>2</sup> Nafion, Fully-pretreated.		
<b>V (V)</b>	<b>I (A)</b>	<b>I (mA/cm<sup>2</sup>)</b>	<b>P (mW/cm<sup>2</sup>)</b>
0.2	0.49	98	19.6
0.3	0.26	52	15.6
0.4	0.06	12	4.8
0.52	0	0	0

**MEA 023**

<b>Nafion 115</b>	Anode:Pt/Ru black 4mg/cm <sup>2</sup> , Cathode: Pt black 4mg/cm <sup>2</sup> , (E-TEK microporous GDL). hot -pressed:1 tonne & 2min, 3M 1ml/min MeOH, 70ml/min O <sub>2</sub> , T=70C humidifer =35C. 0.7 mg/cm <sup>2</sup> Nafion, Post-treated		
<b>V (V)</b>	<b>I (A)</b>	<b>I (mA/cm<sup>2</sup>)</b>	<b>P (mW/cm<sup>2</sup>)</b>
0.2	0.91	182	36.4
0.3	0.31	62	18.6
0.4	0.03	6	2.4
0.49	0	0	0

**MEA 024**

<b>Nafion 115</b>	Anode:Pt/Ru black 4mg/cm <sup>2</sup> , Cathode: Pt black 4mg/cm <sup>2</sup> , (E-TEK microporous GDL). hot -pressed:0.5 tonne & 2min, 3M 1ml/min MeOH, 70ml/min O <sub>2</sub> , T=70C humidifer =35C. 0.7 mg/cm <sup>2</sup> Nafion, Post-treated		
<b>V (V)</b>	<b>I (A)</b>	<b>I (mA/cm<sup>2</sup>)</b>	<b>P (mW/cm<sup>2</sup>)</b>
0.2	0.51	102	20.4
0.3	0.16	32	9.6
0.4	0.01	2	0.8
0.47	0	0	0

**MEA 036**

<b>Bilayer</b>	Anode:Pt/Ru black 4mg/cm <sup>2</sup> , Cathode: Pt black 4mg/cm <sup>2</sup> , (E-TEK microporous GDL). hot -pressed:2 tonne & 2min, 3M 1ml/min MeOH, 70ml/min O <sub>2</sub> , T=70C humidifer =35C. 0.7 mg/cm <sup>2</sup> Nafion, Post-treated		
<b>V (V)</b>	<b>I (A)</b>	<b>I (mA/cm<sup>2</sup>)</b>	<b>P (mW/cm<sup>2</sup>)</b>
0.2	0.55	110	22
0.3	0.26	52	15.6
0.4	0.06	12	4.8
0.5	0.01	2	1
0.53	0	0	0

**MEA 036**

<b>Bilayer</b>	Anode:Pt/Ru black 4mg/cm <sup>2</sup> , Cathode: Pt black 4mg/cm <sup>2</sup> , (E-TEK microporous GDL). hot -pressed:2 tonne & 2min, 5M 1ml/min MeOH, 70ml/min O <sub>2</sub> , T=70C humidifer =35C. 0.7 mg/cm <sup>2</sup> Nafion, Post-treated		
<b>V (V)</b>	<b>I (A)</b>	<b>I (mA/cm<sup>2</sup>)</b>	<b>P (mW/cm<sup>2</sup>)</b>
0.2	0.48	96	19.2
0.3	0.23	46	13.8
0.4	0.05	10	4
0.5	0	0	0

**MEA 036**

<b>Bilayer</b>	Anode:Pt/Ru black 4mg/cm <sup>2</sup> , Cathode: Pt black 4mg/cm <sup>2</sup> , (E-TEK microporous GDL). hot -pressed:2 tonne & 2min, 7M 1ml/min MeOH, 70ml/min O <sub>2</sub> , T=70C humidifer =35C. 0.7 mg/cm <sup>2</sup> Nafion, Post-treated		
<b>V (V)</b>	<b>I (A)</b>	<b>I (mA/cm<sup>2</sup>)</b>	<b>P (mW/cm<sup>2</sup>)</b>
0.2	0.45	90	18
0.3	0.18	36	10.8
0.4	0.03	6	2.4
0.49	0	0	0

**MEA 037**

<b>3.5 wt% Silica</b>	Anode:Pt/Ru black 4mg/cm <sup>2</sup> , Cathode: Pt black 4mg/cm <sup>2</sup> , (E-TEK microporous GDL). Hot -pressed:2 tonne & 2min, 3M 1ml/min MeOH, 70ml/min O <sub>2</sub> , T=70C humidifer =35C. 0.7 mg/cm <sup>2</sup> Nafion, Post-treated		
<b>V (V)</b>	<b>I (A)</b>	<b>I (mA/cm<sup>2</sup>)</b>	<b>P (mW/cm<sup>2</sup>)</b>
0.2	0.85	170	34
0.3	0.35	70	21
0.4	0.05	10	4
0.5	0	0	0

**MEA 037**

<b>3.5 wt% Silica</b>	Anode:Pt/Ru black 4mg/cm <sup>2</sup> , Cathode: Pt black 4mg/cm <sup>2</sup> , (E-TEK microporous GDL). Hot -pressed:2 tonne & 2min, 5M 1ml/min MeOH, 70ml/min O <sub>2</sub> , T=70C humdifer =35C. 0.7 mg/cm <sup>2</sup> Nafion, Post-treated		
<b>V (V)</b>	<b>I (A)</b>	<b>I (mA/cm<sup>2</sup>)</b>	<b>P (mW/cm<sup>2</sup>)</b>
0.2	0.88	176	35.2
0.3	0.3	60	18
0.4	0.01	2	0.8
0.47	0	0	0

**MEA 037**

<b>3.5 wt% Silica</b>	Anode:Pt/Ru black 4mg/cm <sup>2</sup> , Cathode: Pt black 4mg/cm <sup>2</sup> , (E-TEK microporous GDL). Hot -pressed:2 tonne & 2min, 7M 1ml/min MeOH, 70ml/min O <sub>2</sub> , T=70C humdifer =35C. 0.7 mg/cm <sup>2</sup> Nafion, Post-treated		
<b>V (V)</b>	<b>I (A)</b>	<b>I (mA/cm<sup>2</sup>)</b>	<b>P (mW/cm<sup>2</sup>)</b>
0.2	0.84	168	33.6
0.3	0.25	50	15
0.4	0.01	2	0.8
0.45	0	0	0